44
12 R

OPERATION CHARACTERISTICS OF FIXED-IMPELLER HYDROCLONES

Approved:

Joseph M. DallaValle

W. B. Harrison

Joseph B. Moder

Date Approved by Chairman: December 1, 1955

OPERATION CHARACTERISTICS OF FIXED-IMPELLER HYDROCLONES

A THESIS

Presented To

The Faculty of the Graduate Division

Georgia Institute of Technology

In Partial Fulfillment

of the Requirements for the Degree

Doctor of Philosophy in the School

of Chemical Engineering

By
Henry Howard Sineath

November 1955

ACKNOWLEDGEMENTS

The author wishes to make the following acknowledgements: to Doctor J. M. DallaValle and Doctor J. J. Moder for their assistance and guidance throughout the course of this work; to Doctor Paul Weber, Doctor W. N. Newton, and other members of the Chemical Engineering Department for their interest and helpful suggestions; to Doctor T. W. Jackson of the Engineering Experiment Station for his interest and suggestion on design; to Doctor W. B. Harrison for editing the manuscript; to Mr. John Bierman and Mr. Jones Scoggins for their assistance in experimentation and analytical work; and to Mr. C. A. Mayes for his assistance in construction of experimental equipment.

The author also wishes to express his appreciation to the Dawes Silica Mining Co. of Thomasville, Georgia, for donating the sized sand and to Mr. John L. Gray, Superintendent of the Chemical Products Co. of Cartersville, Georgia, for donating the barytes used in this study.

TABLE OF CONTENTS

TABLE OF CONTENTS (Continued)

LIST OF TABLES

LIST OF FIGURES

LIST OF FIGURES (Continued)

SUMMARY

Within the last decade, the effects of legal and technological changes on many process industries have stimulated the search for more economical separation and classification processes. The liquid-solid cyclone has been developed for classification and desliming of solids at particle sizes below the 200-mesh point and, in many instances, has replaced other less economical separation equipment. The cyclone utilizes centrifugal force for separating solids from liquids and is an efficient device, separating with a high degree of "sharpness." Unfortunately, the cyclone does not give satisfactory separation at larger particle diameters (70 to 200 mesh). Because there are many applications where the desired separation is beyond the range of the cyclone, as presently designed, it appeared desirable to attempt to develop equipment to extend the range of separation to larger particle sizes. With these considerations in mind, Dr. J. M. DallaValle and Dr. J. J. Moder of the Georgia Institute of Technology advanced the idea for and had constructed a 10-inch diameter fixed-impeller centrifugal separator for liquid-solid separation.

The investigation concerned studies to determine the feasibility of such a device as a liquid-solid separator. These studies were to include the effect of various geometric and operative variables on separation efficiency, separation point, and energy loss.

After reviewing previous work on liquid-solid cyclones and conducting a preliminary evaluation of the 10-inch model, equations for

the design of the fixed impeller were developed. Also, a special method of closure, to permit rapid changes in geometry, was designed for the test section. The method incorporated "doughnut" flanges, recessed O-ring gaskets, and tie rods.

Tests were performed in a 5-1/2-inch inside-diameter test section using feed slurries of sand-water and barytes-water containing 10 to 25 per cent solids. The effects of various geometric and operative variables on the 50 per cent separation point and on separation sharpness were investigated. Energy-loss studies were conducted at various underflow diameters, overflow diameters, and water feed rates.

The results of these tests indicated that

1. The impeller as designed operated satisfactorily, and the method of derivation of the design equation should be applicable for deriving equations for other blade contours.

2. The over-all design of the test section with "doughnut" flanges, recessed O-ring gaskets, and tie rods served its purpose excellently. This method of closure should be advantageous in equipment where rapid changes in geometry are desired.

3. For specific geometry and blade angle, an equation was developed for the 50 per cent separation point as follows:

$$\mu = 157 \frac{e^{0.77}}{G^{0.68}} \left[\frac{1.54}{\rho_s - \rho} \right]^{0.5}$$

where μ is the 50 per cent point (microns),

e is the overflow diameter (inches),

G is the feed rate (pounds per second),

ρ_s is the solids density (grams per cubic centimeter), and

ρ is the slurry density in the same units.

It was found that the exponents of this equation did not vary with geometry. Changing geometry was reflected in changes in the K_1 value (157 as shown in the previous equation).

4. For a given flow rate and comparable geometric and operative factors, the fixed-impeller separator produced a higher 50 per cent point than a conventional cyclone. "Sharpness," as defined by Taggart and by efficiencies defined in this work, was approximately the same for the two separators. However, a graphical method presented in this work indicated that the sharpness was less for the fixed-impeller device.

5. Energy-loss equations for the fixed-impeller separator were found to be of the same general form as those for the cyclone. However, an additional variable of underflow diameter is involved. The energy loss was found to be less for the fixed-impeller device. This is exemplified in that the capacity ratio $GPM/F^{0.5}$ was found to vary (at fixed blade angle) as the 0.9 power of the overflow diameter with the underflow diameter as a parameter. The equation expressing this relationship was found to be as follows:

$$\frac{GPM}{F^{0.5}} = K_{CR} e^{0.9}$$

where GPM = feed rate,

F = energy loss,

e = overflow diameter,

$K_{CR} = 9.8 + 6.3\ E^{3.1}$, and

E = underflow diameter.

Within the range investigated, it appears that the fixed-impeller centrifugal separator could be used to extend the separation-point range of the liquid-solid cyclone. However, the following additional work should be undertaken:

1. A study of the ratio of overflow diameter to the section diameter should be conducted. The results of such an investigation would show whether the trend of increased 50 per cent point with increased overflow diameter would continue.

2. The effect of changing blade angle should be investigated in order to determine the relationship of this variable with the 50 per cent point.

3. An investigation of the effect of feed-volume split to the underflow and overflow should be conducted. This should include a consideration of 50 per cent point and separation sharpness.

4. Additional energy-loss studies shoud be performed in order to develop a generalized relationship for energy loss as a function of geometric and operative variables.

5. Based on the results of the present investigation, a larger model should be designed and constructed for use in extending various geometric variables.

The pursuit of the recommendation presented above and the continued development of the fixed-impeller centrifugal separator could lead to its acceptance into the industrial family of separation equipment.

CHAPTER I

INTRODUCTION

In recent years, legal, economic, and technological changes have necessitated a diligent search for a more efficient classification and separation process for certain industries. Among these, the following may be included:

1. Many plants have been forced to operate on lower percentages of make-up material because of economic considerations, shortages, or legal restrictions on waste disposal.

2. Mechanization of mining and processing has greatly increased the amount of refuse in the materials to be processed.

3. The necessity of using lower grade ores has imposed economic restrictions on many operations and has intensified the search for more economically feasible processes to up-grade material.

4. The general increased cost of labor and material in this country has resulted in greater cost for conventional process equipment and necessitated higher physical plant investments.

The development of the liquid-solid cyclone has met the challenge of those changes in many instances, particularly in the field of classification and deslurring of particles below the 200-mesh point (74 microns). In many instances, the cyclone has replaced other separation devices such as drag and spiral classifiers, settling cones, and hydro-separators with their relatively large area requirements per gallon of through-put. (1)

The application of solid-liquid cyclones to many industrial separation processes has been rapid, since it offers many advantages. Among these are: (1) economy in terms of low initial cost and low operating cost, (2) simplicity--it has no moving parts, (3) high capacity per unit of floor space, and (4) sharp separation at fine-particle sizes. (1, 2, 3, 4, 5, 6, 7, 8, 9, 10)

The cyclone (Figure 1) consists of a cylindrical section above a truncated cone. The slurry to be processed enters the cylindrical section through a tangential inlet nozzle. The feed, with the tangential velocity, creates a spiral or vortex of high centrifugal force. Solid particles are forced to the periphery of the conical section and are discharged out of the underflow nozzle located at the apex of the cone. The clarified liquid is discharged through the overflow pipe, which is centered in the cylindrical section at the top of the cyclone. (11) Experimental studies have been conducted concurrently with the applications for the liquid-solid cyclone to determine design and operating factors for increasing its application and usefulness. Several investigators have presented results of detailed studies permitting the accurate design of separators for specific applications. (1, 2, 3, 6, 12, 13, 14, 15, 16) These investigators have also pointed out some of the limitations of the liquid-solid cyclone. Dahlstrom (3) has indicated that one of the problems of the cyclone has been that for certain applications the separation point needed to be raised to a higher micron size. It has also been demonstrated that as the separation point is increased by manipulation of variables, the sharpness of separation decreases for the cyclone.

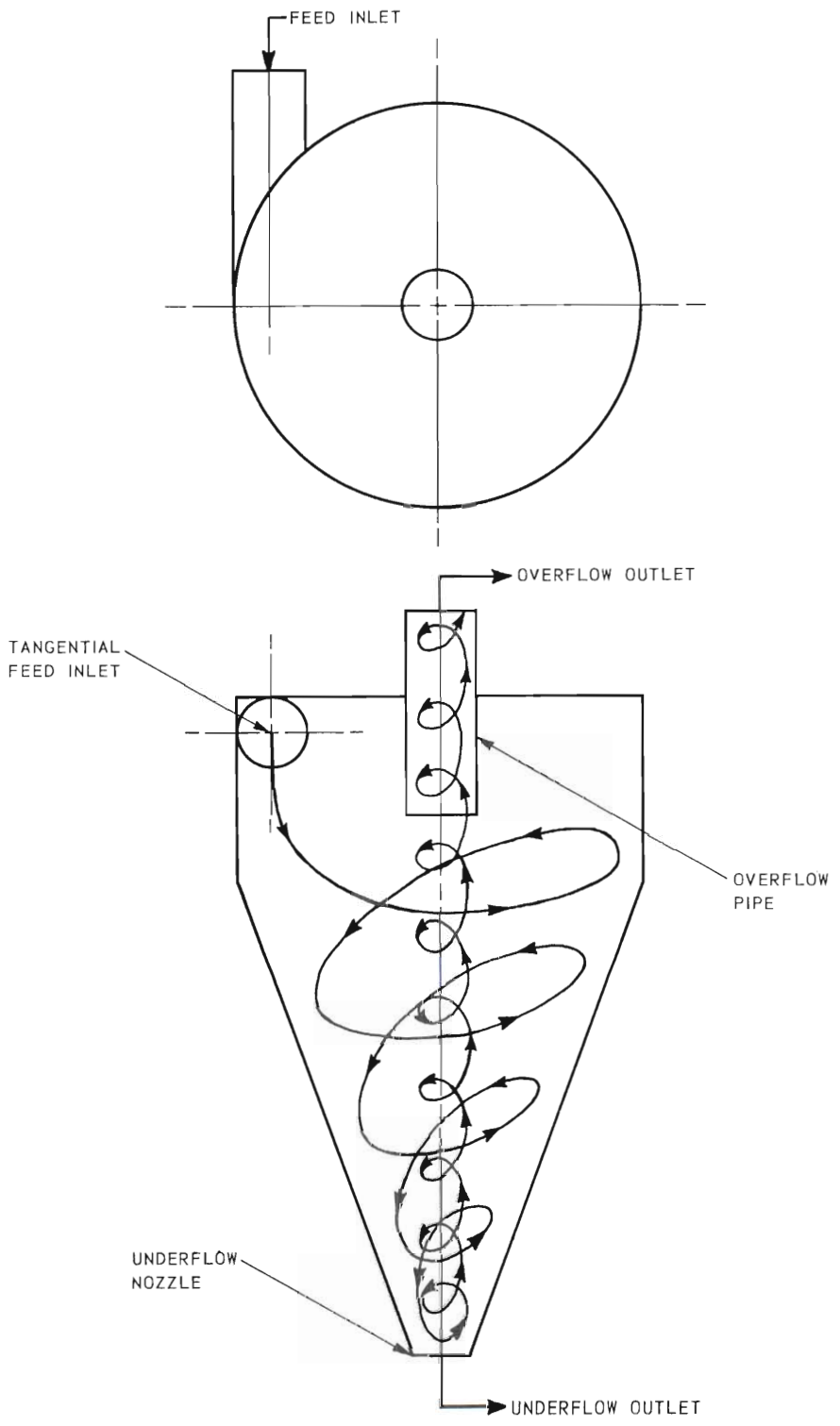

Figure 1. Conventional Liquid-Solid Cyclone.

Because there are many operations in the mining, chemical, and agricultural fields where the separation desired is beyond the range of the cyclone as presently designed, it appeared desirable to develop a device which would extend the range of operation of the cylone. Furthermore, because the cyclone has been very successfully employed in certain industrial applications, it was reasoned that the principles embodied in the cyclone, with its resulting simplicity, would be a good starting point for developing a device to extend its range of sharp separation to large-particle sizes.

With these considerations in mind, Dr. Joseph M. DallaValle and Dr. Joseph J. Moder, Jr., of the Georgia Institute of Technology, advanced the idea for a fixed-impeller centrifugal separator. This separator (Figure 2), as intuitively designed, embodied a fixed impeller, an overflow pipe with bottom discharge concentrically located in the device, and a break or baffle plate. The impeller idea was incorporated as a means for providing the "whirl" velocity necessary for the vortex. It was based on a use of similar fixed blades or veins in gas-solid separators. The overflow pipe with bottom discharge was included in place of the overflow pipe with top discharge used in conventional cyclones. This was done since it appeared that such a design would provide lower energy loss. The break plate was placed in the device to act as a false bottom, which would eliminate irregularities in the flow probably set up by the unsymmetrical bottom design. The fixed impeller was a six-bladed design made of 1/8-inch sheet brass. The straight blades were turned at about 30 degrees from the horizontal. (See Figures 2 and 6.)

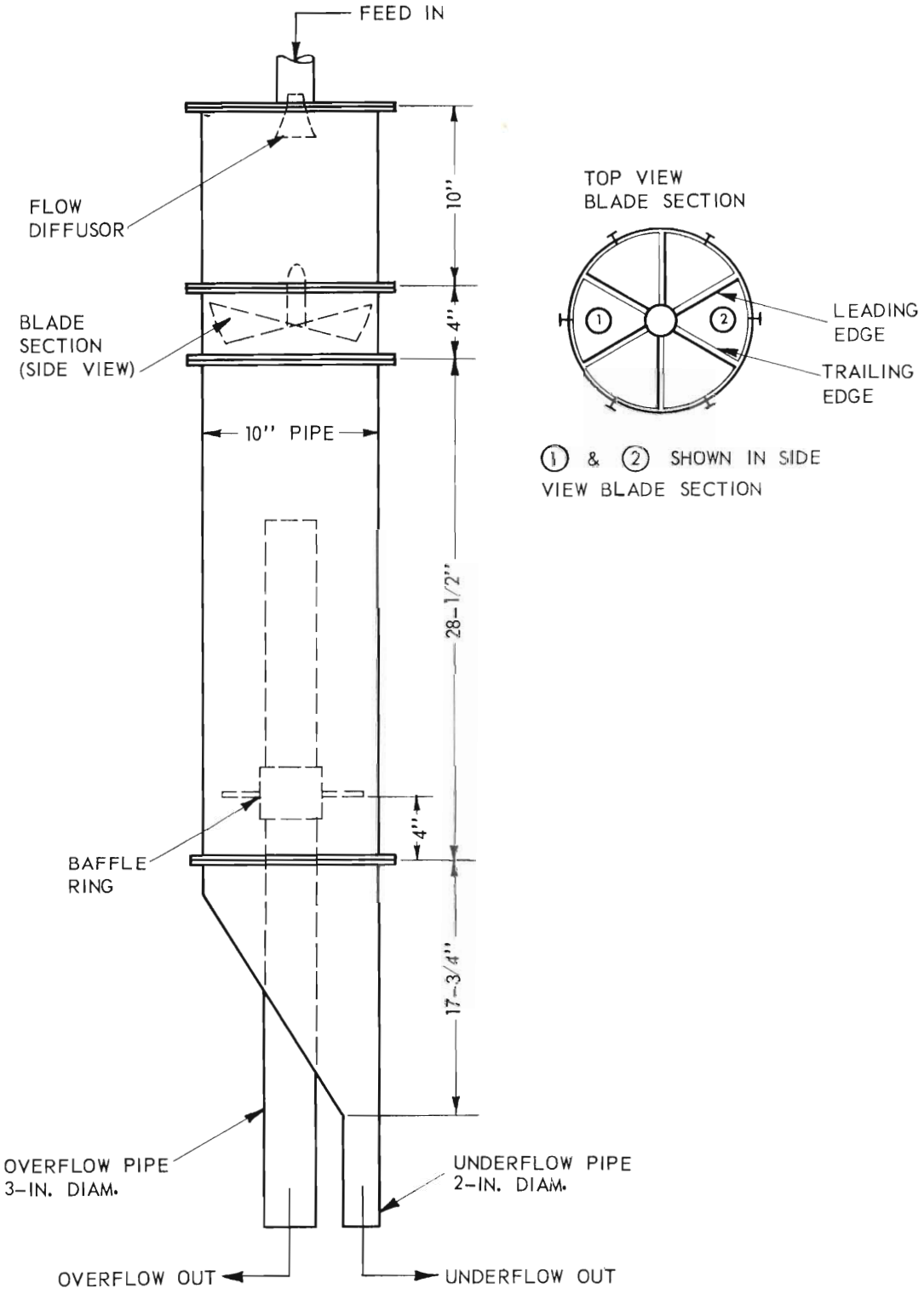

Figure 2. The 10-Inch Fixed-Impeller Separator.

If a slurry of solid and liquid were introduced at the top of the device, it would flow down through the impeller. The mixture would receive a whirl velocity, which would be a function of the initial velocity striking the blades and the blade angle. The resulting whirl would set up a vortex for separation. The overflow with a small amount of solids would discharge out the overflow pipe, and the underflow with high-solids concentration would discharge out the underflow pipe. The lower energy loss (with the overflow pipe discharge out the bottom) and the added variable of impeller design should provide a means for extending the separation range on conventional liquid-solid cyclones.

It was the purpose of this investigation, using this device as a basis, to develop equipment for liquid-solid separation and to indicate its feasibility for separation at larger particle diameters than are obtainable with conventional cyclones. This study included a consideration of the effect of various geometric and operative factors on separation point and separation sharpness as well as a preliminary investigation of energy loss.

The program outlined at the outset of the work included:

1. After a literature search was completed in the general fields of cyclone separation, a preliminary study of the DallaValle-Moder fixed-impeller model would be conducted. Initial evaluation studies should give indicative design data for future work.

2. Based on these preliminary studies and from the literature considerations, a model would be designed for detailed study. The results of such a study should present the necessary information for evaluating this type of a device as a liquid-solid separator.

After reviewing previous work on liquid-solid cyclones, it was concluded that several of the variables involved with the fixed-impeller device should be the same as some of the important variables of the liquid-solid cyclone. This conclusion can be drawn when the similarity between the two devices is considered. (1) Both have a means for producing a whirl velocity with a resulting centrifugal force, which is a principal factor effecting separation. (2) Both devices have overflow pipes concentrically located. (3) Both have a means for eliminating solids through underflow outlets. Also, since both are serving as solid-liquid separation devices, the effect of the physical properties of the systems on classification efficiency should be similar, e.g., concentration of slurries and density of solids. With these observations in mind, it was decided to approach the problem based on Dahlstrom's analysis (3) of the solid-liquid cyclone. He has shown that an equation of the following form is applicable to conventional cyclone operation at and below a feed concentration of 15 per cent solids by weight.

$$\mu = \frac{K(eb)^a}{Q^c}\left[\frac{T}{\rho_s - \rho}\right]^q \qquad (1)$$

where μ = particle size at 50 per cent point (particle size which reports 50 per cent by weight to underflow and overflow) (microns),

e = overflow diameter (inches),

b = inlet diameter (inches),

Q = flow rate (gallons per minute),

K = proportionality constant,

ρ_s = specific gravity of solid (grams per cubic centimeter),

ρ = specific gravity of slurry (grams per cubic centimeter), and

T, q, a, and c = constants.

It should be noted that classification efficiency, according to Dahlstrom, is a function of centrifugal force (represented by e, b, and Q in the equation) and specific gravity of particle and slurry. Thus, if e, b, and the physical properties of the systems are fixed, classification efficiency varies inversely with the flow rate raised to the proper power. A similar equation could be assumed for the fixed-impeller device; however, a different term corresponding to the inlet-nozzle diameter would have to be included. One approach that could be used to arrive at this is: Take a section of the fixed impeller, i.e., two blades with an entrance velocity at the blade equal to V_1, entrance area equal to A_1, discharge area equal to A_2, and discharge velocity equal to V_2.

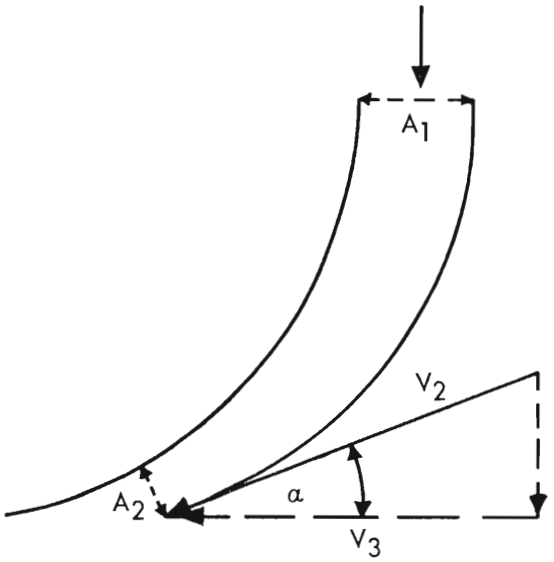

By continuity,

$$V_2 = \frac{V_1 A_1}{A_2} . \quad (2)$$

Then, whirl velocity = V_3

$$V_3 = V_1 \frac{A_1}{A_2} \cos \alpha . \quad (3)$$

Thus, the whirl velocity, V_3, could be calculated as a function of blade angle

and entrance velocity. Because it is convenient to represent the effect that the overflow nozzle has on centrifugal force in terms of diameter, it would perhaps be desirable to express V_3 as some equivalent round pipe diameter, D_R, or

$$V_3 = \frac{4Q}{\pi D_R^2} \tag{4}$$

where Q = volumetric flow rate and

D_R = equivalent round pipe diameter to give a velocity V_3 for a flow rate Q.

Then,

$$D_R = \left(\frac{4Q}{\pi V_3}\right)^{0.5} = \left[\frac{4Q}{\pi V_1 \left(\frac{A_1}{A_2}\right) \cos \alpha}\right]^{0.5}, \tag{5}$$

or, by continuity,

$$D_R = \left(\frac{4A_2}{\pi \cos \alpha}\right)^{0.5} = b. \tag{6}$$

Then, the assumed equation for the fixed-impeller device becomes

$$\mu = \frac{K(eb)^a}{(Q)^c} \left[\frac{T}{\rho_s - \rho}\right]^q \tag{7}$$

$$\mu = \frac{K_1 \left[e\left(\frac{A_2}{\cos \alpha}\right)^{0.5}\right]^a}{(Q)^c} \left[\frac{T}{\rho_s - \rho}\right]^q. \tag{8}$$

This indicates that if the blade angle, the other geometric variables, and the physical properties and operating conditions of the system were fixed, an investigation of the overflow diameter as a function of flow rate should characterize a, c, and K_1. Also, by investigating different physical systems of solid and slurry density, T and q should be evaluated. A plot of μ versus $[e(A_2/\cos\alpha)^{0.5}]^a/Q^c$ with log-log coordinates should yield a straight line for a given geometry and set of operating conditions. As the geometry and operating conditions of the system are varied, K_1 should change but a and c should remain constant. In order to determine variations in the value of K_1 for a given impeller, it would be necessary to consider various geometric and operating variables. Intuitively, one would expect the following to have significance: (See Figure 2.) (1) the diameter of the test section, (2) the diameter of the break plate, (3) the position of the break plate with reference to the top of the overflow pipe, (4) the length of the section between the impeller and the bottom section, (5) the distance between the top of the overflow pipe and the impeller, (6) the concentration of solids in the feed, and (7) the concentration of solids in the underflow, which is also related to the volume split between overflow and underflow.

Since in a vortex, centrifugal force has been shown to be proportional to the square of the velocity divided by the radius of curvature, the diameter of the device should have an effect on operation. However, investigators (11, 17) have shown that diameter has a negligible effect on classification size and energy requirements (2, 3, 6) of the cyclone. An empirical rule has been advanced based on the experiences of one writer, which apparently is adequate for industrial application (18). It is:

> To obtain the sharpest classification at the minimum particle size for a certain pair of inlet and overflow diameter, the latter should cover a definite portion of the cyclone diameter. Generally speaking, twice the feed diameter plus its overflow diameter divided by the cyclone diameter should range from 0.4 to 0.65".

In view of the similarity between the cyclone and the fixed-impeller device, it may be assumed that the effect of diameter on classification and energy requirements is probably not significant for the fixed-impeller separator.

Criner (11) has shown that in a vortex, particles are moved toward the core by a radial velocity V_r but are retarded by the centrifugal acceleration V_t^2/r, where V_t is equal to tangential velocity and r is equal to the radius. A particle of a specific size being acted upon by V_r and V_t^2/r would find a radius at which the velocity of settling equaled V_r.

The circle formed by this radius is referred to as the equilibrium radius. Particles of other sizes would find other radii--larger particles nearer the periphery and smaller particles nearer the core.

This mechanism would provide a series of concentric strata of particles, each stratum containing a range of particle sizes. Thus, it would appear that the diameter of the break plate would affect separation, since it would select which stratum to pass to the underflow and which to turn upward toward the overflow outlet.

Since the source of the fluid is at the periphery of the vortex, there must be a radial velocity, V_r, imposed upon the vortex motion. The radial flow carries energy to the inner area of the vortex to replace that dissipated through turbulence. This energy thus transported is used to maintain the strength of the vortex. Criner (11) has shown

that V_r can be considered independent of axial position in a vortex. Therefore, it would seem that the radial flow along the axis would be constant per unit area, and the total flow to the core would be proportional to the length of the vortex along the axis. Consequently, the distance between the impeller and the top of the overflow pipe and the length of the section between the impeller and the bottom plate should affect the separation characteristics of the device.

The discussions above are concerned with the primary or main vortex of the system, which is the primary factor in the operation of the system when the break plate is at the same level as the top of the overflow pipe. When the break plate is moved a finite distance below the overflow outlet, a secondary vortex is created which would initiate around the outside of the overflow pipe. This vortex should turn in the same direction as the main vortex, but its vertical velocity component is turned in the upward direction or opposite to that of the main vortex. All other factors being fixed, the classification size should vary inversely as some function of the distance between the break plate and the overflow outlet. That is, as the distance is increased, the size of separation of the particles should decrease. This would appear reasonable when it is considered that the secondary vortex would provide a second chance for particles to be exposed to a centrifugal separation force.

The concentration of the solids in the feed should affect the separation point because if high enough concentration is used, hindered settling effects due to crowding of the particles should be evidenced. However, investigations (2, 3, 6) have been reported which show that

hindered settling effects are negligible at or above a feed-volume ratio of eight parts of liquid to one part of solid. Since no quantitative expressions are known to be available, the effect of feed concentration on separation size should be investigated for the fixed-impeller device.

Dahlstrom (3) has investigated the effect of concentration of solids in the underflow in a 9-inch cyclone. He reported that the separation point was decreased slightly with an increased volume to the underflow. This could have a greater effect on separation, since liquid with its accompanying fine solids would be taken from the overflow and discharged in the underflow. Conversely, the minor effect appears feasible when it is considered that no greater centrifugal force should occur with higher volume splits to the underflow. In the fixed-impeller device, the presence of the break plate could considerably modify the general situation found in a cyclone. As the volume split is increased to the underflow at a specified rate, the volume of material turned from the primary vortex toward the overflow outlet could be decreased.

The energy requirements for the cyclone have been reported (3) as

$$\frac{GPM}{F} = K'(eb)^{0.9} \qquad (9)$$

where F = energy loss (feet of fluid),

GPM = flow rate (gallons per minute),

e = overflow diameter (inches),

b = inlet diameter (inches), and

K' = constant.

Feed solid concentrates (0 to 14 per cent), percentage of feed slurry reporting to the underflow (0 to 30 per cent), and cyclone diameter (3 to 14 inches) were found to have a negligible effect on K'. The constant K' increased with length of cylindrical section and increased with decreasing included angle of the conical section.

Because the energy requirement for the secondary vortex should be less in the fixed impeller than in the cyclone, the fixed-impeller device should operate at lower pressure drops than a conventional cyclone. This seems evident after considering that the secondary vortex within a cyclone extends almost the entire length of the device. Within the fixed-impeller device, the secondary vortex length is a function of the position of the break plate and, by design, could always be less than the length of the secondary vortex of the conventional cyclone.

The equation as assumed earlier should define the classification point and the following relationship should define the sharpness of separation.

$$\text{Percentage of coarse-particle separation} = \left[\frac{W_v}{W_c}\right] 100 \qquad (10)$$

and

$$\text{percentage of fine-particle separation} = \left[\frac{W_o}{W_F}\right] 100 \qquad (11)$$

where W_v = weight of solids greater than the 50 per cent separation point in the underflow

W_c = weight of solids greater than the 50 per cent separation point in the feed,

W_o = weight of solids less than the 50 per cent point in the overflow, and

W_F = weight of solids less than the 50 per cent point in the feed.

Thus, if equations of the type assumed were true, it should be possible to define the separation point and the sharpness of separation.

The Dahlstrom equation (3) for (4- to 14-inch cyclones) separation is:

$$\mu = 81 \frac{(eb)^{0.68}}{(GPM)^{0.53}} \left[\frac{1.73}{\rho_s - \rho}\right]^{0.5} \tag{12}$$

where μ = 50 per cent separation (microns),

e = overflow diameter (inches),

b = inlet diameter (inches),

GPM = flow rate (gallons per minute),

ρ_s = specific gravity of solid (grams per cubic centimeter), and

ρ = specific gravity of slurry (grams per cubic centimeter).

For assumed equation for the fixed-impeller device, it would be expected that the exponents e, b, GPM, and the constant K_1 would be different from those on the Dahlstrom equation above. Since the flow pattern has been modified in such a way as to reduce the height of the secondary vortex appreciably, one would expect that for a given flow rate, the centrifugal force would be applied for a shorter period of time. This would result in an increased 50 per cent separation point and would probably be evidenced by a raising of the exponent on e and b. Because the geometry of the device is different from the cyclone, the K_1 value should be different; it would probably increase.

CHAPTER II

EQUIPMENT

Preliminary tests.--Since the 10-inch fixed-impeller device was available, preliminary separation tests were conducted to obtain indicative design information before proceeding with model design. A discussion of these investigations is included in the Appendix.

Design of test section.--In view of the size and the rigid construction of the 10-inch DallaValle-Moder device, it was decided to construct a smaller, more flexible model for detailed study. In order to facilitate construction and provide the desired flexibility, it was decided to use a 5-1/2-inch inside diameter as the design diameter for the test section. This permitted the use of 6-inch plastic and steel tubing with a 0.25-inch wall thickness. Because geometric variables were to be studied, the test section was designed using "doughnut" flanges with recessed O-ring gaskets. The sections of the tubing would then be held in place between two flanges by four 0.25-inch tie rods; sections above and below would be held in place similarly. The details of the flanges and method of closure are illustrated in Figure 3. This arrangement permits rapid change in length of test section or change from plastic to steel by manipulation of tie rods.

Bottom plate and discharge assembly.--Since the overflow diameter would have to be varied over a convenient range, a bottom plate was designed to provide the necessary flexibility. The assembly is shown in Figure 4. A recessed groove was provided in the plate for an O-ring gasket.

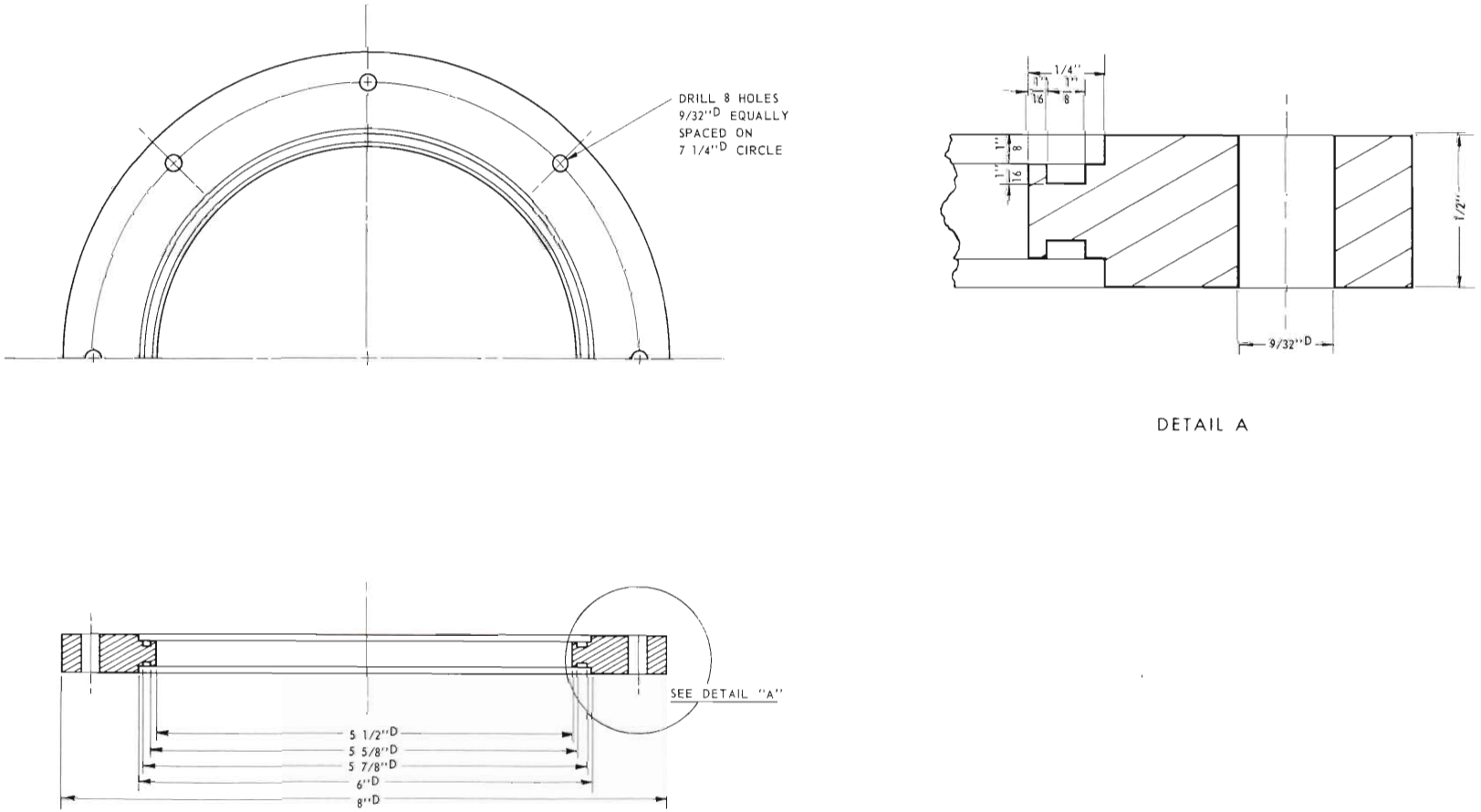

Figure 3. Test-Section Flange Detail.

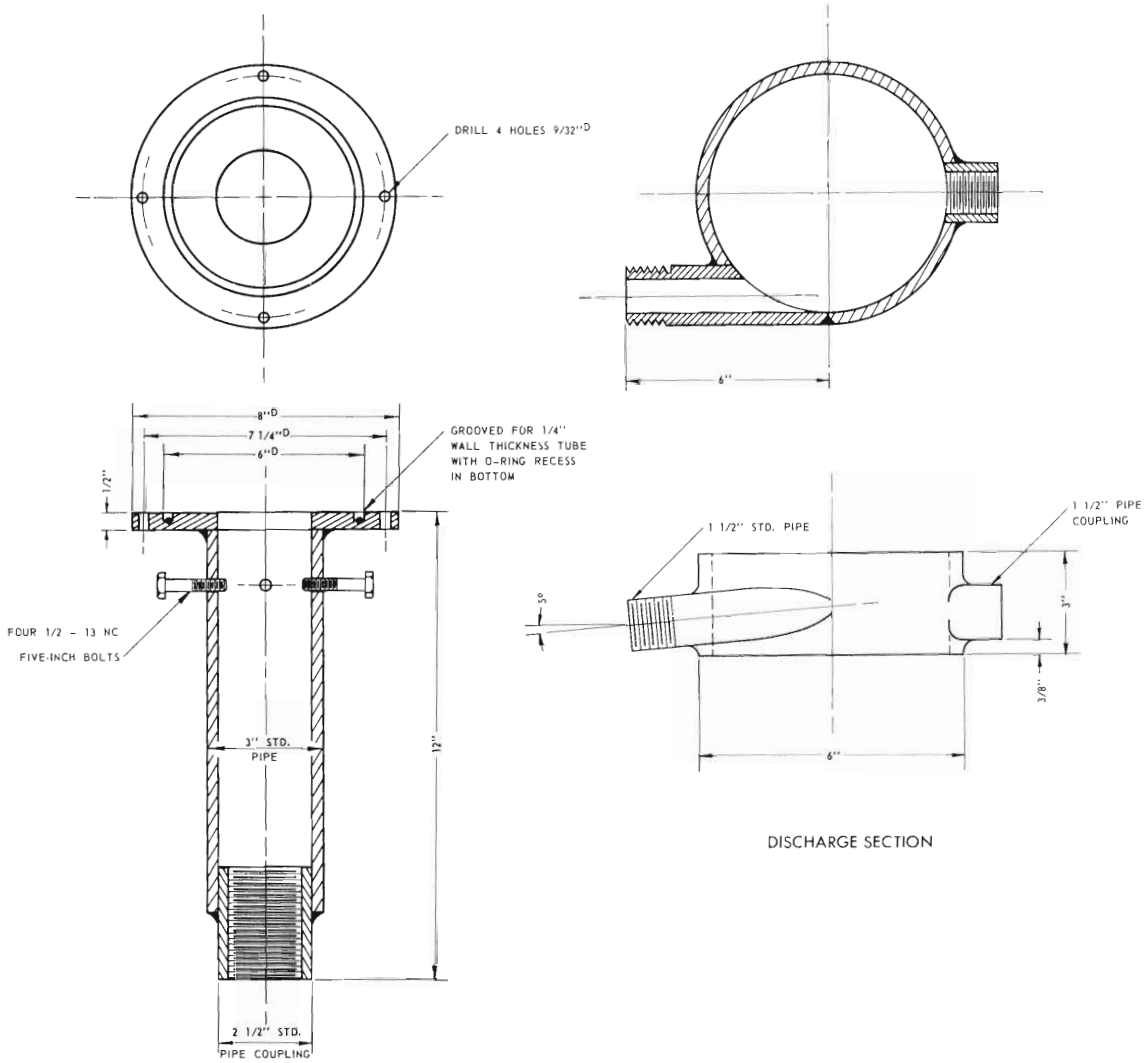

Figure 4. Test-Section Discharge Assembly.

This provided the closure between the plate and the tubing of the underflow discharge section. By using standard pipe bushings, the various overflow pipes could be screwed into the bottom plate assembly and centered by means of the four centering screws. The underflow discharge section was provided with a tangential and perpendicular outlet for comparison studies. This discharge assembly not only provided flexibility but eliminated the irregularities present in the bottom of the 10-inch model.

Break-plate assembly.--Since it appeared desirable to investigate break-plate diameter and position, the break-plate assembly shown in Figure 5 was designed for each diameter overflow pipe. Thus, the ring diameter could be varied for each overflow-pipe diameter, if desired. Also, the assembly could be moved up or down the overflow pipe and secured at the desired elevation by set screws.

Impeller design and construction.--After the preliminary investigation with the DallaValle-Moder 10-inch device (Figure 6) was completed, it was concluded that any new models should involve a major modification in impeller design. As the first step toward such a modification, it seemed desirable to determine why the impeller had not performed adequately. If one of the blades from this model is considered as an inclined plane with a jet of liquid impinging on it with a velocity V_1,

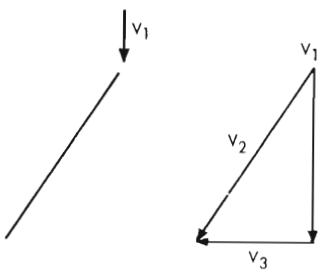

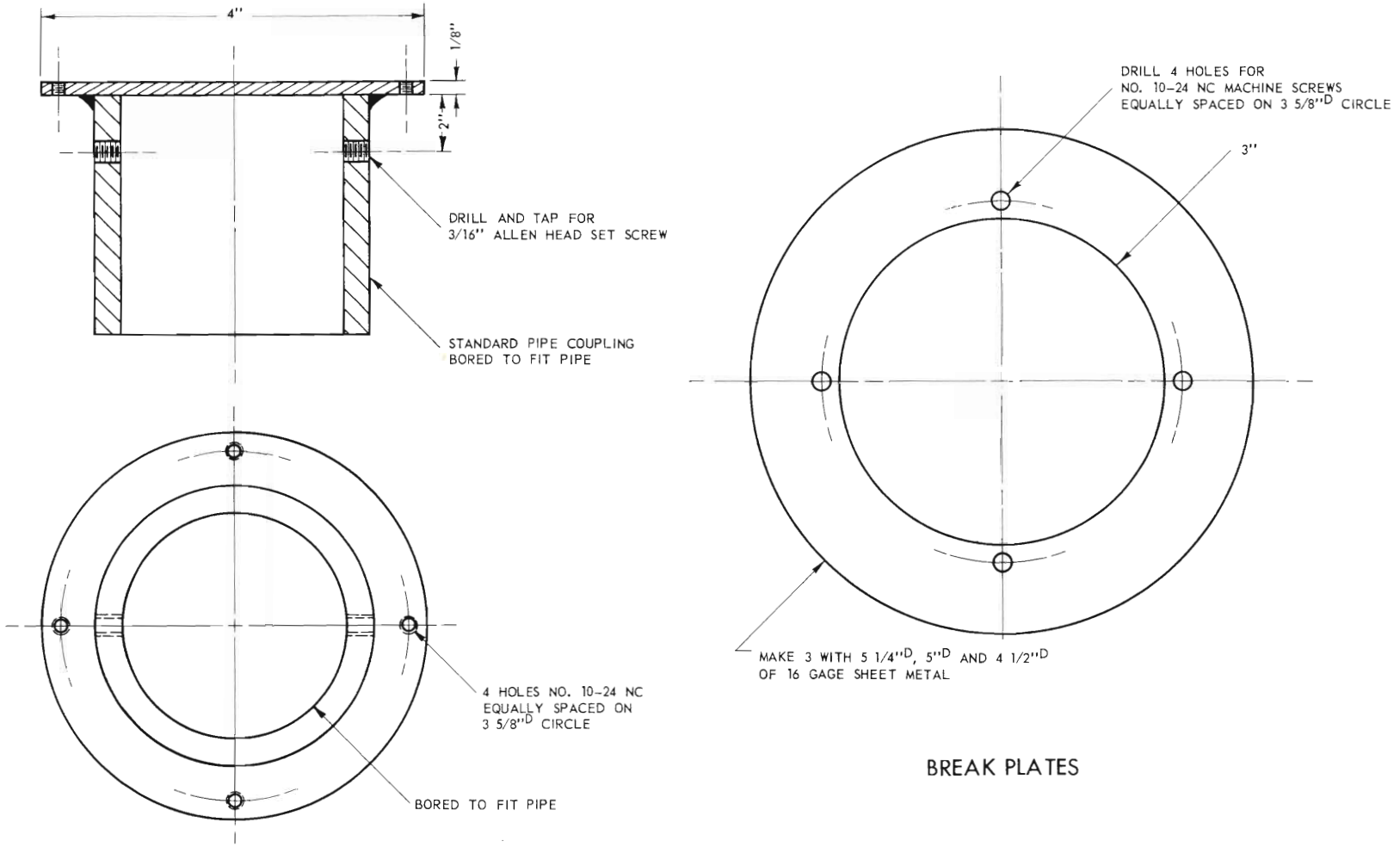

Figure 5. Break-Plate Assembly.

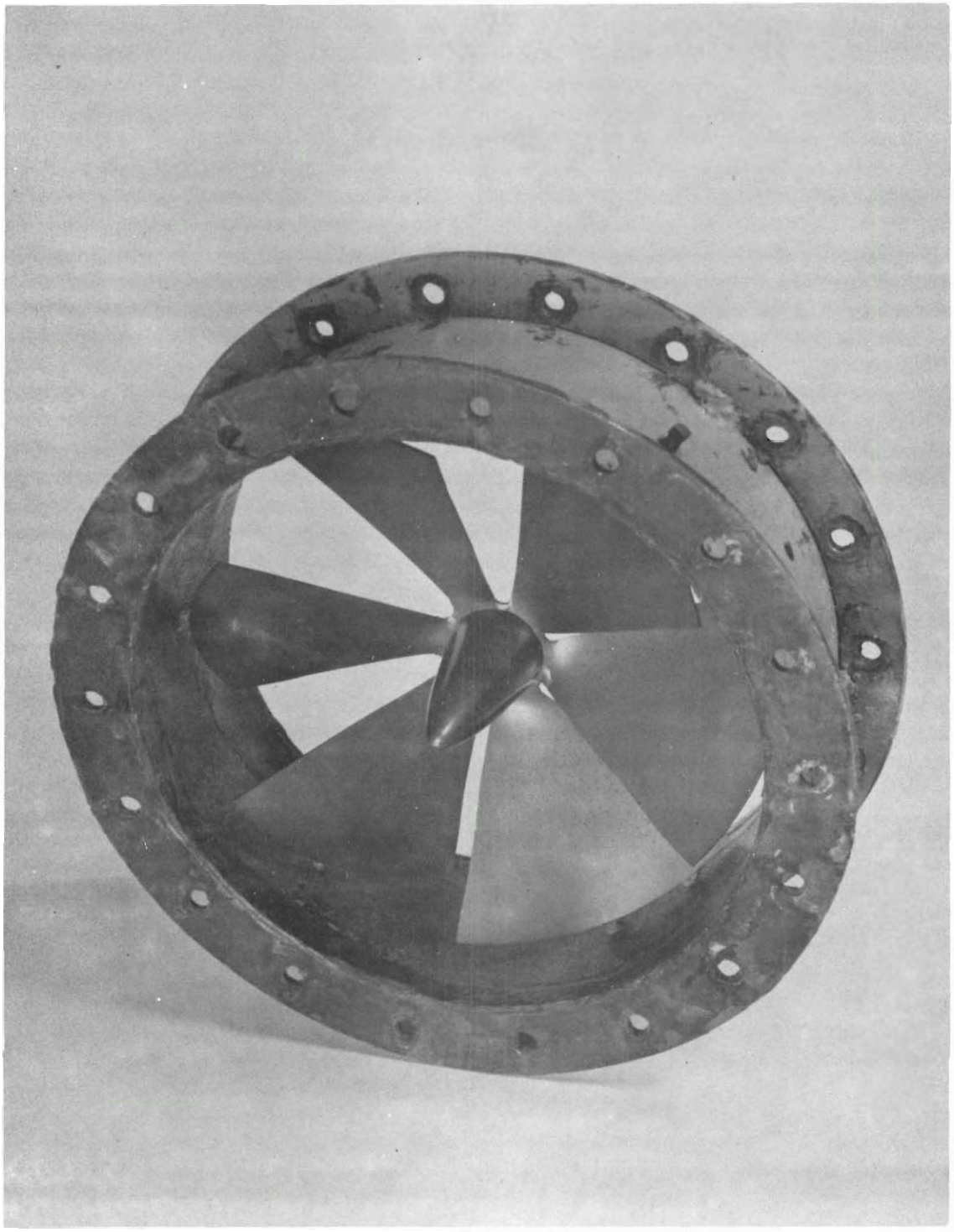

Figure 6. The 10-Inch Fixed Impeller.

the whirl velocity (V_3) is immediately generated at the leading edge of the blade. This should result in turbulent conditions at the leading edge and along the plate. Also, the jet would be separated by the leading edge of the plate and, because of its characteristic shape, separation of the liquid or cavitation should occur. These conditions could produce unstable flow downstream of the impeller which would affect the vortex. From Figure 7 it is apparent that between the blades of the impeller, from the periphery to the hub, free-flow area occurred, that is, area through which liquid could flow relatively unaffected by the impeller. This, of course, would result in unstable flow conditions and would permit direct short-circuiting to the overflow pipe. (See Figure 2.) Another limitation of this impeller is the fact that there is no appreciable increase in velocity of the fluid along the axis of the tube. An impeller contained in an annulus would increase the velocity and result in a higher whirl velocity for a given flow rate and blade angle. Thus, it seemed necessary to design a blade which would gradually accelerate the liquid and eliminate any free-flow area, particularly near the center of the section; however, design would have to be simple enough to be constructed economically. With these conditions in mind, it was decided that perhaps the simplest shape would be that of an arc of a circle contained in an annulus. This shape would produce a gradual whirl acceleration of the liquid, would be relatively simple to layout, and would be relatively simple to build. It would also permit the elimination of free-flow area, and, because of the annular construction would give a higher whirl velocity; it should also eliminate short-circuiting. Since final design for hydraulic impellers necessitates an

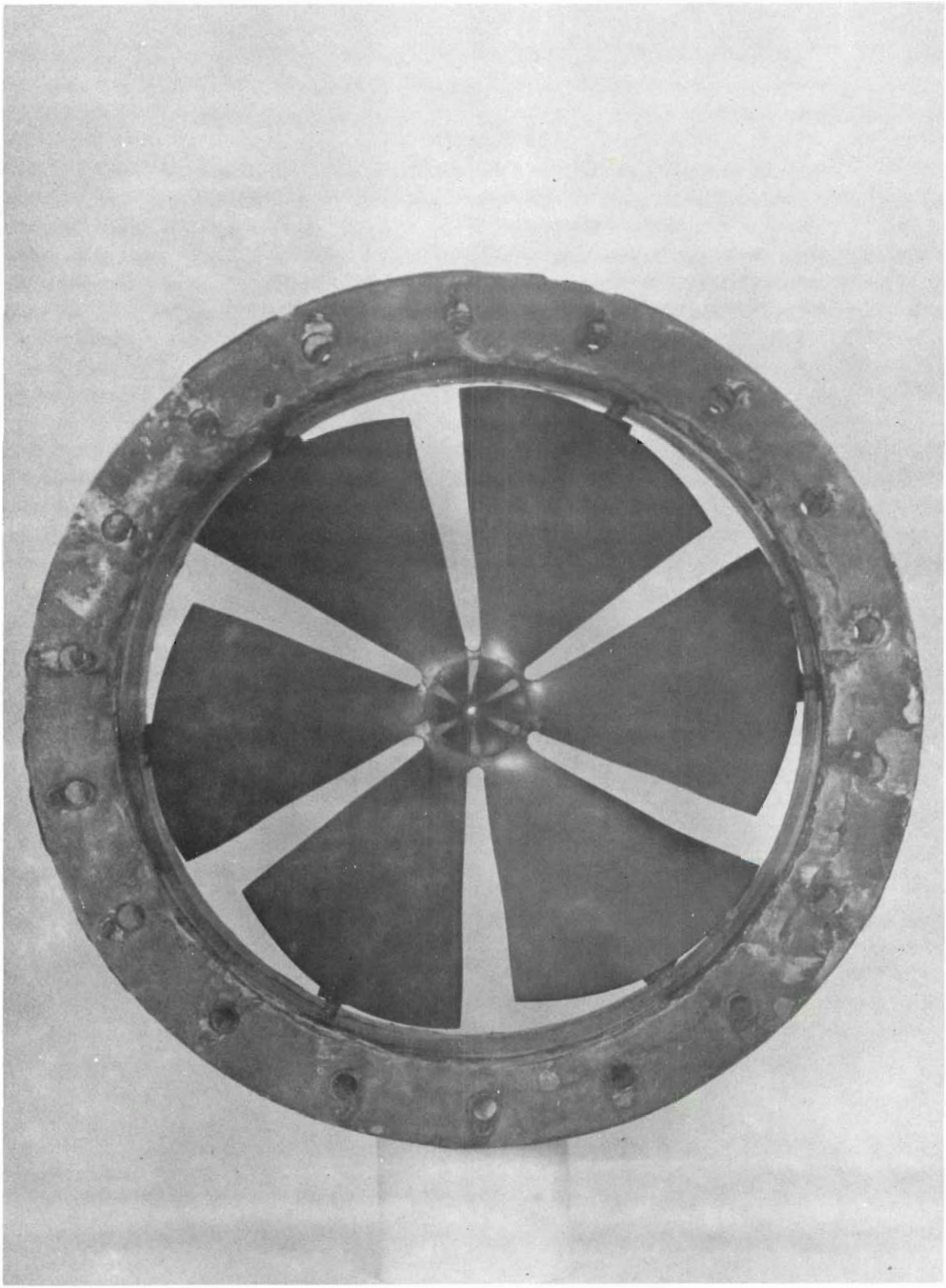

Figure 7. The 10-Inch Fixed Impeller--Top View.

empirical approach, it was decided to design, to construct, and to test an impeller using blades based on the arc of a circle. Modifications could then be made in blade design, if necessary.

The essentials of blade construction may be separated into four parts [See Figure 8(a)]:

1. the trailing edge angle,
2. the blade length,
3. the distribution of curvature between leading and trailing edges, and
4. the blade thickness.

Since the arc of a circle has been chosen for the shape of the blade, the distribution of curvature has been fixed. However, consideration must be given to the other essentials of blade construction. In order to develop relationships for the length of the blade and the trailing edge angle, assume that a fixed vane is contained in a tube of radius r. [See Figure 8(b).] A fluid flows in the tube with an approach velocity u, and the vane adds a tangential or whirl velocity V_3 to the original velocity u. It is desired to produce a flow downstream of the vane such that the pressure graduation in the radial direction within the fluid exactly balances the centrifugal force caused by the whirl. This would give a stable rotational flow without secondary flows with the exception of the wake flow produced by the central body or hub. In two dimensions, this flow has been investigated and is known as vortex flow (19). It is characterized by the formula

$$V = \Gamma/2\pi r \qquad (13)$$

where Γ is a constant for any one flow and is known as the circulation.

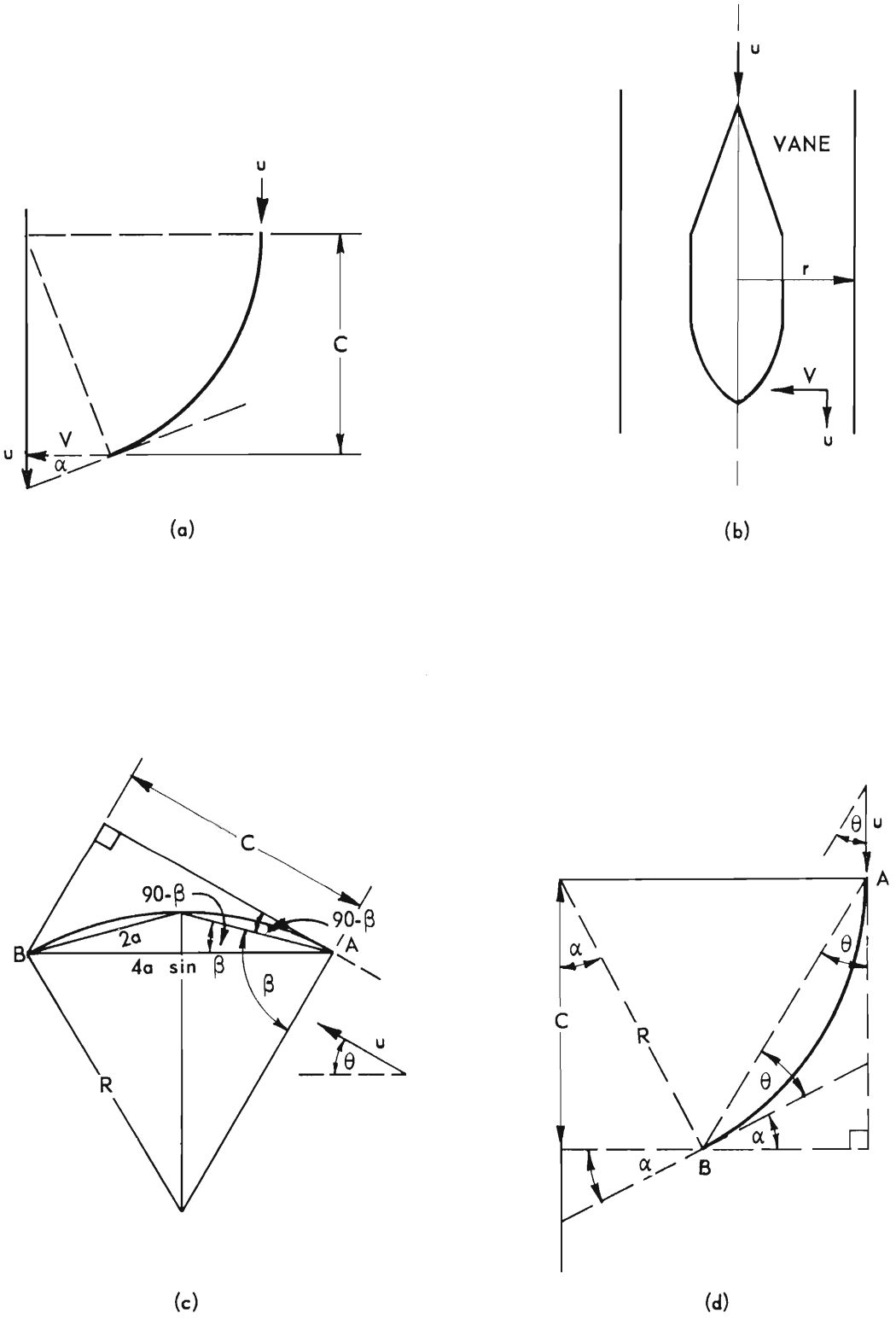

Figure 8. Sketches in Design Development.

The whirl velocity must be very high in order to produce separation. The approach velocity u adds very little to the total resultant velocity, and the vortex velocity distribution would produce the balance between pressure gradient force and the centrifugal force.

From Figure 8(a) it can be seen that

$$\tan \alpha = \frac{u}{V} \text{ or } \alpha = \tan^{-1} \frac{u}{v}. \qquad (14)$$

The tangential velocity V can be obtained from equation 13. The circulation Γ is a constant which depends on the magnitude or strength of the vortex. The value of Γ for any particular installation will depend upon the force required for separation. The approach velocity u will depend upon the inner body design and entrance effects in the tube. This velocity is a function of radius r and equation 14 becomes

$$\alpha = \tan^{-1}(2\pi ru/\Gamma). \qquad (15)$$

Equations 13 and 15 should break down at r = 0. The vortex as it actually exists takes care of this fact by having an air core at its center. Behind any central body, there is an unstable wake region having a width of the order of magnitude of the body diameter. The wake and the vortex core can be considered to coincide. Calculation from equation 15 and subsequent equation for the blade length must then be made over values of radius from the radius of the central body to the internal radius of the tube carrying the flow.

The size of the vanes may be determined by a consideration of the forces acting on the vanes. The mass of fluid per second entering and

annulus of width dr and radius r is $2\rho\pi ru \cdot dr$, where ρ is the density of the fluid and u is as previously defined. The torque dT needed to import a tangential velocity V to the mass flow $2\pi\rho ru \cdot dr$ may be calculated from

$$dT = \frac{d(\text{angular momemtum})}{dt} = \frac{d(MrV)}{dt} , \tag{16}$$

where M = mass,

r = radius,

V = velocity, and

t = time.

$$dT = r \cdot dF_1 \tag{17}$$

where dF_1 is the force acting on an annulus of width dr. Equating equations 16 and 17

$$dF_1 = 2\pi\rho ruV \cdot dr. \tag{18}$$

If there are N blades in the fluid turning system, the force dF acting on an infinitesimal area $C \cdot dr$, where C = blade length, is

$$dF = \frac{2\pi}{N} \rho ruV \cdot dr. \tag{19}$$

Streeter (19) has shown that for a circular arc [See Figure 8(c).]

$$L = 4\pi a u^2 \rho \cos(\theta + \beta) \tag{20}$$

where L = lift force (pounds),

ρ = density (lb. $sec.^2/ft.^4$),

$a = R \cos \beta$ when R = arc radius,

θ = approach angle as measured from the chord of the arc, and

β = angle formed by lines R and 2A.

By construction, it can be seen that

$$C = \cos \theta \, (4a \sin \beta) \tag{21}$$

$$a = \frac{C}{4 \cos \theta \sin \beta} \tag{22}$$

$$L = 4\pi\rho u^2 \frac{\cos(\theta + \beta)}{4 \cos \theta \sin \beta}$$

$$L = C\pi\rho u^2 \frac{\cos(\theta + \beta)}{\cos \theta \sin \beta} \tag{23}$$

if u is taken perpendicular to R at point A, then

$$\theta = (90° - \beta) + (90° - \beta)$$

$$\theta = 180° - 2\beta$$

$$\beta = 90° - \frac{\theta}{2} \tag{24}$$

$$L = C\pi\rho u^2 \frac{\cos\left(90° + \frac{\theta}{2}\right)}{\cos \theta \sin\left(90° - \frac{\theta}{2}\right)} . \tag{25}$$

Now θ can be shown to be[See Figure 8(d).]

$$\theta = \frac{90° - \alpha}{2} . \tag{26}$$

Then,

$$L = C\pi\rho u^2 \frac{\cos\left(90° + \frac{90° - \alpha}{4}\right)}{\cos\left(\frac{90° - \alpha}{2}\right) \sin\left(90° - \frac{90° - \alpha}{4}\right)} .$$

The force equation for an infinitesimal area C·dr then becomes

$$dF = \frac{2\pi}{N} \rho r u V dr = C\pi\rho u^2 \frac{\cos\left(90° + \frac{90° - \alpha}{4}\right) dr}{\cos\left(\frac{90° - \alpha}{2}\right) \sin\left(90° - \frac{90° - \alpha}{4}\right)}. \quad (27)$$

Solving for C, the blade length

$$C = \frac{2rV \cos\left(\frac{90° - \alpha}{2}\right) \sin\left(90° - \frac{90° - \alpha}{4}\right)}{Nu \cos\left(90° + \frac{90° - \alpha}{4}\right)}. \quad (28)$$

If V is the velocity needed to produce stable flow downstream of the vanes as given by equation 13,

$$C = \frac{\Gamma \cos\left(\frac{90° - \alpha}{2}\right) \sin\left(90° - \frac{90° - \alpha}{4}\right)}{N\pi u \cos\left(90° + \frac{90° - \alpha}{4}\right)}. \quad (29)$$

Thus, the blade length is a function of the number of blades, the approach velocity, the amount of whirl, and the leading edge angle α. Referring again to Figure 8(d), it is evident that

$$\cos \alpha = \frac{C}{R} \text{ or } R = \frac{C}{\cos \alpha} \quad (30)$$

where R = radius of curvature of the arc and

C = blade length.

Now, it is necessary to consider the thickness of the blade. From equation 19,

$$dF = \frac{2\pi}{N} \rho r u V \cdot dr.$$

Since for a given set of conditions $\frac{2\pi}{N} \rho u V$ = constant,

$$F = \frac{2\pi}{N} \rho u V \frac{r^2}{2} \Bigg|_{r_1}^{r_2} . \tag{31}$$

In order to maintain flexibility, it was decided to pin the blades to the hub and to the wall of the outside tube.

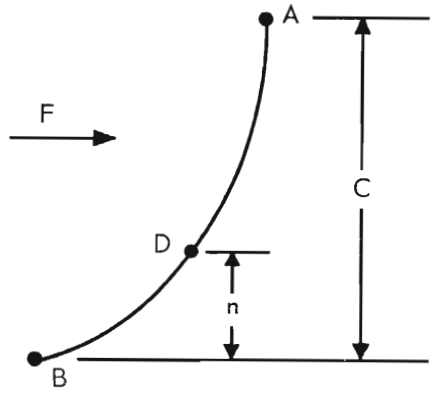

Referring to the sketch, it is evident that the force on the segment DB is

$$F_{DB} = F \frac{n}{C} \tag{32}$$

From mechanics, it can be shown that (20)

$$Y = \frac{Wn^3}{8\,EI} \tag{33}$$

where Y = maximum deflection (inches),

W = load on cantilever (inches),

E = modulus of elasticity (pounds per square inch),

n = length of cantilever (inches),

I = moment of inertia = $\frac{bd^3}{12}$,

b = width of beam (inches),

d = thickness of beam (inches),

then,

$$Y = \frac{12\ Wn^3}{8\ Ebd^3} = \frac{1.5\ Wn^3}{Ebd^3} . \qquad (34)$$

Thus, design relationships have been developed for considering

1. the trailing edge angle,
2. the blade length C and the radius of curvature of the blade R, and
3. the thickness of the blade d.

Using these relationships, the impeller calculations were performed and are included in the Appendix. The results of these calculations indicate that for a flow rate of 150 gallons per minute with an average tangential velocity equal to 29.7 feet per second:

$R = 0.34$ feet,

$C = 0.33$ feet,

$d = 0.125$ inch, and

$\alpha = 8$ degrees 32 minutes.

Figure 9 presents the layout used for the blades. The blade blanks were cut and drilled from 0.125-inch steel plate according to template B and were hot-formed on the jig shown in Figure 10. The jig was cast from steel using a pattern of the same characteristic shape, and the pattern was made by using template A which gave the necessary curvature. The blades formed on the jig were tapered and mounted on

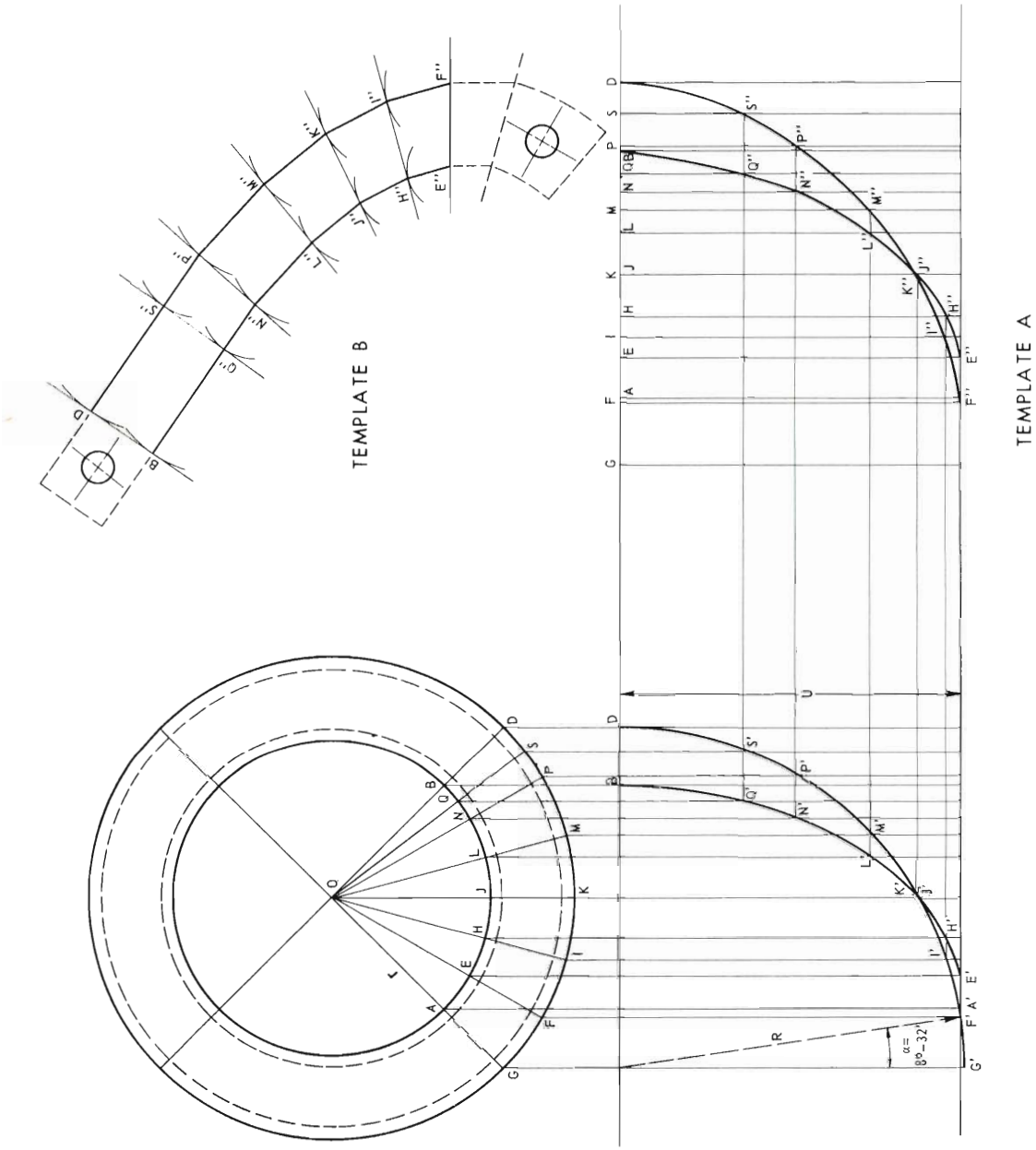

Figure 9. Layout of Impeller Blades.

Figure 10. Blade Forming Jig.

the core, and the core was extended with an upstream and downstream cone to reduce turbulence. The impeller was held within the tubing section by means of eight rolled pins (0.625 inch in diamter and 0.5 inch in length). The pins were placed in holes drilled through the outside tubing into the edge of the blades. The completed impeller is shown in Figure 11.

An assembly drawing without the detail of the impeller design is shown in Figure 12.

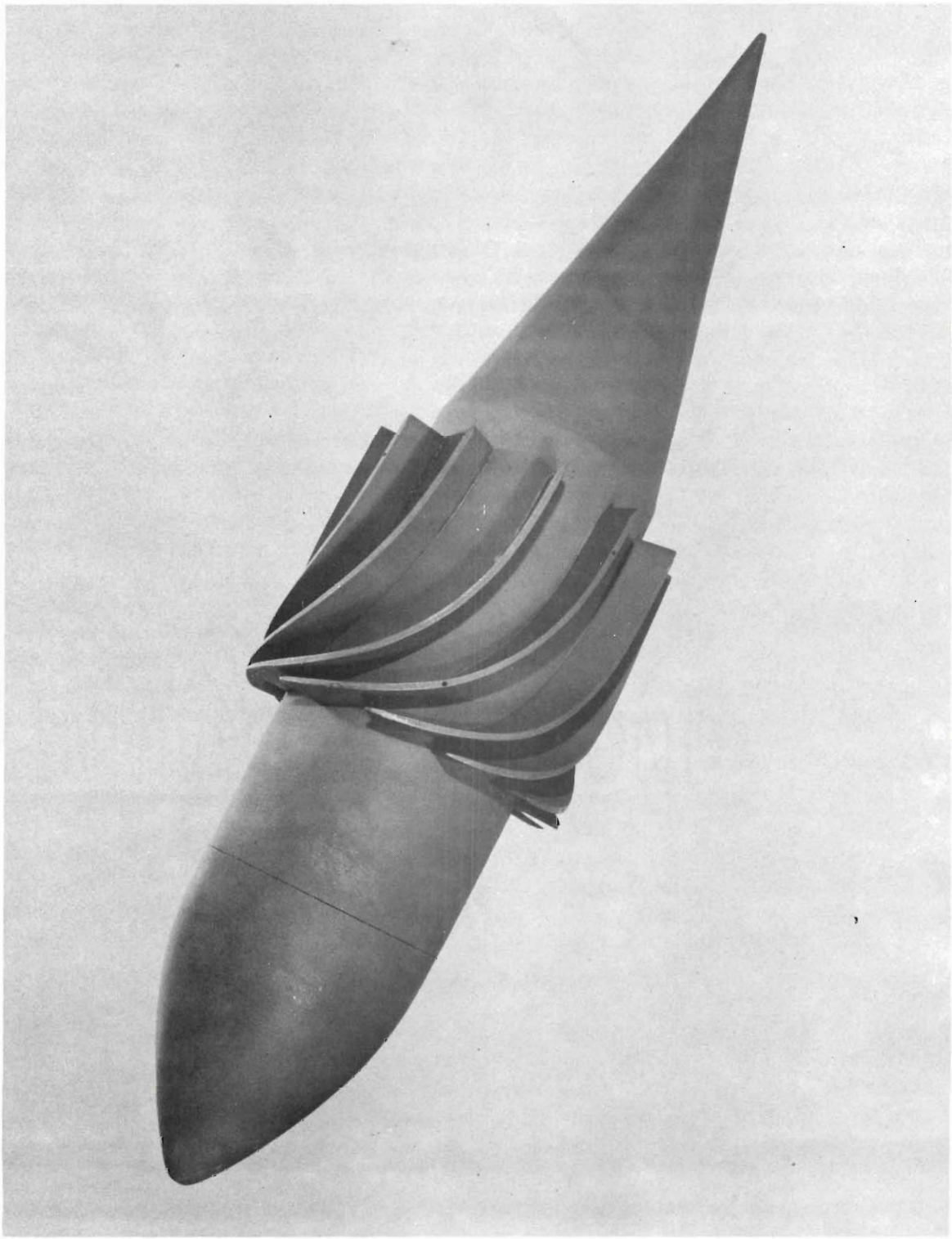

Figure 11. The 5-1/2-Inch Fixed Impeller.

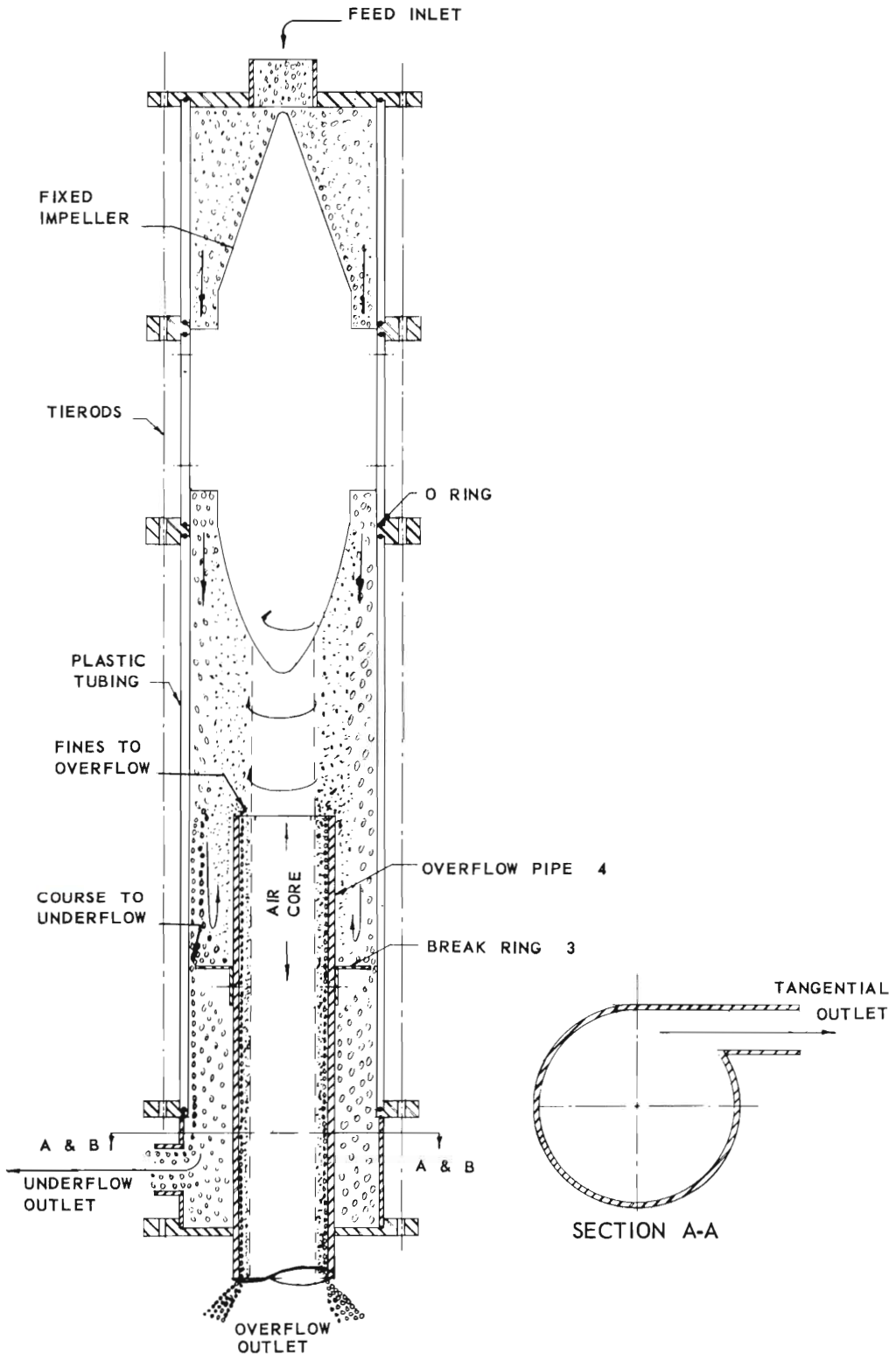

Figure 12. Assembly Drawing of 5-1/2-Inch Fixed-Impeller Separator.

CHAPTER III

PROCEDURE

SETUP OF EQUIPMENT

The 5-1/2-inch fixed-impeller separator was assembled and installed in a closed circuit with a reservoir and pump. (See Figure 13.) Two 1/4-hp mixers and a cooling coil were placed in the reservoir. A pressure tap was provided above the impeller section, and a Bourbon pressure gauge (0 to 30 pounds per square inch) was installed for use as a pressure indicator. Two 55-gallon steel drums with discharge valves at the bottom were provided as weighing tanks, and two sheet metal ducts were used for transferring the overflow and underflow to the weighing tanks.

VISUAL STUDIES

In order to determine if the impeller, as designed and constructed, performed adequately and to observe the flow operation of the test section, the initial setup was made using transparent plastic tubing. A compressed air line was inserted through the underflow pipe into the main body of the test section. Figure 14 is a photograph of a test section in operation. Water is flowing through the device with a counter current stream of air. Using the water-air system, high-speed motion pictures were taken of the operation. (See Figure 15.) It was then possible to trace the path of the air bubbles and, thus, get an indication of flow pattern.

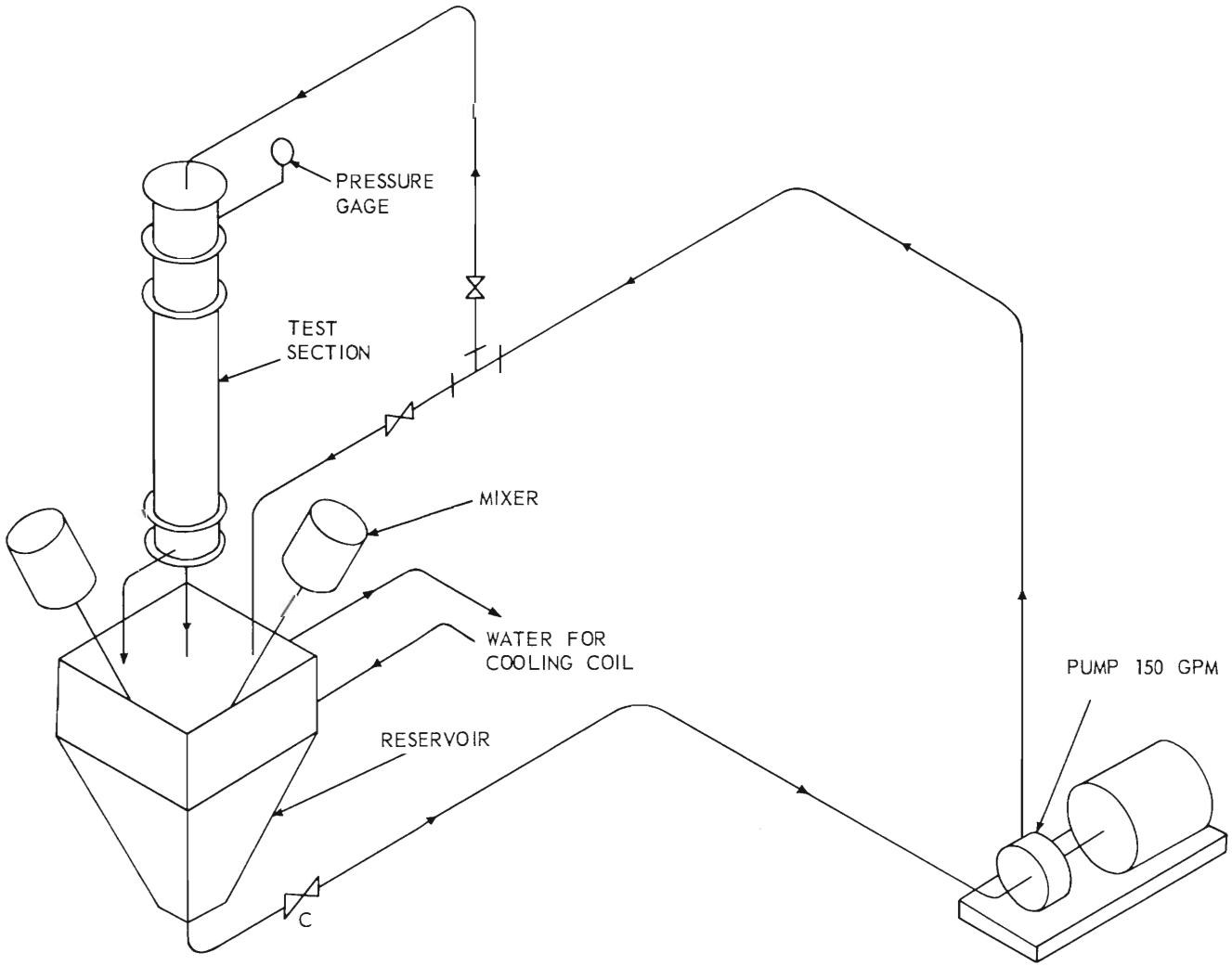

Figure 13. Sketch of Equipment Setup.

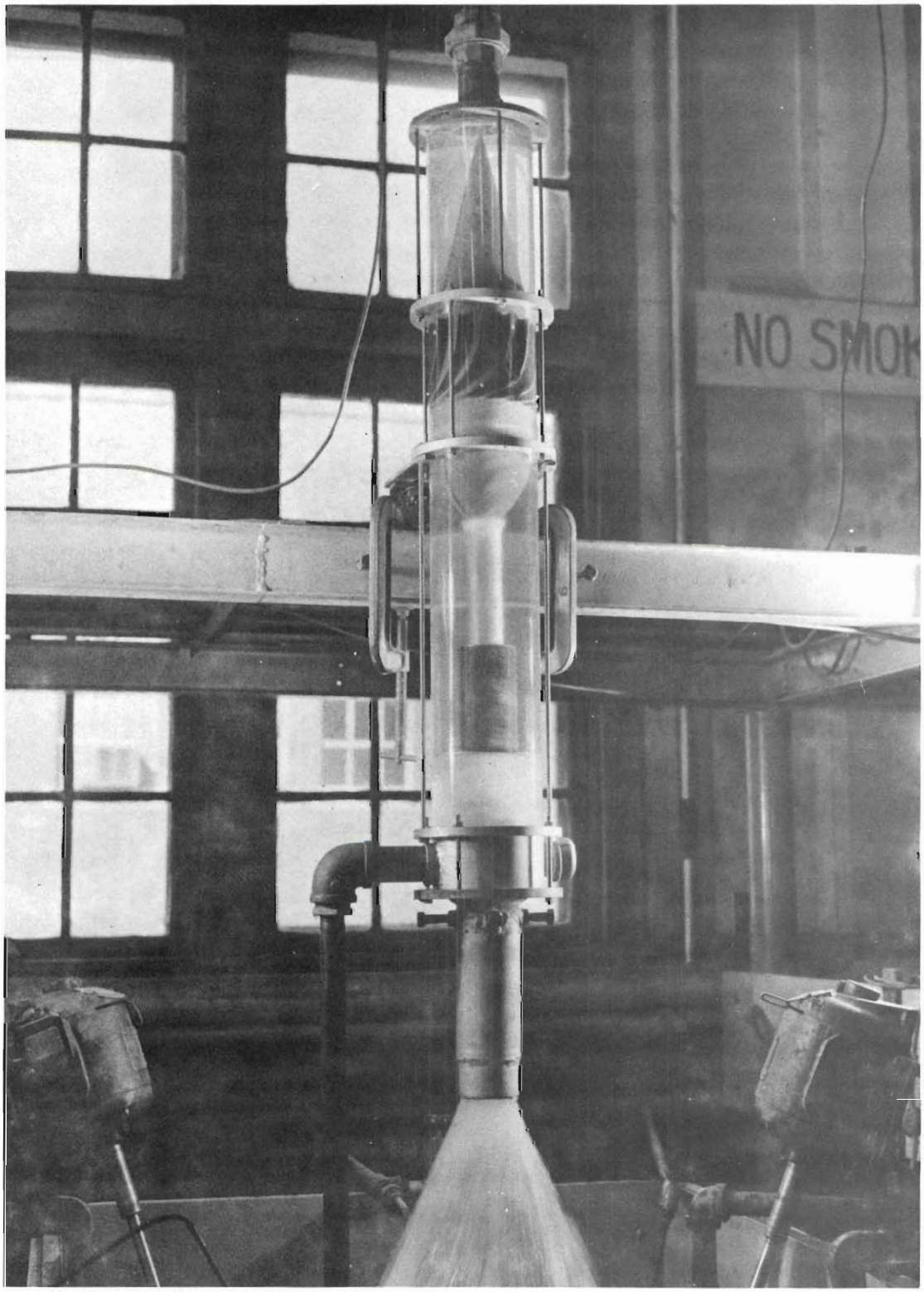

Figure 14. Plastic Test Section.

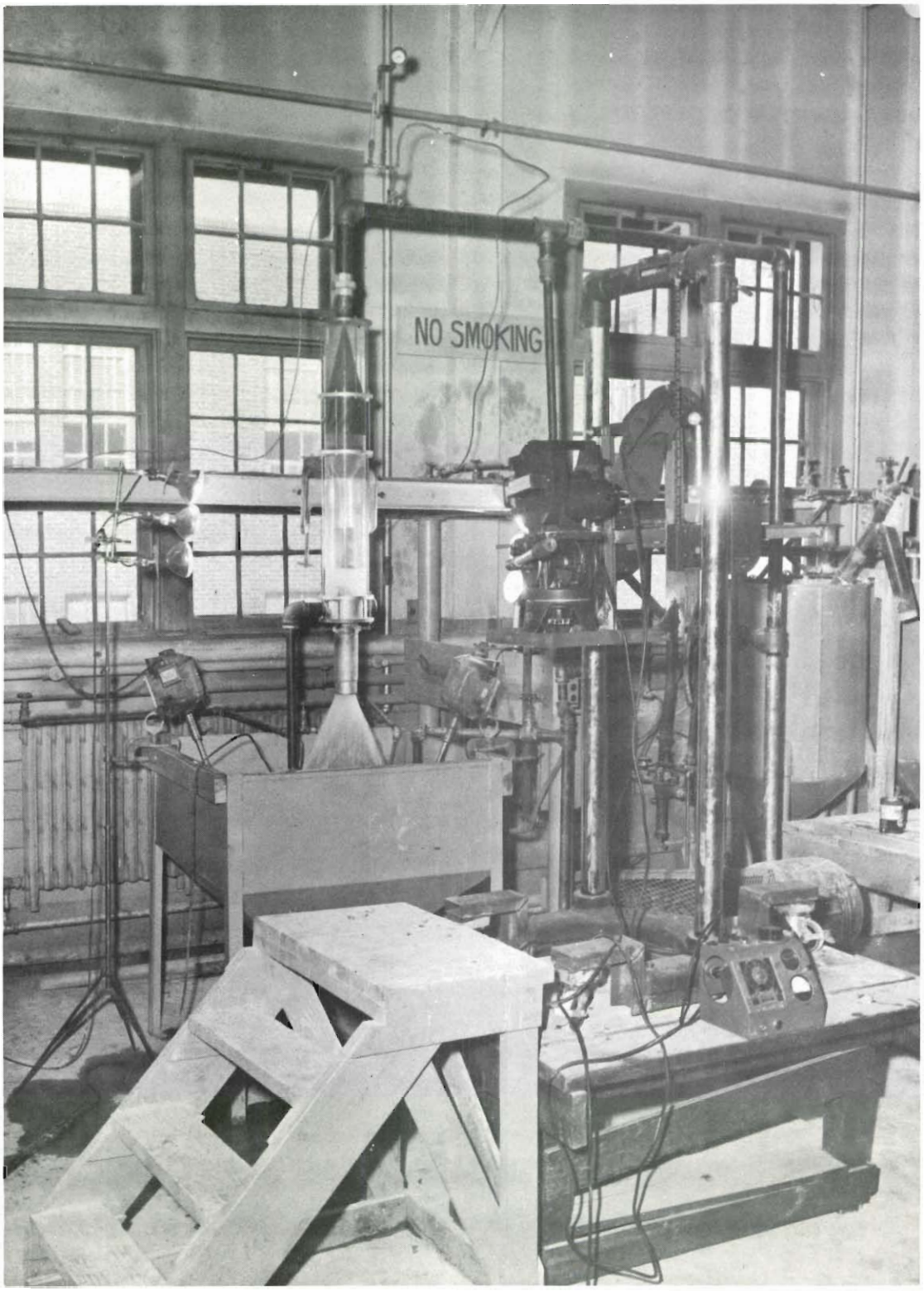

Figure 15. High-Speed Camera and Test Section.

SEPARATION STUDIES

Method of Operation

In solid-liquid separation studies, it is desirable to select a physical system which is relatively uniform and easily reproducible. For these reasons the system, sand and water, was chosen for the separation studies. Sand of three graded sizes was obtained from the Thomasville, Georgia, plant of the Dawes Silica Mining Company. The screen analyses of the sands are shown in Table 1 in the Appendix. The feed slurries were prepared using the following weights of sand:

Dawes No. 2035	10 lbs.
No. 45 AFS	20 lbs.
No. 85-90 AFS	30 lbs.

The composition of the mixture is given in Table 1, under the column entitled "Mixture 3-2-1 Proportion."

Several tests were made to determine the density of the sand. The displacement method consistently gave the density of the material at 2.63 grams per cubic centimeter. In order to study the effect of the solids density on separation, a sample of native ground barytes was obtained. This material had a density of 4.42 grams per cubic centimeter as determined by the displacement method.

Operative Procedure

After replacing the plastic tubing sections with steel tubing, the reservoir was filled with a weighed amount of tap water, and the pump and the mixers were started. The desired amount of solid was slowly added to the reservoir. The flow rate to the test section was adjusted by means

of valves and the by-pass line. (See Figure 13.) The underflow solids concentration was maintained at the desired value by adjusting the diameter of the underflow discharge valve. The percentage of solids in the underflow was approximated by weighing samples of the underflow. The method used was based on the following:

ρ = density (gram cubic centimeters),

W = weight (grams), and

V = volume (cubic centimeters).

Subscripts:

s = solids,

w = water, and

t = total mixture.

S = percentage of same by weight in mixture = $\frac{W_s}{W_t} \times 100$

$$V_t = V_s + V_w$$

$$W_t = W_s + W_w$$

$$V_w = W_w$$

$$V_s = \frac{W_s}{\rho_s} = \frac{W_s}{2.63}$$

$$\frac{W_s}{2.63} + W_w = \frac{W_t}{\rho_t}$$

$$W_s + W_w = W_t$$

$$W_s - \frac{W_s}{2.63} = W_t - \frac{W_t}{\rho_t}$$

$$W_s = \frac{W_t \left(1 - \frac{1}{\rho_t}\right)}{0.62}$$

$$W_s = \frac{SW_t}{100}$$

$$S = 1.612 \left(1 - \frac{V_t}{W_t}\right) \times 100. \qquad (35)$$

A plot of S versus $\frac{V_t}{W_t}$ yields a straight line from which values of S can be rapidly obtained for a specific value of $\frac{V_t}{W_t}$.

For each test performed, pressure drop was recorded, and samples were taken of the underflow and overflow. Flow rates of these two streams were taken simultaneously by diverting the streams through metal ducts to the weighing tanks. After recording the weights, the slurries in the weighing tanks were returned to the reservoir.

Tests Performed

Overflow diameter as a variable.--Four runs (runs I-M through IV-M) were made in order to obtain the relationship between flow rate and overflow diameter. The geometry of the test section was fixed with the exception of the overflow-pipe diameter. Five pipe diameters were used. They were: 1-, 1-1/4-, 1-1/2-, 2-, and 2-1/2-inch standard steel pipe. Details of the geometry for each run are given in Table 2 in the Appendix.

Variation of break-plate diameter.-- In order to obtain information on the variation of break-plate diameter with flow rate, run IV-M was repeated, with the exception that the break-plate diameter was decreased to four inches (run V-M).

Position of the break plate.--Run VI-M was conducted to determine the effect of the break-plate position relative to the overflow nozzle. This run was a repeat of run IV-M with the exception that the break plate was 1-1/2 inches from the top of the overflow pipe.

Dimensions of test section.--The effects of length of test section and height of overflow pipe were investigated in runs VII-M and VIII-M. In run VII-M, the distance between the overflow nozzle and the trailing edge cone of the impeller was the same as for run IV-M (4-5/8 inches), but the test section was extended to 32-1/4 inches below the impeller flange. During run VIII-M, the same test-section length (32-1/4 inches) was used, but the overflow nozzle was placed 18.9 inches below the trailing edge cone of the impeller.

Tangential discharge investigation.--Runs I-M through VIII-M were conducted with the underflow being drawn off through an outlet perpendicular to the axis of the test section. In order to determine the effect of a tangential underflow discharge, the perpendicular discharge was closed, and run IX-M was conducted using the tangential discharge port in the discharge assembly. (See Figure 4.)

Underflow-solids concentration.--The effect of the percentage of solids in the underflow was investigated by repeating run IV-M with underflow solids concentration of approximately 44 per cent (run X-M). Thus, by comparing IV-M with X-M, an indication of the variation of underflow solids concentration could be obtained. Run XII-M was carried out with an underflow solids concentration of approximately 70 per cent with the concentration of feed solids of about 25 per cent.

Feed-solids concentration.--In order to get information of the effect of feed-solids concentration on separation point, runs XI-M and XII-M were carried out with a feed increased to approximately 25 per cent solids by weight.

Effect of solids density.--Since it appeared that the solids density should be investigated, run XIII-M was conducted. This run was a repeat of run IV-M with regard to geometry, but barytes (a density of 4.42 grams per cubic cemtimeter) was substituted for the sand of run IV-M. The recorded data for all of these runs are presented in Table 2 in the Appendix.

METHOD OF ANALYSIS AND CALCULATION

Sample Analysis

Since certain information was necessary in order to evaluate the 50 per cent separation point and percentage of coarse- and fine-particle solids separation efficiency, the underflow and overflow samples taken in runs I-M through XIII-M were processed in the laboratory.

The analytical procedure was as follows:

1. The jar plus the sample was weighed to one-tenth of a gram.
2. The sample was wet screened on U. S. Standard Sieve Screens:

30	70	200
40	100	250
50	140	325

3. The material retained on each screen was dried and weighed.
4. The jar was dried and weighed.

From the total weight of the sand and the total weight of the sample, the percentage of solids in the sample was calculated. Since the weight of solids retained on each individual screen was recorded for the underflow and overflow, it was possible to calculate the 50 per cent point and a percentage coarse-and fine-particle separation.

Calculation of Data

Fifty per cent point (μ).--The 50 per cent separation point was calculated as follows:

μ = percentage of a specific size in the feed reporting to the underflow

$$= \frac{YMy}{XMx + YMy} \times 100 \qquad (36)$$

where X = overflow rate (pounds per second),

Y = underflow rate (pounds per second),

Mx = weight of solid retained on a specific screen in the overflow sample, and

My = weight of solid retained on a specific screen in the underflow sample.

Since the solids retained on a specific screen contain material that would just pass the next larger screen, the arithmetic average of the screen openings in microns of the screen on which the material was retained and the next larger screen was used as the particle size of the material. For example, solids retained on a U. S. Standard Sieve No. 140 were assigned a particle size as follows:

Sieve No.	Sieve Opening
140	105 microns
100	149 microns
Total	254 microns

Average: $\frac{254 \text{ microns}}{2} = 127$ microns

Solids which passed a U. S. Standard Sieve No. 325 (44 microns) were assigned a particle size of 22 microns.

Plots were made of the percentage of a specific size reporting to the underflow versus the particle size. The 50 per cent point in microns was read from the curve at its intersection with the 50 per cent line. This graphical procedure is illustrated in Figure 16. The calculated data are presented in Tables 2 and 3, and sample calculations are included in the Appendix.

Coarse- and fine-particle separation efficiency.--Although the 50 per cent point is an excellent method of defining the separation point, it does not give any indication of sharpness of separation. For this reason, a coarse- and fine-particle separation efficiency has been defined from equation 10

$$W_y = \text{percentage of coarse-particle separation} = \left[\frac{W_w}{W_c}\right] \times 100$$

where W_w is equal to the weight of solids greater than the 50 per cent separation point in the underflow, and W_c is equal to the weight of solids greater than the 50 per cent in the feed, and from equation 11

$$W_x = \text{percentage of fine-particle separation} = \left[\frac{W_o}{W_F}\right] \times 100$$

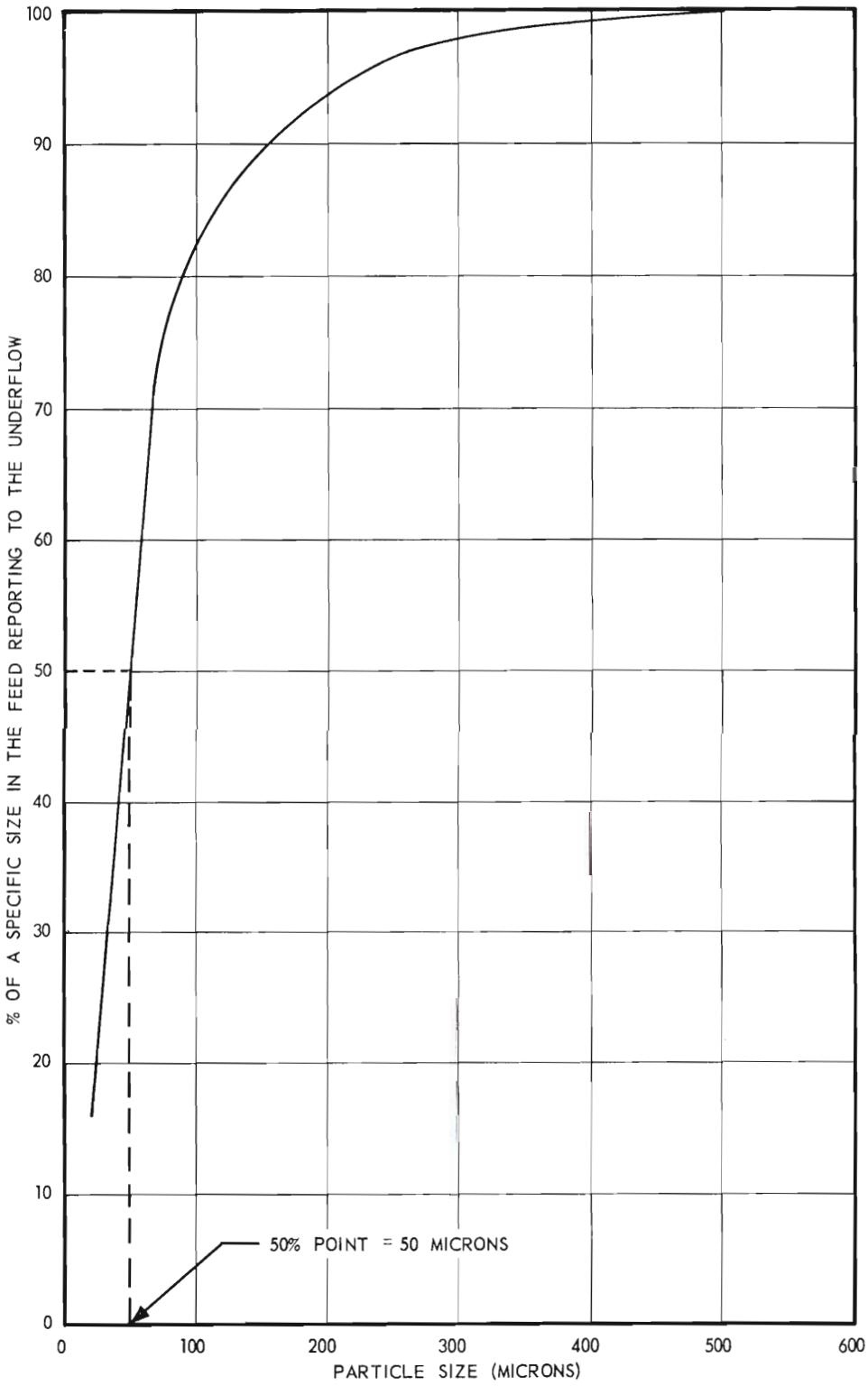

Figure 16. Fifty Per Cent Point Determination.

where W_o = the weight of solids less than the 50 per cent point in the overflow and

W_F = the weight of the solids less than the 50 per cent point in the feed.

Calculated data are presented in Table 3 in the Appendix, and sample calculations are included in the Appendix. For comparison, Taggart (21) efficiencies were calculated and are given in Table 3.

PRESSURE DROP STUDIES

Although detailed energy-loss studies were not included in the scope of the work, it appeared to be of interest to undertake a preliminary investigation of energy loss and compare it with the loss for a conventional cyclone. The energy loss for a cyclone has been shown to be (3) related to the inlet and overflow diameter. It was reasoned that an additional variable of underflow diameter would have to be considered in studying the fixed-impeller device. Runs were made at fixed blade angle with varying underflow diameter and overflow diameter.

Dahlstrom's (3) capacity ratio was calculated for a conventional cyclone operating at the same flow rate by obtaining an equivalent round-inlet pipe diameter for the impeller device by equation 6. Using this as the inlet diameter, the capacity ratio was calculated from

$$Q/(F)^{0.5} = 5.68(eb)^{0.9}$$

where $Q/(F)^{0.5}$ = capacity ratio,

Q = gallons per minute of feed,

F = energy loss (feet),

e = inlet diameter (inches), and

b = overflow diameter (inches).

CHAPTER IV

RESULTS

Data.--Tables 2 and 3 (in the Appendix) contain the calculated data for runs I-M through XIII-M. Tables 4 and 5 (in the Appendix) contain the operative data and analytical data for the samples from runs I-M through XIII-M.

Correlation of Data.--Figure 17 is a plot on log-log coordinates of 50 per cent point versus flow rate with overflow diameter as a parameter for runs I-M through IV-M. These data indicate a family of straight lines with a slope calculated by method of least squares to be 0.68 (the 50 per cent point increasing with decreasing flow rate and increasing with increasing overflow diameter).

The 50 per cent point versus overflow diameter is plotted on log-log coordinates in Figure 18. A straight line can be fitted to these points by least-squares method with slope 0.77.

Since both overflow diameter and flow rate vary as a log function of the 50 per cent point, it appeared that a correction coefficient should exist as a function of the 50 per cent point. Since Dahlstrom (3) has shown that for a conventional cyclone the 50 per cent point varies directly with the product of the overflow diameter and flow rate (raised to the proper powers) at fixed-nozzle diameter, a product coefficient was tried. The results are plotted to log-log coordinates in Figure 19. From Figure 19 it is apparent that the data can be

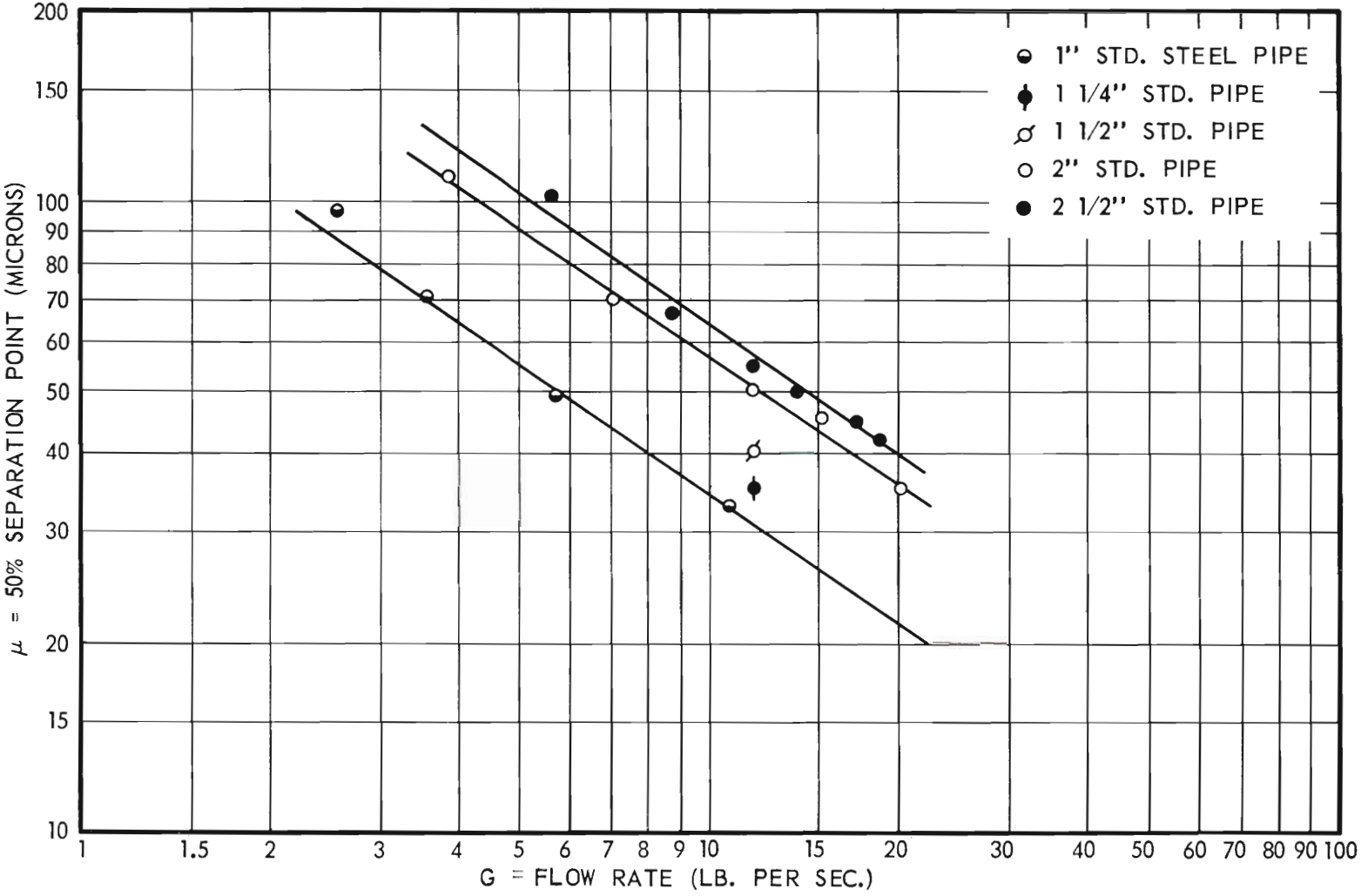

Figure 17. Fifty Per Cent Point Versus Flow Rate.

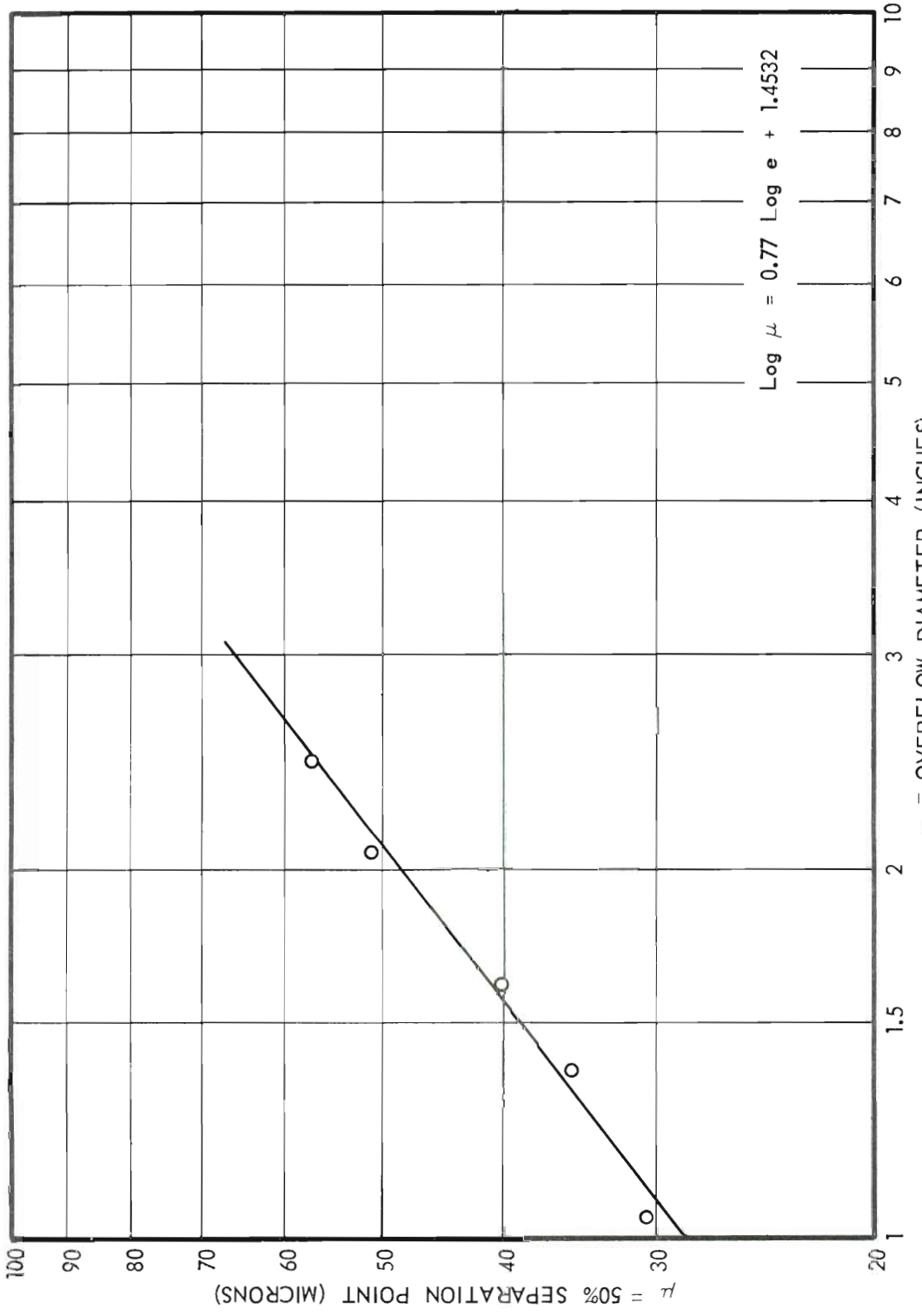

Figure 18. Fifty Per Cent Point Versus Overflow Diameter.

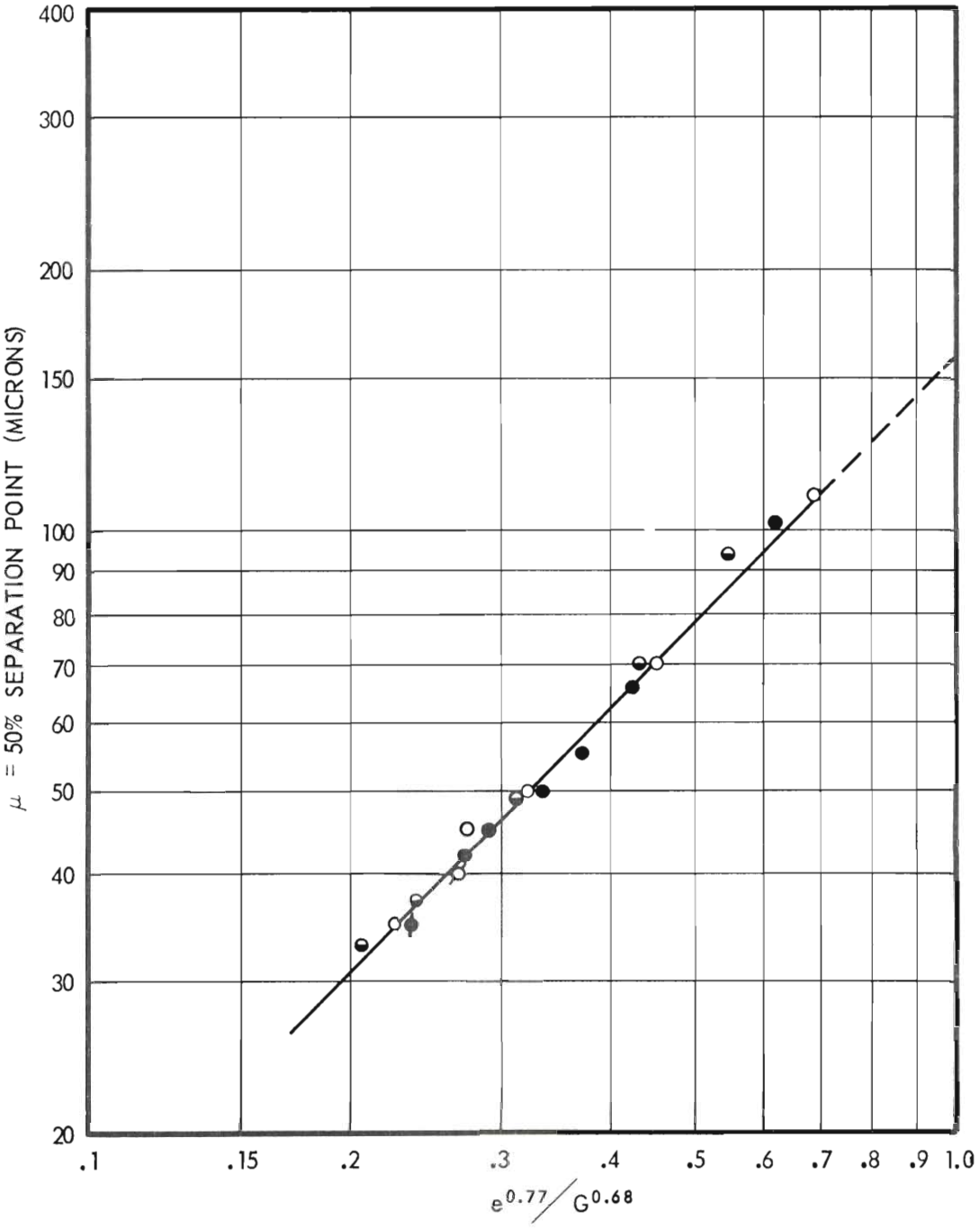

Figure 19. Fifty Per Cent Point Versus Correlation Coefficient.

represented by a linear relationship with a slope of 1.00, and the intercept 157 calculated by the method of least squares.

Thus,

$$\mu = 50 \text{ per cent point (microns)} = 157 \frac{e^{0.77}}{G^{0.68}} . \qquad (37)$$

Figure 20 is a photograph of the plastic test section showing flow lines of the primary and secondary vortex. The effect of various geometric and physical factors is presented in Figures 21 through 27. In each case, the correlation coefficient for each test is plotted versus the 50 per cent point, and the base line represented by equation 37 is plotted for reference. Figure 28 is a plot of the results of run XIII-M. This run was made with the same geometry as the base line, but solids (barytes) of density 4.42 grams per cubic centimeter were used as the material to be separated. If Stokes' law applies:

$$u_s = \frac{(\rho_s - \rho)\ 62.4 g D_s^{\ 2}}{18 \mu_s} . \qquad (38)$$

Then, the diameter ratio of equal settling velocity particles of different densities (assuming the same slurry viscosity) is

$$\frac{D_{s_1}}{D_{s_2}} = \left[\frac{\rho_{s_2} - \rho_2}{\rho_{s_1} - \rho_1} \right]^{0.5} . \qquad (39)$$

If this statement were true, then density parameter lines could be drawn parallel to the base line. Figure 28 contains the base line for reference and the predicted performance line on the basis of equation

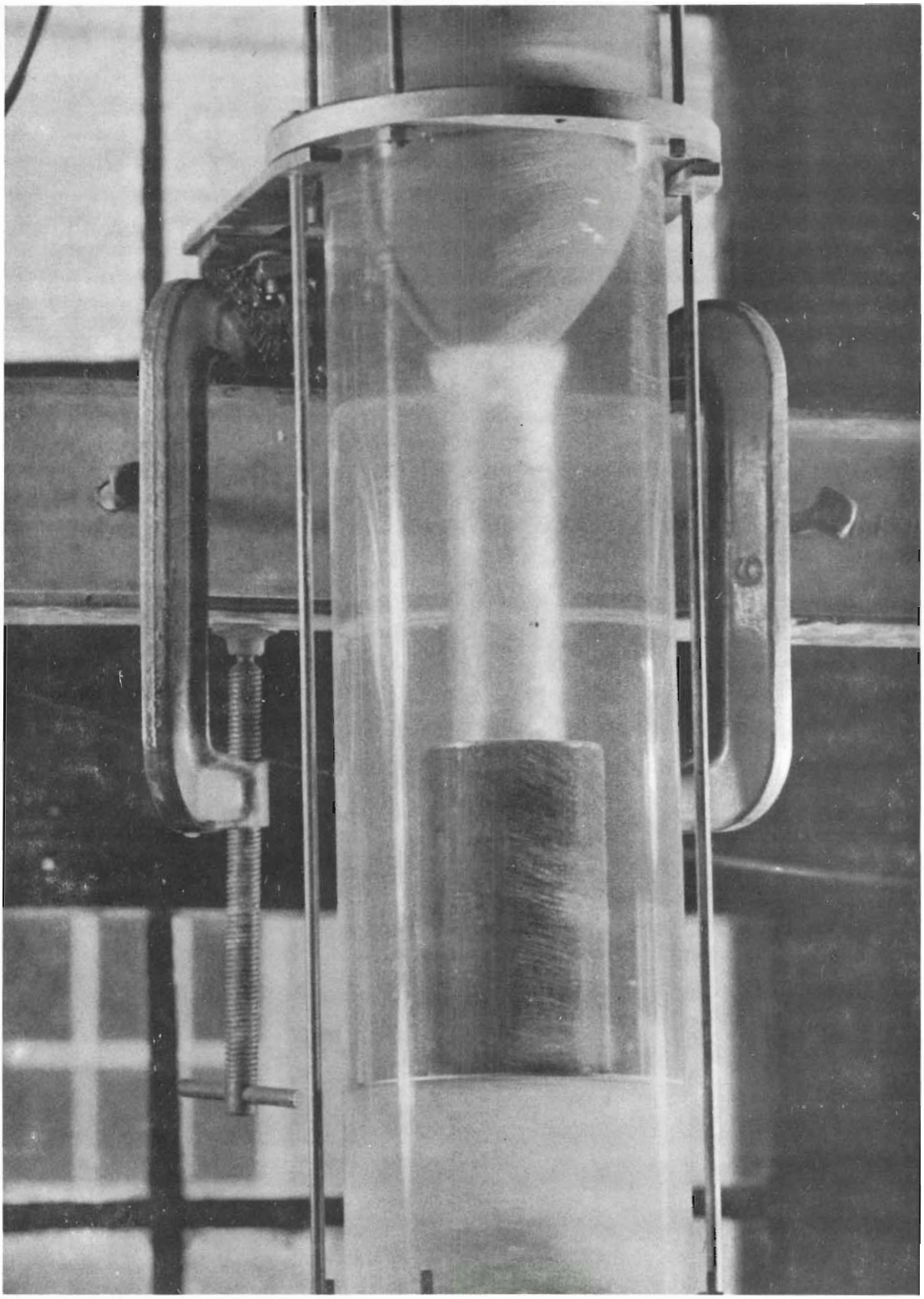

Figure 20. Test Section with Visible Flow Lines.

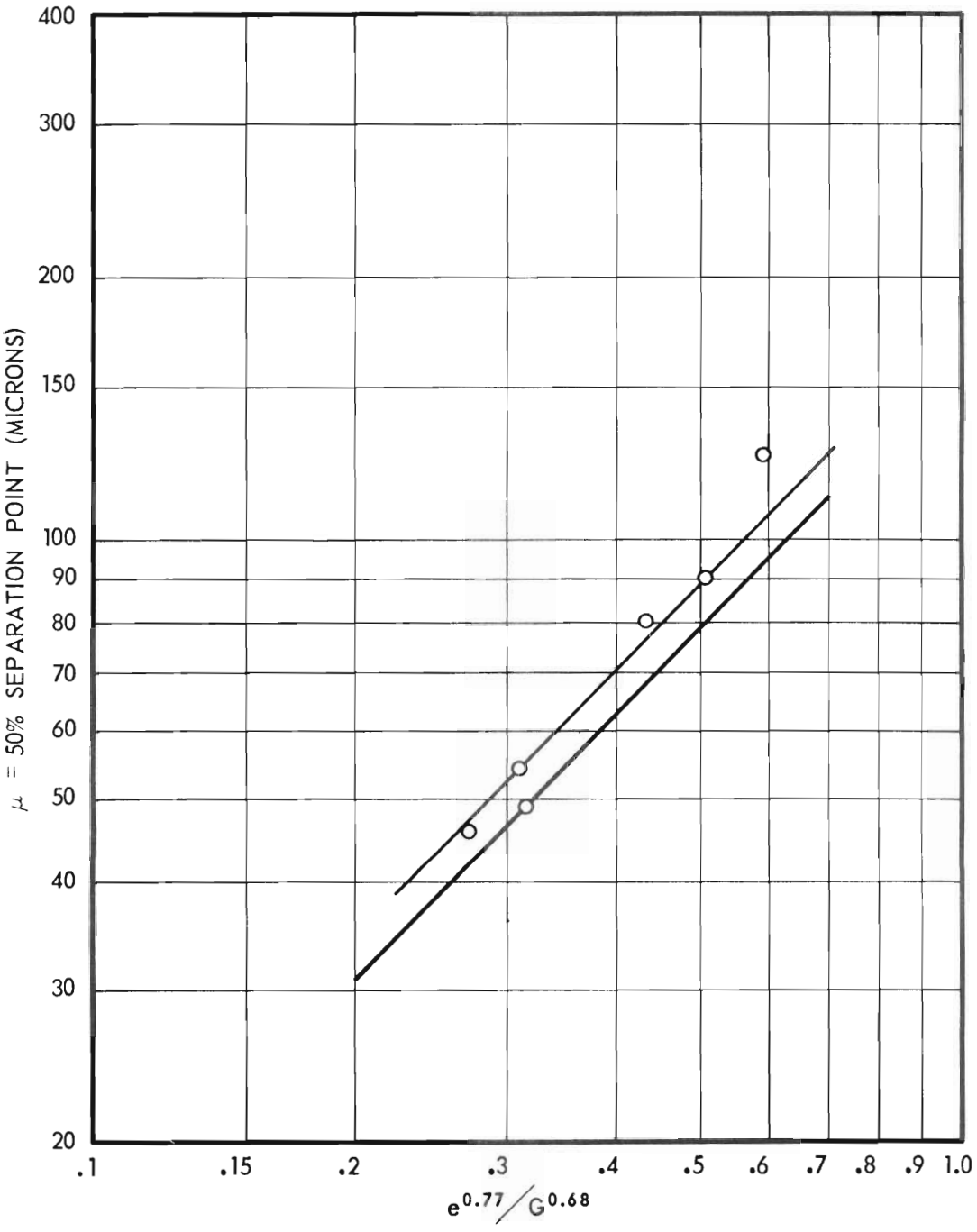

Figure 21. Effect of Break-Plate Diameter on 50 Per Cent Point.

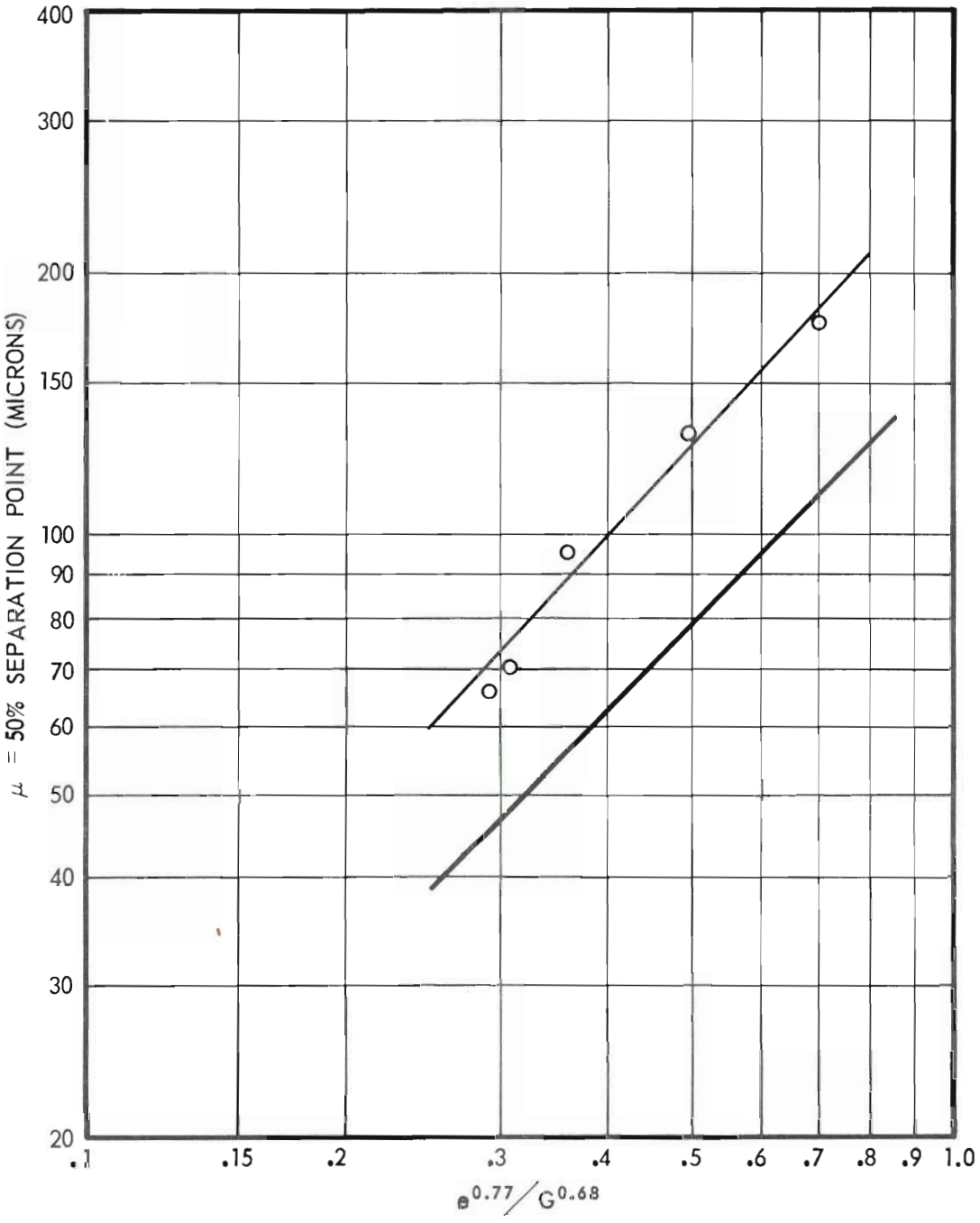

Figure 22. Effect of Break-Plate Position on 50 Per Cent Point.

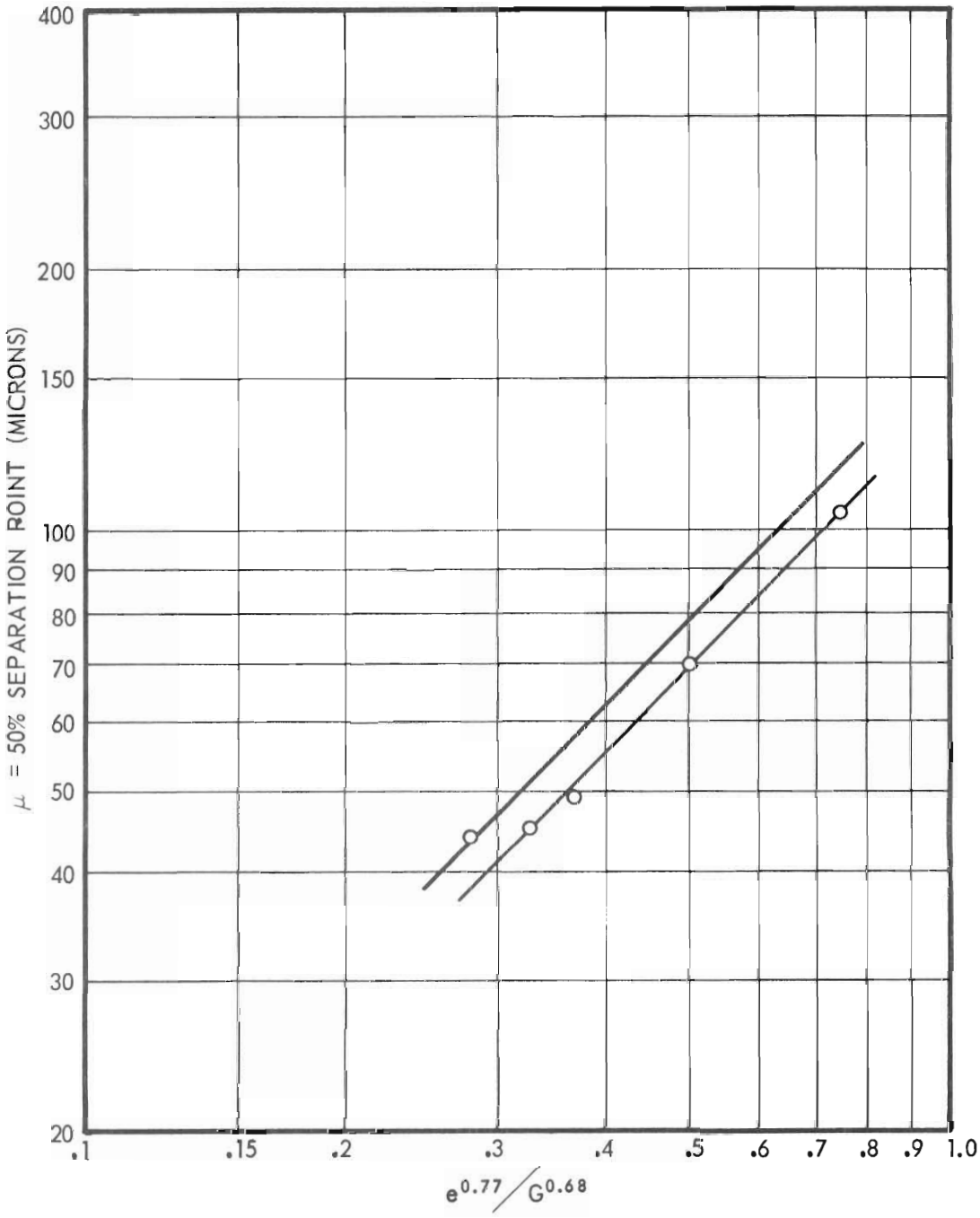

Figure 23. Effect of Length of Test Section on 50 Per Cent Point.

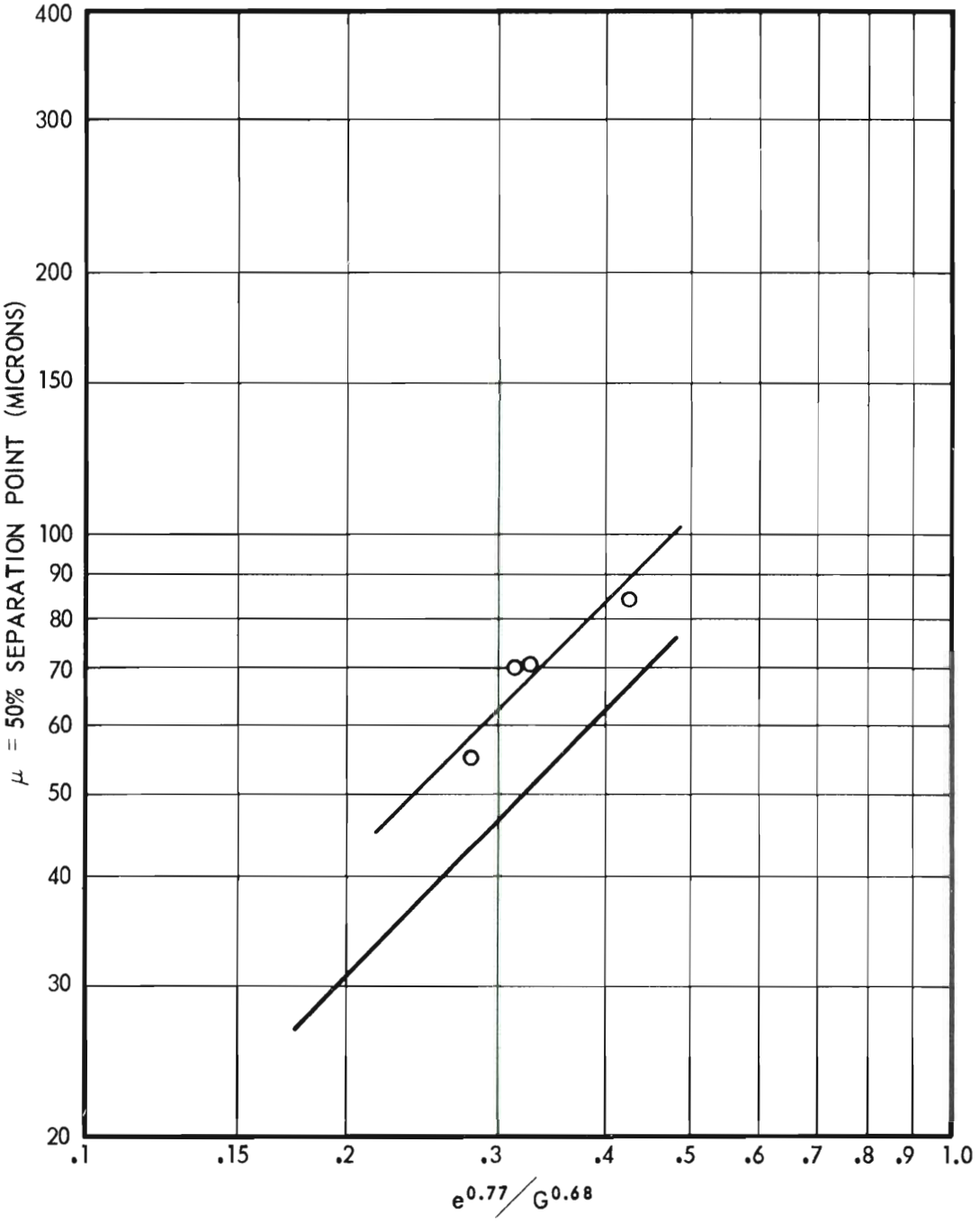

Figure 24. Effect of Distance Between Impeller and Overflow Pipe on 50 Per Cent Point.

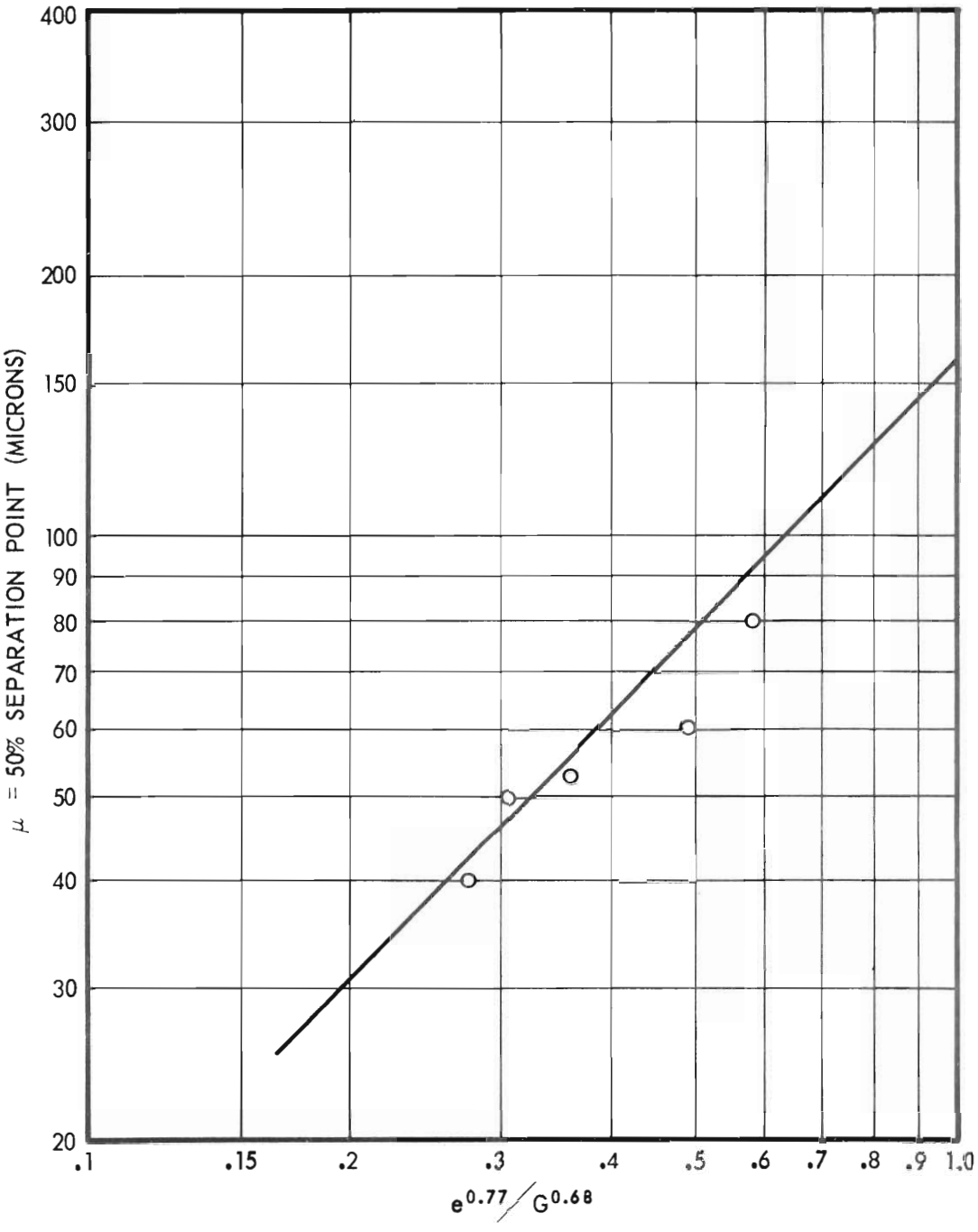

Figure 25. Effect of Tangential Discharge on 50 Per Cent Point.

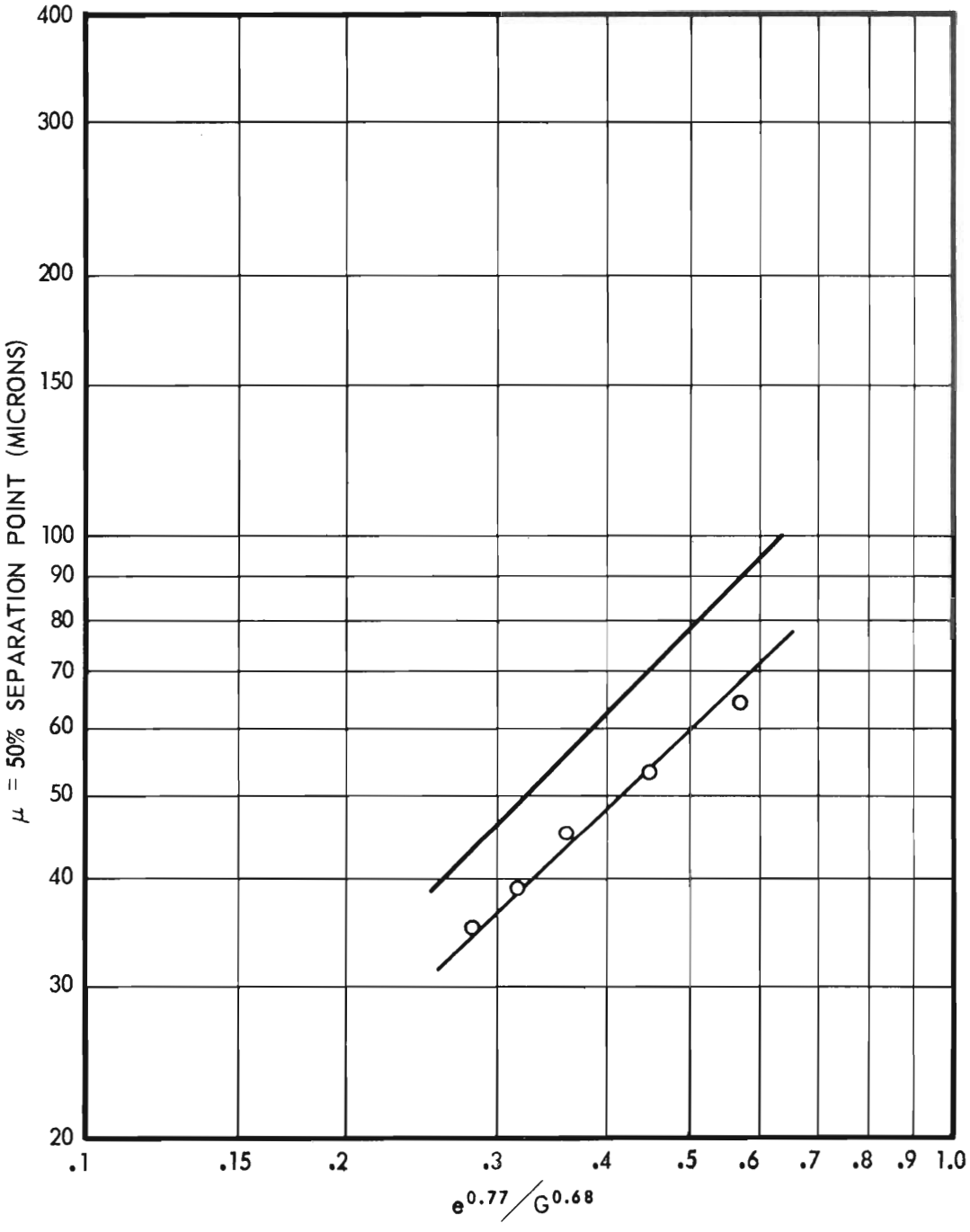

Figure 26. Effect of Solid Concentration in Underflow on 50 Per Cent Point.

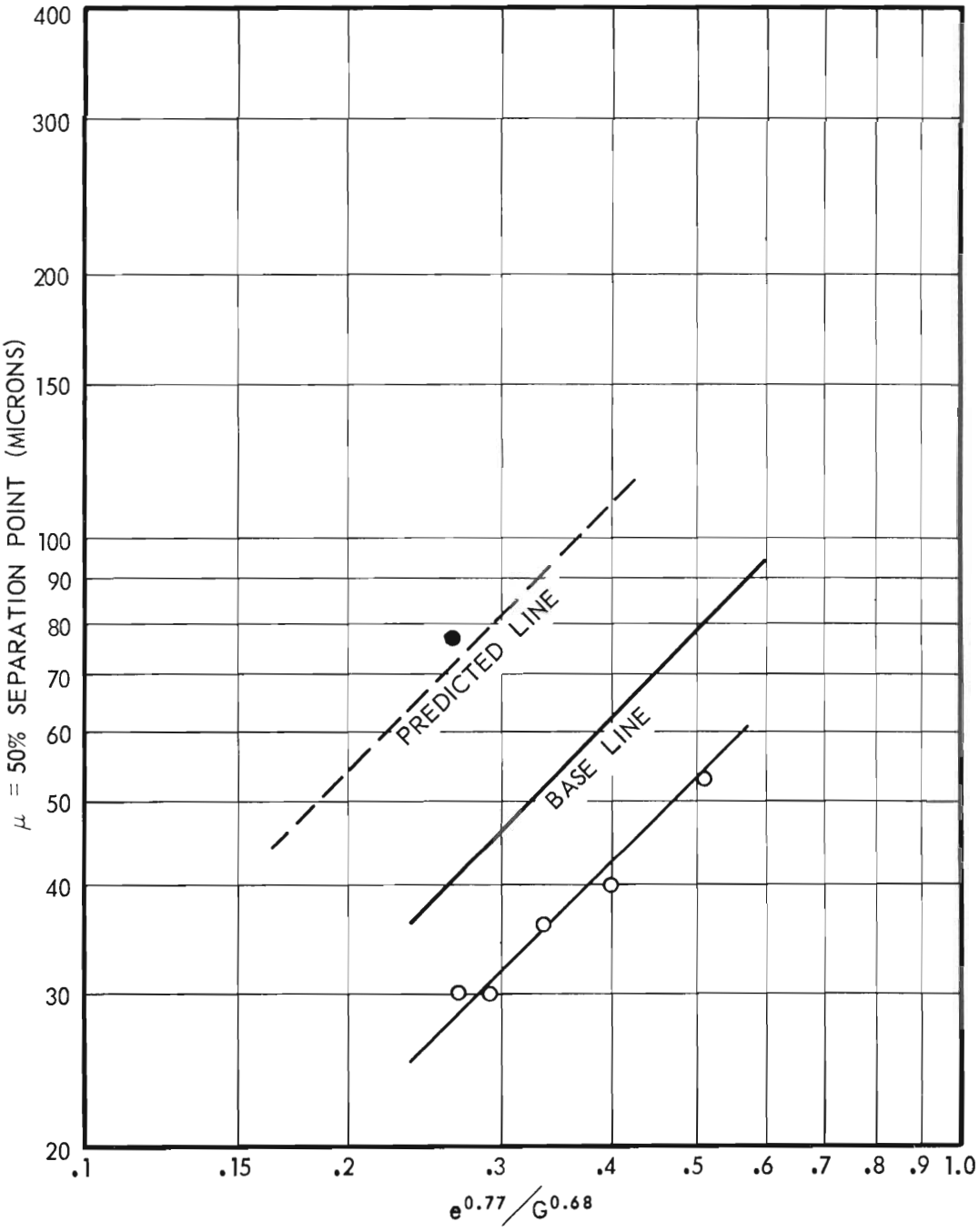

Figure 27. Effect of Solid Concentration in Feed on 50 Per Cent Point.

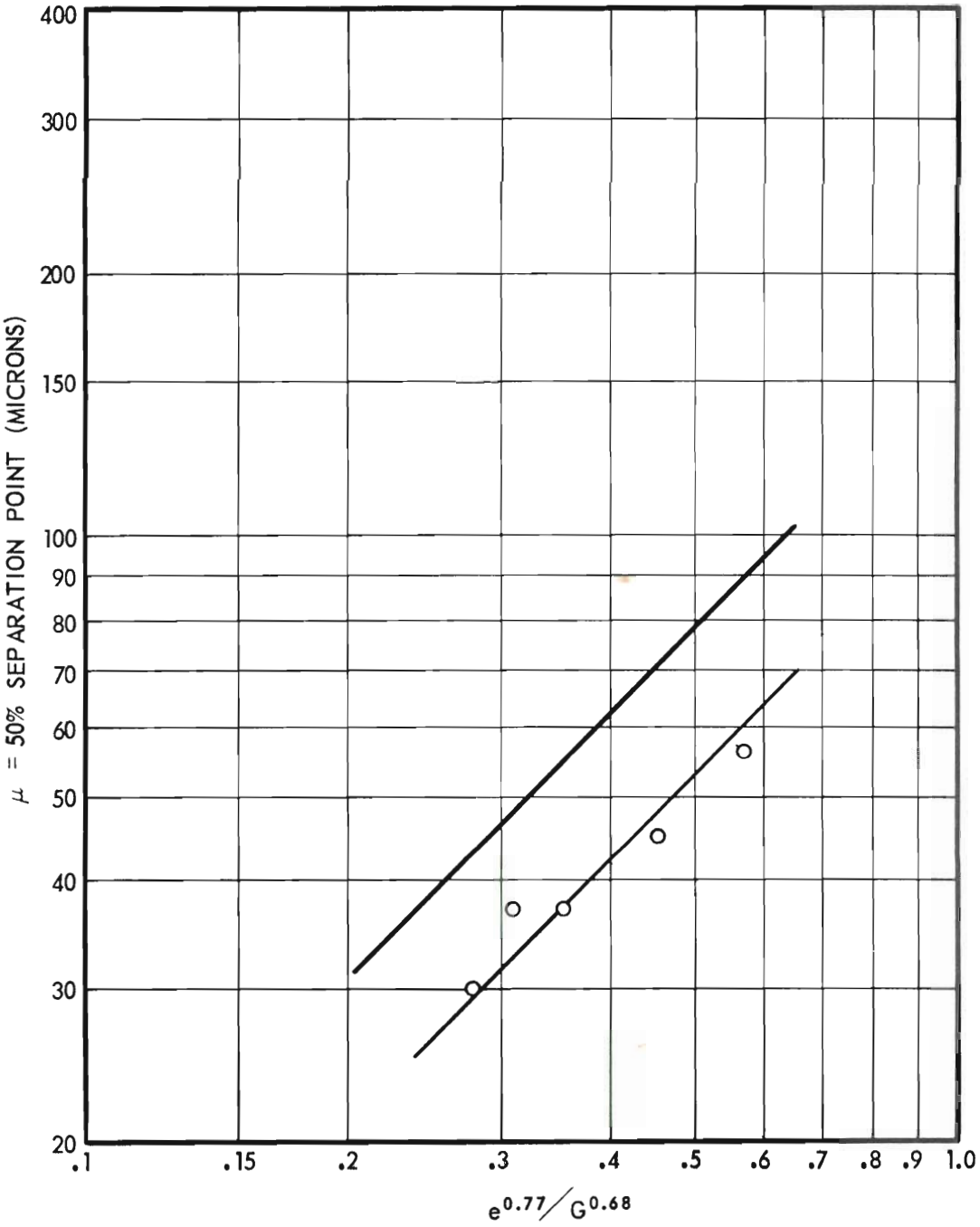

Figure 28. Effect of Solids Density on 50 Per Cent Point.

39. It is apparent from Figure 28 that agreement between predicted and experimental performance is satisfactorily indicated. Equation 39 is applicable to the operation of the device.

Combining equations 37 and 39,

$$\mu = 157 \frac{e^{0.77}}{G^{0.68}} \left[\frac{1.54}{\rho_s - \rho}\right]^{0.5}. \qquad (40)$$

The data obtained in the preliminary energy-loss studies are presented in Tables 5 and 6 in the Appendix. The results are shown graphically in Figure 29. A comparison with the conventional cyclone as calculated from equation 9 is shown in Figure 29.

Figure 30 is a plot of K_{CR} (the intercept of the various underflow diameters of Figure 28) versus underflow diameter.

Figure 31 presents a comparison among the fixed-impeller separator, the cyclone, and the open-top cyclone. The line for the cyclone was calculated from Dahlstrom's equation (3) and the line for the fixed-impeller equipment from equation 40. The inlet diameter for the cyclone was calculated as an equivalent round pipe diameter by equation 6. The overflow diameter was selected as 2.067 inches for both calculations. The data shown for the open-top cyclone was taken from Emmett (22).

Figure 32 is a plot of the percentage of a specific particle size in the feed reporting to the underflow versus the particle size in microns. Data are given for a typical cyclone run from Dahlstrom (3), two fixed-impeller runs and run 117 from Emmett (22). The slope and the shape of the curves indicate the sharpness of separation. From Table 3

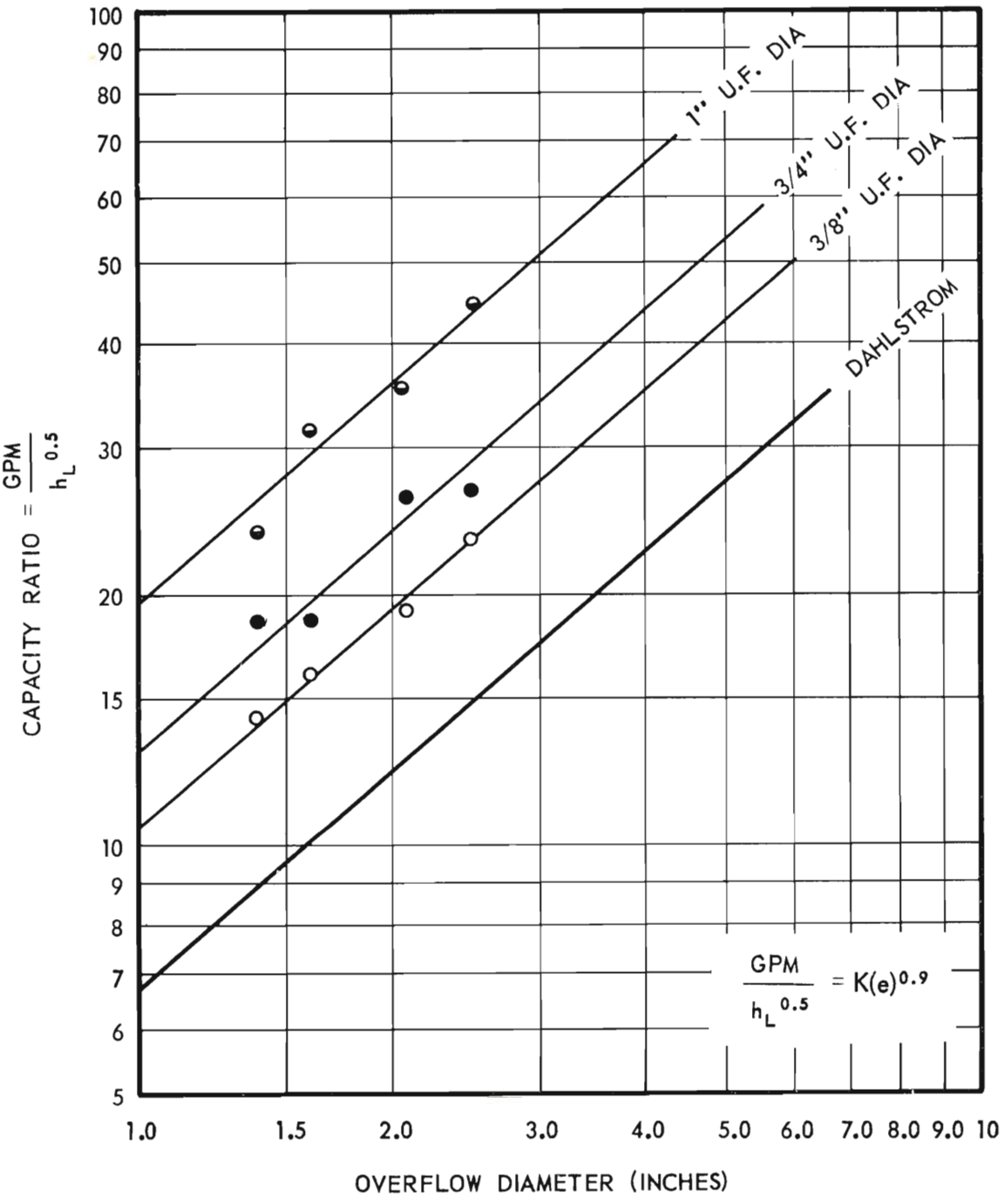

Figure 29. Capacity Ratio Versus Overflow Diameter.

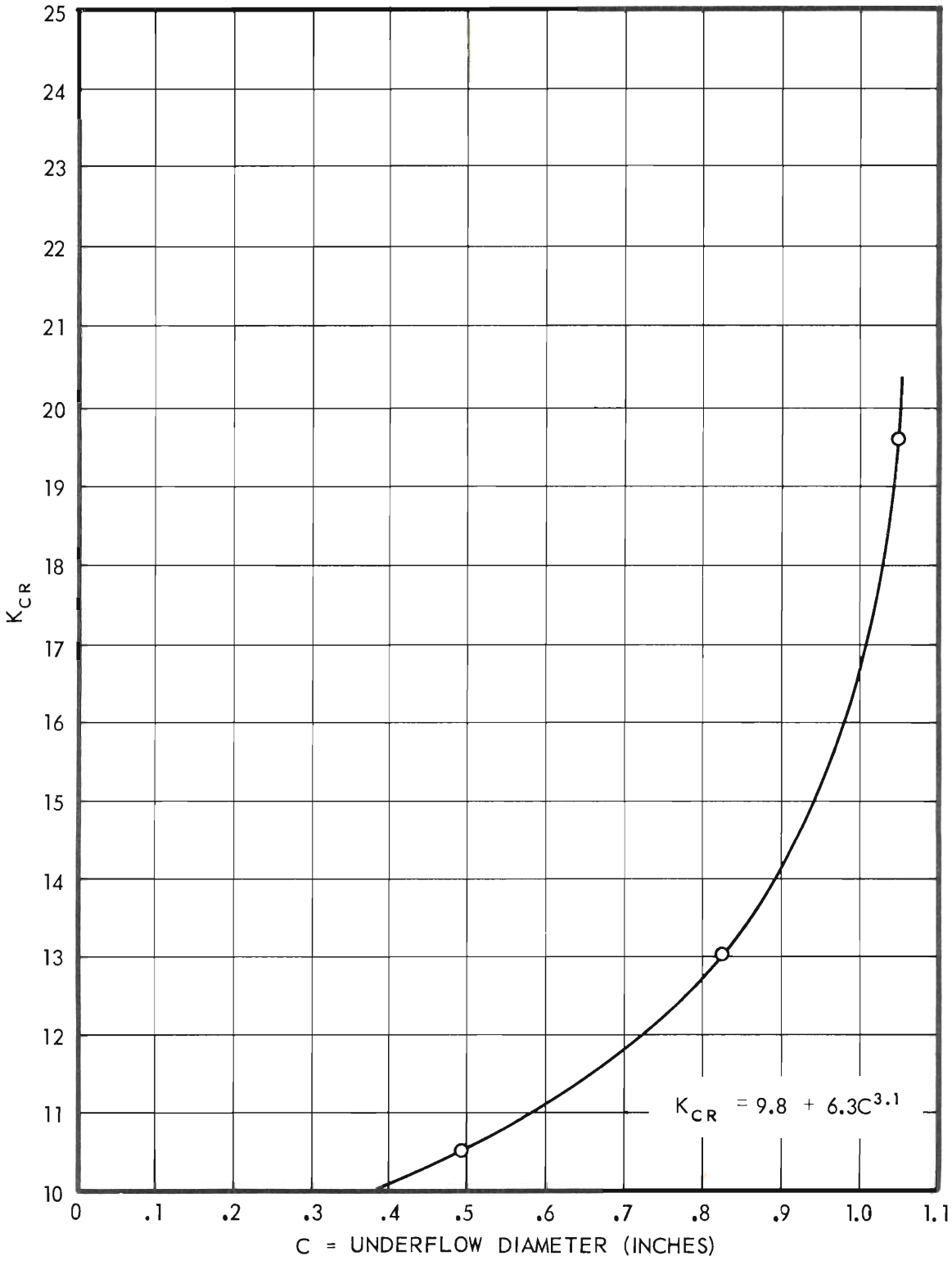

Figure 30. K_{CR} of Capacity Ratio Equation Versus Underflow Diameter for Energy Loss.

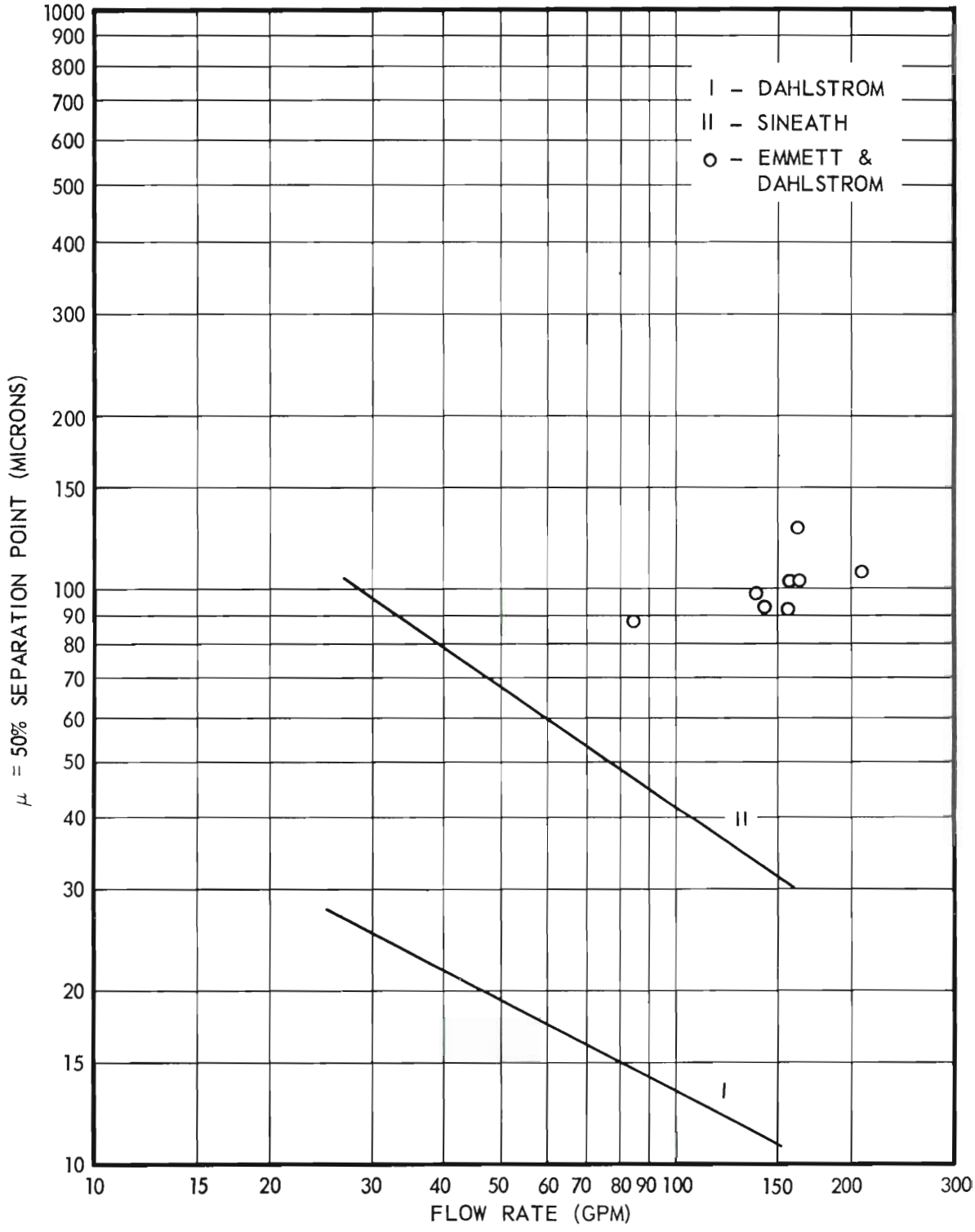

Figure 31. Comparison of Cyclones with Fixed-Impeller Separator.

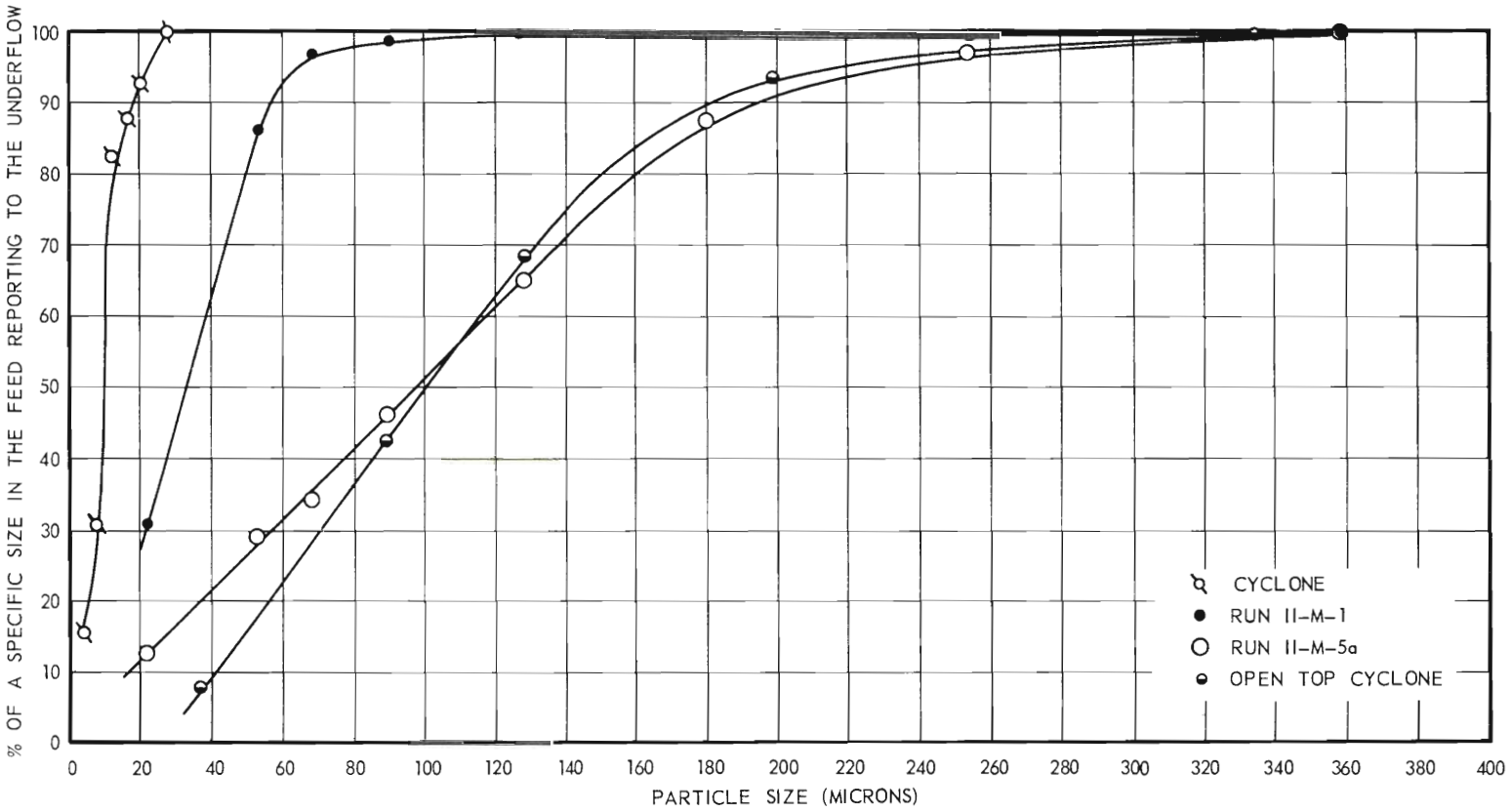

Figure 32. Comparison of Sharpness of Separation.

another comparison of sharpness of separation can be obtained by comparing coarse-particle, fine-particle, and Taggart (21) efficiencies.

CHAPTER V

DISCUSSION OF RESULTS

Visual Studies

A high-speed motion picture of the device with a plastic test section in operation confirmed the premise that the break plate did cause the formation of a secondary vortex around the overflow pipe. This effect is apparent upon close examination of Figure 20. The streamlines of the primary vortex are visible on the surface of the impeller tail cone in the upper part of the photograph, and those of the secondary vortex are visible on the surface of the overflow pipe in the lower part. It is apparent that the lines of the primary vortex slope downward to the left and those of the secondary vortex slope upward to the left. The photographs of the blade section indicated that some turbulence existed just below the trailing edge of the blade; however, separation of the liquid from the blade edge was not observed. The turbulence could probably be reduced by varying blade design, but this would be difficult in view of the velocities involved (25 to 40 feet per second).

Separation Studies

Earlier in this work equation 8 was assumed for the device which related the 50 per cent separation point to overflow diameter, blade angle, flow rate, density of solids, and density of the slurry. Equation 40 was developed based on experimental data from runs I-M through IV-M

and run XIII-M. This equation is of the same form as the assumed equation with the exception of the blade angle. Since experimental work was performed at a fixed blade angle, this effect of the variable has not been evaluated. In view of Dahlstrom's equation (equation 12) and other considerations presented earlier in this work, it seems logical to assume that the function $\left(\frac{A_2}{\cos \alpha}\right)^{0.5}$ (from equation 8) should vary with the same power as the overflow diameter e. Using this assumption, it would be possible to predict μ for a given set of conditions. From a consideration of equation 40 and the data for runs I-M through IV-M of Table 2, it is apparent that the 50 per cent separation point increases with decreasing flow rate and increasing overflow diameter. Also, the separation point decreases with increasing solids density and increases with increasing feed-slurry density. Thus, if it is desired to increase the 50 per cent separation point, it can be accomplished by increasing the overflow diameter and feed-slurry density and by decreasing the flow rate. Other factors which must be considered are the coarse- and fine-particle separation efficiency. From run I-M through IV-M, Table 2, it is evident that the coarse-particle separation efficiency decreases with decreasing flow rate and 50 per cent separation point. This efficiency decreases about 14 per cent over the range of flow rate from 20.2 to 3.9 pounds per second. There does not appear to be a trend for the fine-particle separation efficiency as a function of flow rate.

The effect of increasing overflow diameter on the separation efficiencies is represented by runs I-M-3, II-M-1, and IV-M-6. All of these runs were conducted at approximately the same flow rate. It appears that decreasing diameter of the overflow pipe has the effect of

decreasing coarse-particle separation efficiency by about 4.5 per cent over the range of diameters 1.05 to 2.47 inches. However, the 94 per cent separation efficiency for the 2.47-inch diameter of run IV-M-6 should be acceptable for most applications of the device.

The fine-particle separation efficiency trends toward an increasing efficiency with increased overflow diameter. This efficiency exhibits about a 10 per cent rise over the diameter range of 1.05 to 2.47 inches.

The effects discussed above would be expected, since as flow rate is decreased, less centrifugal force is acting on the particles of the slurry; consequently, separation efficiency is lower and the 50 per cent point is higher. Also, increased overflow diameter would reduce centrifugal force, producing the same effect. It is of interest to note that the flow rate had a much greater effect on 50 per cent point and separation efficiency than the overflow diameter. It appears that if a higher 50 per cent point is desired, the best approach would be to increase overflow diameter and maintain as low flow rate as possible to give a coarse-particle separation efficiency in excess of 90 per cent.

It was advanced earlier that the various physical and geometrical operating factors should affect the K_1 value but not the constants a, c, T, and q of equation 8. In order to determine the validity of this premise, runs V-M through XII-M were performed.

The diameter and position of the break plate (run V-M, Figure 21).--From Figure 21 it is evident that by decreasing the diameter of the break plate an increase in the 50 per cent point occurred. This is contrary to the ideas advanced earlier in this work in that the smaller diameter

plate did not permit passage of the smaller particle strata to the underflow. This difference may be explained by consideration of run VI-M, Figure 22. Run VI-M was conducted with the break plate 1.5 inches below the overflow-pipe discharge. By decreasing the distance between the break plate and overflow pipe from 5.75 to 1.5 inches, a considerable increase in the 50 per cent point was experienced. This is attributed to a decrease in the height of the secondary vortex resulting in a decrease in retention time of particles in the centrifugal force field. This is substantiated further by the decrease in coarse-particle separation efficiency (Table 2). Another factor contributing to the effect of the secondary vortex is the volume of the slurry moving upward in the secondary vortex. That is, since the break-plate diameter was reduced for run V, less material would be diverted upward, and since less material was being subjected to centrifugal force, less total separation would take place.

Length of test section and distance between impeller and overflow-pipe outlet.--From run VII-M, Figure 23, it can be observed that a slight decrease in the 50 per cent point was experienced by extending the test-section length. The effect of lengthening the vortex core, that is, the distance between the impeller and overflow outlet, is shown in run VIII-M, Figure 24. It is apparent that by extending the distance between the impeller and the overflow outlet from 4.63 to 19 inches, an increase in the 50 per cent point is experienced. This increase is about 10 microns at 15 to 20 pounds per second feed rate and about 20 microns at 5 to 10 pounds per second feed rate. Run VIII-M exhibits a slightly lower coarse-particle separation efficiency than run IV-M and a slightly higher fine-particle separation efficiency. This indicates that by increasing the

area through which liquid can flow to the core, more coarse solids are carried out in the overflow, resulting in a high percentage of the total feed being transferred out of the overflow and a decrease in the percentage of water volume split to the underflow. By comparing the data in Table 2 for runs IV-M and VIII-M, it can be seen that the above trends are evident.

Effect of tangential underflow discharge.--Run IX-M, Figure 25, shows the data obtained using a tangential discharge for the underflow. It appears from the scatter of the data around the base line that the tangential discharge had little affect on the operation of the device.

Effect of solids concentration in the underflow and water volume split to the underflow.--A consideration of run X-M, Figure 26, indicates that a decrease in underflow solids resulted in separation at a lower 50 per cent point. This would be expected, since as water is robbed from the overflow, accompanying fine solids would be split into the underflow. This result would tend to decrease the 50 per cent separation point. The increase in water volume split for run X-M over IV-M, shown in Table 2, indicates that a greater percentage of the total water in the feed did report to the underflow. This indicates that as less liquid is moving through a given area of the vortex to the core, the velocity normal to the core is decreased, and smaller particles are permitted to move toward the periphery of the section and out of the underflow.

Effect of feed-slurry concentration.--Run XI-M, Figure 27, was conducted at approximately 25 per cent solids in the feed. Since the base line is representative of runs made at about 15 per cent solids, Figure 27 should indicate the effect of an increase in solids concentration in the feed.

However, while maintaining an underflow, solids concentration of 50 to 55 per cent, the percentage of feed water split to the underflow was increased to about 30 per cent in run XI-M. Thus, it would be better to state that Figure 27 indicates the effect of an increased feed-solids concentration at approximately constant underflow-solids concentration. Run XII-M was conducted with the same feed as run XI-M, but the underflow-solids concentration was increased to about 72 per cent. The resulting point was plotted on Figure 27 for reference. This run indicates that increased feed-solids concentration produces an increase in 50 per cent point at increased underflow-solids concentration. This can be explained by considering the volume split to the underflow. In run XI-M, the volume split (Table 2) was about 30 per cent and in run XII-M about 9 per cent. It is interesting to note that by applying simple proportions to runs X-M and XII-M, the predicted lines shown in Figure 27 for 72 per cent solids were obtained. This was done as follows:

Average underflow solids--run IV-M = 51.7 per cent

Average underflow solids--run X-M = 44.4 per cent

Intercept of the base line--Figure 26 = 157

Intercept of operative line--Figure 26 (run X-M) = 115

Underflow solids--run XII-M = 72.2

$$\frac{157 - 115}{51.7 - 44.4} = \frac{\text{XII-M intercept} - 157}{72.2 - 51.7}$$

Solving this for run XII-M intercept, the intercept would be equal to 272.

It is of interest also that the coarse-particle separation efficiency remained in the middle 90's for run XII-M, but the fine-particle efficiency was drastically reduced. After considering runs X-M, XI-M, and XII-M, it is apparent that detailed investigations need to be made on the effect of volume-split and underflow-solids concentration; however, it seems reasonable to state that the fixed-impeller device as designed perhaps should be operated with feed-solids concentration between 20 and 25 per cent and underflow-solids concentration in excess of 60 per cent to achieve separation at larger particle sizes than was experienced with the base-line operation shown in Figure 27.

Effect of density of solids.--Run XIII, Figure 28, indicates that an increase in the density of the solids in the feed slurry results in separation at finer particle sizes. It is of interest to note that if the densities of the slurries (equation 39) are taken as 1.0 gram per cubic centimeter, that the intercept of the predicted line would be increased from 107.4 to 108.6. This slight difference indicates that for water-solids slurries, a negligible error will be introduced by using 1.0 gram per cubic centimeter for the density of slurry in equation 40, up to a feed concentration of about 15 per cent solids.

Pressure Drop Studies

From Figure 29 it appears that the energy requirements for the fixed-impeller device are less than that of the conventional cyclone. Another variable, the underflow diameter, must be considered in addition to the inlet and overflow diameters in calculating the capacity ratio for the fixed-impeller device. Since the underflow parameter lines are

approximately parallel, a consideration of the intercept of these lines should permit an evaluation of capacity ratio for the device for underflows in the range investigated. Figure 30 is a plot of these K_{CR} values as a function of underflow diameter, and the equation shown on the figure is applicable over the range studied. For example, if the capacity ratio was desired for a 0.8-inch underflow pipe and a 1.75-inch overflow pipe, the 0.8-inch diameter would be substituted in the equation of Figure 30 and the K_{CR} value obtained. Using this K_{CR} value in the equation of Figure 29, the capacity ratio could be calculated, and at a specific flow rate, the energy loss could be determined. It should be pointed out that the relationships of Figures 29 and 30 are applicable only to the over-all geometry of runs I-M through IV-M. In order to obtain a more generalized relationship for energy loss in the fixed-impeller device, a detailed investigation of this variable as a function of geometric and operative factors will have to be performed. However, in view of the results shown in Figure 29, the reasoning advanced earlier in this work concerning energy loss is sound. That is, because of the overflow discharges out of the bottom of the device, the energy loss should always be lower for the fixed-impeller device than for a comparable conventional cyclone.

Comparison with Cyclone and Open-Top Cyclone

From Figure 31 it can be seen that for a specific flow rate, the fixed-impeller device separates at a considerably higher 50 per cent point than a conventional cyclone but lower than an open-top cyclone. In this comparison Dahlstrom's equation (3) has been used with equivalent overflow

and inlet diameters to those of the fixed-impeller device. However, the open-top cyclone data were obtained by Emmett (22) on a 30-inch diameter model. These data were included for interest, but, in view of the size of the equipment, it does not appear to be a fair comparison. Since completing the planned investigation of this work, it has become apparent that the diameter of the device should be investigated for its effect on separation.

Figure 32 presents a comparison of "sharpness" of separation for the cyclone, the fixed-impeller device and the open-top cyclone. Run 117 of the open-top cyclone and run II-M-5a were plotted on the basis of approximately equivalent 50 per cent separation points. The flow rate for the open-top cyclone was about eight times that of the fixed-impeller device. It is evident that the cyclone gives a sharper separation than the fixed-impeller device, but for some applications, this difference in sharpness would be acceptable with separation at a large 50 per cent point. The comparison of run II-M-5a with the open-top cyclone is of interest since the separation is slightly sharper with the open-top cyclone. Here, as in the case of point of separation (Figure 31), it must be remembered that the sizes and flow rates of the two devices are vastly different.

In Figure 32 the cyclone has been considered to separate more sharply than the fixed-impeller device on the basis of the slopes of the curves. The graphical representation of sharpness presents a better picture of the separation sharpness than either course- or fine-particle separation efficiencies, as defined, or Taggart efficiency (21). This seems evident when one considers that the Taggart efficiency calculated for the

cyclone data of Figure 32 is equal to about 75 per cent whereas this efficiency for run II-M-1 is equal to about 73. The coarse- and fine-particle separation efficiencies for the cyclone run have been calculated to be 98.5 and 82.4, respectively, whereas these same efficiencies were 98.50 and 69.90 for run II-M-1. However, the coarse-particle separation efficiency, as defined, should be useful for applications where it is desirable to maintain an overflow with a minimum of +50 per cent point particles. In this case, the higher the coarse-particle separation efficiency, the better the assignment would be accomplished. The fine-particle efficiency should be useful when the opposite of the above is the case.

CHAPTER VI

CONCLUSIONS AND RECOMMENDATIONS

The conclusions resulting from the present investigation may be summarized as follows:

1. The equations developed for the impeller design proved to be satisfactory and should be useful in future blade design using a segment of a circle as the blade contour. Also, the method of derivation of the equations should be applicable for deriving equations for other blade contours.

2. The test section designed with "doughnut" flanges, recessed O-ring gaskets, and tie rods permitted a rapid change in length of test section and other geometric variables. It would be applicable and should find wide acceptance to experimental equipment where rapid change in geometric variables is desired.

3. An equation (number 40) has been developed for predicting the 50 per cent separation point for the fixed-impeller device with a specific blade contour, blade angle, and for a specific geometry. This equation relates the overflow diameter, the flow rate, and the solid and slurry density to the 50 per cent point.

4. It has been demonstrated that the exponents of this equation do not vary appreciably with geometry. The effect of changing geometric variables is a change in the K_1 value of the equation.

5. It has been advanced that the exponent on the blade-angle relationship of equation 8 should be the same as that of the overflow

diameter, i.e., 0.77. It has been shown that the 50 per cent point increases with decreasing flow rate and increasing overflow diameter.

6. An increase in the break-plate diameter results in separation at a larger 50 per cent point with little change in separation sharpness.

7. A decrease in the distance between the break plate and overflow-pipe outlet results in separation at a larger 50 per cent point with a decrease of about 7 per cent in coarse-particle separation sharpness.

8. An increase in the length of the vortex produces separation at a larger 50 per cent point with a decrease of about 4 per cent in separation sharpness (as defined by coarse-particle separation efficiency).

9. The change from perpendicular to tangential discharge for the underflow pipe indicates no appreciable change in 50 per cent point or separation sharpness.

10. A decrease in underflow-solids concentration results in a lower 50 per cent point with negligible effect on separation sharpness.

11. An increase in feed-solids concentration produces a lowering of the 50 per cent point at fixed underflow solids. However, when underflow solids were increased along with feed solids, the result was an increase in 50 per cent point with a decrease in separation sharpness.

12. The capacity ratio ($GPM/F^{0.5}$) for the fixed-impeller device is larger than for the conventional cyclone. Thus, as predicted, the energy loss is less for the fixed-impeller separator. Capacity ratio was found to vary (at fixed inlet velocity) with overflow diameter, with underflow diameter as a parameter.

13. For a given flow rate, comparable geometric and operating factors, the fixed-impeller separator produces a higher 50 per cent point

than the conventional cyclone. The sharpness of separation, as defined by Taggart (21) and by coarse- and fine-particle separation efficiencies defined in this work, was about the same for the two separations. However, a graphical method presented for determining separation sharpness indicates that the cyclone produces a sharper separation than the fixed-impeller separator. Comparison tests with the open-top cyclone were considered inconclusive in view of the drastic difference in size and flow rates of the two devices. However, it is of interest to note that for comparable 50 per cent point, the separation sharpness, by the graphical method, is slightly sharper for the open-top cyclone than for the fixed-impeller separator.

Within the range investigated, it appears that the fixed-impeller centrifugal separator could be used to extend the separation-point range of the liquid-solid cyclone. However, additional work should be undertaken as follows:

1. Tests should be performed with an increase in the ratio of overflow diameter to the section diameter. The results of such an investigation would show whether the trend of increased 50 per cent point with increased overflow diameter would continue.

2. The effect of changing blade angle should be investigated to determine the relationship of this variable with the 50 per cent point.

3. A detailed investigation of the effect of feed volume split to the overflow and underflow should be conducted. This should include a consideration of 50 per cent point and separation sharpness.

4. The effect of section diameter should be investigated with an extension in the range (above and below) of the ratio between the overflow diameter and section diameter.

5. Detailed energy-loss studies should be performed in order to develop a relationship for energy loss as a function of geometry and operating variables.

The pursuit of these recommendations and continued development of the fixed-impeller centrifugal separator could well lead to its acceptance into the industrial family of separation equipment.

APPENDICES

NOMENCLATURE

A_b	Cross-sectional area (square inches)
A_1	Entrance area of impeller at leading edge of blades
A_2	Discharge area of impeller at trailing edge of blades
b	Inlet diameter (inches)
C	Height of blade (feet)
c	Constant in equations 1, 7, and 8
D	Diameter (inches)
D_R	Equivalent round pipe diameter to give a velocity V_3 for flow rate Q
D_s	Diameter of particles (feet)
d	Thickness of blade (inches)
E	Underflow diameter (inches)
e	Overflow diameter (inches)
F	Energy loss (feet)
G	Flow rate (pounds per second)
g	Acceleration due to gravity (32.2 feet/second/second)
GPM	Flow rate (gallons per minute)
h_L	Head loss (feet)
K	Proportionality constant, equation 7
K_1	Proportionality constant, equation 8
K_{CR}	Proportionality constant, equation 41
K^1	Proportionality constant, equation 9
Mx	Weight of solids retained on a specific screen in overflow sample

My	Weight of solids retained on a specific screen in underflow sample
P	Pressure (pounds per square inch)
Q	Flow rate (cubic feet per second)
$\frac{Q}{F^{0.5}}$	Capacity ratio (or $GPM/F^{0.5}$)
q	Constant in equations 1, 7, and 8
R	Radius of arc of blade (feet)
r	Radius of tube section (inches)
S	Percentage of solids in feed
T	Constant in equations 1, 7, and 8
t	Time (seconds)
U.F.	Underflow
u	Approach velocity to vane (feet per second)
u_s	Settling velocity of particle (feet per second)
V	Tangential velocity
V_r	Radial velocity
V_1	Velocity at blade entrance
V_2	Velocity at trailing edge of blade
V_3	Whirl velocity
W_c	Weight of solids greater than the 50 per cent point in feed
W_F	Weight of solids less than the 50 per cent point in feed
W_o	Weight of solids less than the 50 per cent point in overflow
W_v	Weight of solids greater than the 50 per cent point in overflow
x	Overflow rate (pounds per second)

Y	Underflow rate (pounds per second)
α	Blade angle as measured between a tangent to the blade at the trailing edge and the horizontal
Γ	Circulation (constant)
μ	Partical size in microns at the 50 per cent point (point at which a particle of specific size reports equally by weight to the overflow and underflow)
μ_s	Viscosity of slurry
π	Constant (3.1416)
ρ	Density of slurry
ρ_s	Density of solid

Table 1. Sieve Analysis of Sand

U. S. Standard Sieve No.	A.F.S.† 85-90	A.F.S.† No. 45	Dawes No. 2035	Mixture 3-2-1†† Proportion
20	----	----	9.8	0.99
30	0.1	6.5	52.0	6.56
35	----	----	19.5	1.89
40	3.3	27.5	9.0	7.50
50	9.2	30.3 -(40)	9.7	8.07
70	16.7	19.5	----	8.15
100	27.2	9.9	----	10.72
140	24.8	4.5	----	9.09
200	12.4	1.1	----	4.24
270	4.5	0.2	----	1.32
-270	1.4	0.1	----	0.45

†A.F.S. (American Foundrymen's Society Standard).

††3 parts No. 85-90, 2 parts No. 45, and 1 part No. 2035.

Table 2. Calculated Data for Separation Studies

Run I-M

U.F. Diameter - 3/8-inch--(I-M-4) and I-M-5; 1/2-inch--I-M-2 and I-M-3, 3/4-inch--I-M-1.
O.F. Diameter - 2-inch standard pipe.
O.F. Height - 4-5/8-inch from tail cone of impeller.
Section Height - 18 inches.

Ring Height - 10-3/8 inches.
Ring Diameter - 5.00 inches.
Distance between break plate and overflow pipe - 5-3/4 inches.

Run	ΔP (psig)	Flow Rate (lbs./sec.) O.F.	U.F.	Total	Percentage[1] to U.F.	Percentage of Solids Feed	O.F.	U.F.	50 Per Cent Separation Point (microns)	Correlation Coefficient
I-M-1	17.0	11.00	9.20	20.20	34.4	17.20	0.41	37.30	35	0.226
I-M-2	10.1	9.94	5.32	15.26	21.4	18.37	1.41	50.07	45	0.274
I-M-3	7.0	7.89	3.97	11.86	20.6	17.46	1.53	49.13	50	0.325
I-M-4	2.5	3.93	2.20	6.13	24.8	17.10	2.72	42.80	60[2]	0.510
I-M-5	1.0	2.97	0.907	3.877	14.6	14.11	3.80	47.90	110	0.693
I-M-4a	2.6	5.35	1.76	7.11	14.2	15.02	3.48	50.10	70	0.459

Run II-M

U.F. Diameter - 3/4-inch rubber tubing (variable from 3/4 inch to 0).
O.F. Diameter - 1-inch standard pipe.
O.F. Height - 4-5/8 inches.
Section Height - 18 inches.

Ring Height - 10-3/8 inches.
Ring Diameter - 5.00 inches.
Distance between break plate and overflow pipe - 5-3/4 inches.

Run	ΔP (psig)	Flow Rate (lbs./sec.) O.F.	U.F.	Total	Percentage to U.F.	Percentage of Solids Feed	O.F.	U.F.	50 Per Cent Separation Point (microns)	Correlation Coefficient
II-M-1	25.0	7.30	3.38	10.68	17.3	17.74	0.52	54.96	33	0.207
II-M-2	17.0	6.00	2.56	8.56	19.5	13.26	0.44	43.31	37.5	0.240
II-M-3	10.0	4.57	1.20	5.77	9.2	9.90	0.65	53.47	49.0	0.314
II-M-4	3.5	2.85	0.715	3.565	8.9	13.51	1.36	61.97	70	0.434
II-M-5	1.0	1.765	0.367	2.132	8.4	12.15	2.99	56.00	131[3]	0.617
II-M-5a	2.0	2.03	0.503	2.533	10.7	13.99	4.25	53.30	97	0.549

Run III-M

O.F. Diameter - 1-1/4-inch standard pipe--III-M-1; 1-1/2-inch--III-M-2; 2-1/2-inch--III-M-3.
U.F. Diameter - 3/4-inch rubber tubing (variable from 3/4 inch to 0).
O.F. Height - 4-5/8 inches.
Section Height - 18 inches.

Ring Height - 10-3/8 inches.
Ring Diameter - 5.00 inches.
Distance between plate and overflow pipe - 5-3/4 inches.

Run	ΔP (psig)	Flow Rate (lbs./sec.) O.F.	U.F.	Total	Percentage to U.F.	Percentage of Solids Feed	O.F.	U.F.	50 Per Cent Separation Point (microns)	Correlation Coefficient
III-M-1	17.3	8.18	3.67	11.85	16.9	17.54	0.78	54.90	35	0.239
III-M-2	12.8	8.22	3.60	11.82	16.4	17.65	1.14	55.40	40	0.269
III-M-3	5.0	8.75	3.07	11.82	14.3	15.30	1.93	53.40	55	0.374

(Continued)

Table 2. Calculated Data for Separation Studies (Continued)

Run IV-M

U.F. Diameter - 3/4-inch rubber tubing (variable from 3/4 inch to 0).
O.F. Diameter - 2-1/2-inch standard pipe.
O.F. Height - 4-5/8 inches.
Section Height - 18 inches.

Ring Height - 10-3/8 inches.
Ring Diameter - 5.00 inches.
Distance between break plate and overflow pipe - 5-3/4 inches.

Run	ΔP (psig)	Flow Rate (lbs./sec.) O.F.	U.F.	Total	Percentage to U.F.	Percentage of Solids Feed	O.F.	U.F.	50 Per Cent Separation Point (microns)	Correlation Coefficient
IV-M-1	14.9	13.83	5.05	18.88	13.6	16.55	1.56	57.60	42	0.273
IV-M-2	11.1	11.90	5.32	17.22	18.6	16.42	1.62	49.50	45	0.291
IV-M-3	7.0	9.60	4.25	13.85	18.2	17.15	2.24	50.80	50(4)	0.356
IV-M-4	3.0	6.15	3.35	9.50	23.7	17.02	2.25	44.10	47(4)	0.435
IV-M-5	1.0	4.33	1.30	5.63	14.3	14.48	4.82	46.69	101	0.620
IV-M-6(5)	5.0	8.75	3.07	11.82	14.3	15.30	1.93	53.40	55	0.374
IV-M-7	2.5	5.20	3.60	8.80	25.5	23.40	3.52	52.30	66	0.458
							Ave.	51.7		

Run V-M

Equipment setup same as for run IV-M with the exception that the ring diameter = 4.00 inches.

Run	ΔP (psig)	Flow Rate (lbs./sec.) O.F.	U.F.	Total	Percentage to U.F.	Percentage of Solids Feed	O.F.	U.F.	50 Per Cent Separation Point (microns)	Correlation Coefficient
V-M-1	13.75	15.20	5.40	20.60	14.7	14.95	1.74	52.30	46	0.257
V-M-2	9.50	11.05	4.10	15.15	15.2	14.72	1.72	52.70	49	0.317
V-M-3	7.50	10.50	4.10	15.60	14.6	16.60	2.36	53.20	54	0.310
V-M-4	3.00	7.30	2.23	9.53	12.8	14.90	3.06	53.30	78	0.434
V-M-5	1.00	5.02	1.05	6.07	8.8	13.50	4.54	56.20	125	0.590
V-M-5a	2.00	5.70	1.87	7.57	13.7	17.23	5.133	54.10	92	0.508

Run VI-M

Equipment setup same as for run IV-M with the exception that the break plate was 1-1/2 inches from top of overflow pipe.

Run	ΔP (psig)	Flow Rate (lbs./sec.) O.F.	U.F.	Total	Percentage to U.F.	Percentage of Solids Feed	O.F.	U.F.	50 Per Cent Separation Point (microns)	Correlation Coefficient
VI-M-1	14.00	13.60	3.40	17.00	11.0	12.82	3.05	51.90	72	0.292
VI-M-2	10.75	11.85	3.00	14.85	11.8	12.09	2.82	48.70	75	0.320
VI-M-3	6.90	10.05	2.55	12.60	11.0	13.78	3.75	53.30	95	0.359
VI-M-4	2.50	6.55	1.30	7.85	9.1	12.68	4.77	52.50	130	0.495
VI-M-5	1.25	4.13	0.60	4.73	7.2	11.33	5.61	50.70	175	0.698

(Continued)

Table 2. Calculated Data for Separation Studies (Continued)

Run VII-M

Same conditions as run IV-M except overflow pipe was 14.25 inches longer and test section height was 32.25 inches.

Run	ΔP (psig)	Flow Rate (lbs./sec.) O.F.	U.F.	Total	Percentage to U.F.	Percentage of Solids Feed	O.F.	U.F.	50 Per Cent Separation Point (microns)	Correlation Coefficient
VII-M-1	14.25	14.10	4.05	18.15	12.0	13.42	1.87	53.66	44	0.279
VII-M-2	9.40	10.95	3.40	14.35	12.7	14.27	1.94	54.01	45	0.529
VII-M-3	6.50	9.05	3.055	12.11	13.6	15.56	2.29	54.77	49	0.368
VII-M-4	2.90	5.98	1.75	7.7	13.3	15.47	3.61	55.75	70	0.502
VII-M-5	1.30	3.525	0.750	4.28	9.6	12.50	4.24	51.34	105	0.750

Run VIII-M

Same as run VII-M except that the overflow height was 19 inches from tail cone of impeller.

Run	ΔP (psig)	Flow Rate (lbs./sec.) O.F.	U.F.	Total	Percentage to U.F.	Percentage of Solids Feed	O.F.	U.F.	50 Per Cent Separation Point (microns)	Correlation Coefficient
VIII-M-1	11.50	14.40	4.30	18.40	13.4	13.84	2.56	50.65	55	0.278
VIII-M-2	9.30	12.15	3.16	15.31	10.8	13.51	2.78	54.77	70	0.314
VIII-M-3	6.25	11.00	3.69	14.69	14.5	15.31	3.26	51.25	70	0.324
VIII-M-4	3.00	7.80	2.00	9.80	11.3	13.52	3.67	51.95	84	0.425
VIII-M-5	1.90	4.65	0.865	5.552	8.2	13.45	5.68	55.23	180(6)	0.630

Run IX-M

Same as run IV-M except tangential discharge.

Run	ΔP (psig)	Flow Rate (lbs./sec.) O.F.	U.F.	Total	Percentage to U.F.	Percentage of Solids Feed	O.F.	U.F.	50 Per Cent Separation Point (microns)	Correlation Coefficient
IX-M-1	10.50	12.35	6.27	18.62	21.0	17.97	2.30	48.85	40	0.275
IX-M-2	8.40	11.85	4.25	16.10	14.1	16.60	2.63	55.58	50	0.304
IX-M-3	5.00	9.15	3.44	12.59	17.1	14.97	3.07	46.65	53	0.359
IX-M-4	2.75	5.55	2.28	7.83	16.0	18.47	3.45	55.05	60	0.496
IX-M-5	1.31	4.575	1.54	6.12	15.0	15.86	4.28	50.27	80	0.586

(Continued)

Table 2. Calculated Data for Separation Studies (Continued)

Run X-M

Same as run IV-M except low (approximately 40 per cent) solids in underflow.

Run	ΔP (psig)	Flow Rate (lbs./sec.) O.F.	U.F.	Total	Percentage to U.F.	Percentage of Solids Feed	O.F.	U.F.	50 Per Cent Separation Point (microns)	Correlation Coefficient
X-M-1	10.75	11.95	6.25	18.20	23.4	16.27	2.26	43.08	35	0.279
X-M-2	8.00	10.20	5.15	15.35	22.4	16.36	2.24	44.35	39	0.314
X-M-3	5.10	8.55	3.83	12.38	20.8	14.94	2.46	42.86	45	0.362
X-M-4	2.75	6.15	2.85	9.00	20.2	17.02	3.19	46.88	53	0.451
X-M-5	1.40	4.45	1.97	6.42	20.3	16.46	3.91	44.90	64	0.568

Run XI-M

Same as run IV-M except feed concentration equals approximately 25 per cent solids.

Run	ΔP (psig)	Flow Rate (lbs./sec.) O.F.	U.F.	Total	Percentage to U.F.	Percentage of Solids Feed	O.F.	U.F.	50 Per Cent Separation Point (microns)	Correlation Coefficient
XI-M-1	9.75	10.35	9.13	19.48	30.5	25.49	2.51	51.56	30	0.267
XI-M-2	7.25	8.95	8.15	17.10	32.0	25.24	2.88	49.80	30	0.291
XI-M-3	4.75	7.30	6.70	14.00	29.4	28.84	3.69	56.26	36	0.334
XI-M-4	2.50	5.30	5.48	10.78	33.5	29.87	5.15	53.79	40	0.399
XI-M-5	1.00	3.65	3.86	7.51	34.2	30.82	6.48	53.84	53	0.510

Run XII-M

Same as run XI-M-1 except underflow solids were approximately 70 per cent.

Run	ΔP (psig)	Flow Rate (lbs./sec.) O.F.	U.F.	Total	Percentage to U.F.	Percentage of Solids Feed	O.F.	U.F.	50 Per Cent Separation Point (microns)	Correlation Coefficient
XII-M-1	11.00	14.85	4.80	19.65	8.72	22.41	6.29	72.30	77	0.265

Run XIII-M

Same as run IV except barytes (density of 4.42 gm./cc.) was substituted for the sand.

Run	ΔP (psig)	Flow Rate (lbs./sec.) O.F.	U.F.	Total	Percentage to U.F.	Percentage of Solids Feed	O.F.	U.F.	50 Per Cent Separation Point (microns)	Correlation Coefficient
XIII-M-1	11.9	13.95	4.34	18.29	12.3	16.43	3.90	56.72	30	0.279
XIII-M-2	8.7	12.00	3.55	15.55	11.6	16.38	4.26	57.36	37	0.310
XIII-M-3	6.1	9.90	2.93	12.83	13.1	15.47	4.83	52.45	37	0.354
XIII-M-4	3.1	7.18	1.69	8.87	11.0	14.06	5.52	50.36	45	0.455
XIII-M-5	1.9	5.50	0.883	6.38	7.7	12.48	6.27	51.22	56	0.570

1. Percentage to underflow means percentage by weight of water in feed reporting to underflow.
2. Unexplained experimental error.
3. Unstable operating range.
4. Unexplained experimental error.
5. Same as run III-M-5.
6. Unstable operating range.

Table 3. Separation Efficiencies

Run	50 Per Cent Point (microns)	Particle Separation Efficiency		Taggart Efficiency (21)
		Fine	Coarse	
I-M-1	35	63.80	98.90	57.61
I-M-2	45	84.40	95.30	81.86
I-M-3	50	80.60	94.90	75.39
I-M-4	60	72.72	95.05	-----
I-M-5	110	60.20	83.80	44.03
I-M-4a	70	75.40	89.80	66.80
II-M-1	33	69.90	98.50	72.79
II-M-2	37.5	80.74	89.93	70.37
II-M-3	49.0	82.91	97.09	91.91
II-M-4	70	79.62	92.15	75.28
II-M-5	131	75.37	87.61	-----
II-M-5a	97	77.50	58.20	63.07
III-M-1	35	69.09	98.46	67.53
III-M-2	40	73.01	96.96	69.76
III-M-3	55	77.16	94.02	70.98
IV-M-1	42	77.26	94.68	86.18
IV-M-2	45	71.39	95.04	66.41
IV-M-3	50	73.71	93.24	66.87
IV-M-4	47	70.74	93.45	-----
IV-M-5	101	81.08	79.91	62.71
IV-M-6	55	77.16	94.02	-----
IV-M-7	66	72.08	93.15	65.18
V-M-1	46	82.19	94.26	76.42
V-M-2	49	81.02	95.14	76.10
V-M-3	54	79.78	93.47	73.08
V-M-4	78	57.48	87.10	44.62
V-M-5	125	-----	-----	-----
V-M-5a	92	76.86	85.08	61.97
VI-M-1	72	83.76	87.67	71.41
VI-M-2	75	73.02	88.20	61.23
VI-M-3	95	74.83	85.79	60.60
VI-M-4	130	71.06	80.42	51.52
VI-M-5	175	75.78	76.78	52.61

(Continued)

Table 3. Separation Efficiencies (Continued)

Run	50 Per Cent Point (microns)	Particle Separation Efficiency		Taggart Efficiency (21)
		Fine	Coarse	
VII-M-1	44	80.23	93.03	73.21
VII-M-2	45	79.56	93.20	72.71
VII-M-3	49	81.44	93.17	74.55
VII-M-4	70	79.88	88.00	67.87
VII-M-5	105	77.74	81.85	58.19
VIII-M-1	55	83.22	90.00	73.23
VIII-M-2	70	81.43	90.29	71.71
VIII-M-3	70	79.50	90.43	70.05
VIII-M-4	84	80.99	86.12	67.31
VIII-M-5	180	81.68	86.70	68.39
IX-M-1	40	68.90	93.75	62.58
IX-M-2	50	79.58	92.73	65.75
IX-M-3	53	81.48	90.43	71.92
IX-M-4	60	78.44	91.07	69.56
IX-M-5	80	76.51	83.86	61.28
X-M-1	35	66.19	92.96	59.18
X-M-2	39	70.69	93.32	64.07
X-M-3	45	73.34	92.00	65.35
X-M-4	53	74.64	91.38	66.05
X-M-5	64	73.39	88.73	62.23
XI-M-1	30	62.24	95.42	57.65
XI-M-2	30	58.02	94.80	52.40
XI-M-3	36	64.42	94.45	58.70
XI-M-4	40	61.61	92.69	54.16
XI-M-5	53	60.04	91.75	51.81
XII-M-1	77	54.60	94.67	49.29
XIII-M-1	30	69.42	85.12	54.53
XIII-M-2	37	73.56	86.60	60.14
XIII-M-3	37	74.67	83.61	58.32
XIII-M-4	45	80.35	81.26	61.65
XIII-M-5	56	88.00	85.16	73.09

Table 4. Operative Data of Separation Investigation

Run I-M

U.F. Diameter - (3/8 inch--I-M-4 and 5) (1/2 inch--I-M-2 and 3) (3/4 inch--I-M-1) standard pipe
O.F. Diameter - 2-inch standard pipe
O.F. Height - 4-5/8 inch from tail cone of impeller
Section Height - 18 inches
Ring Height - 10-3/8 inches
Ring Diameter - 5.00 inches
Distance between break plate and overflow pipe - 5-3/4 inches

Run	ΔP (psig)	Underflow			Overflow			Time (sec.)	Flow Rate (lbs./sec.)	
		Tare	Wt.	Lbs.	Tare	Wt.	Lbs.		U.F.	O.F.
I-M-1	17.0	62.5	108.5	46.0	55.0	110.0	55.0	5	9.2	11.0
I-M-2	10.1	62.5	89.1	26.6	55.5	105.2	49.7	5	5.32	9.94
I-M-3	7.0	63.5	103.2	39.7	55.2	134.1	78.9	10	3.97	7.89
I-M-4	2.5	63.6	85.6	22.0	55.3	94.6	39.3	10	2.2	3.93
I-M-5	1.0	63.9	76.5	13.6	55.3	99.9	44.6	15	0.907	2.97

Run II-M

U.F. Diameter - 3/4-inch rubber tubing (variable from 3/4 inch to 0)
O.F. Diameter - 1-inch standard pipe
O.F. Height - 4-5/8 inches
Section Height - 18 inches
Ring Height - 10-3/8 inches
Ring Diameter - 5.00 inches
Distance between break plate and overflow pipe - 5-3/4 inches

Run	ΔP (psig)	Underflow			Overflow			Time (sec.)	Flow Rate (lbs./sec.)	
		Tare	Wt.	Lbs.	Tare	Wt.	Lbs.		U.F.	O.F.
II-M-1	29.0	62.7	97.5	33.8	60.0	133.0	73.0	10	3.38	7.3
II-M-2	17.0	62.7	88.3	25.6	56.0	116.0	60.0	10	2.56	6.0
II-M-3	10.0	62.5	80.5	18.0	56.0	124.5	68.5	15	1.20	4.57
II-M-4	3.5	62.2	76.5	14.3	56.0	113.0	57.0	20	0.715	2.85
II-M-5	1.0	61.5	72.5	11.0	56.0	109.0	53.0	30	0.367	1.765

Run III-M

U.F. Diameter - 3/4-inch rubber tubing (variable from 3/4 inch to 0)
O.F. Height - 4-5/8 inches
Section Height - 18 inches
Ring Height - 10-3/8 inches
Ring Diameter - 5.00 inches
Distance between break plate and overflow pipe - 5-3/4 inches

Run	O.F. Diameter Standard Pipe (inches)	ΔP (psig)	Underflow			Overflow			Time (sec.)	Flow Rate (lbs./sec.)		
			Tare	Wt.	Lbs.	Tare	Wt.	Lbs.		O.F.	U.F.	Total
III-M-1	1-2/4	17.3	61.5	98.2	36.7	56.2	138.0	81.8	10	8.18	3.67	11.85
III-M-2	1-1/2	12.8	61.5	97.5	36.0	56.5	138.7	82.2	10	8.22	3.60	11.82
III-M-3	2-1/2	5.0	62.5	93.2	30.7	55.5	142.0	87.5	10	8.75	3.07	11.82

Run IV-M

U.F. Diameter - 3/4-inch rubber tubing (variable from 3/4 inch to 0)
O.F. Diameter - 2-1/2-inch standard pipe
O.F. Height - 4-5/8 inches
Section Height - 18 inches
Ring Height - 10-3/8 inches
Ring Diameter - 5.00 inches
Distance between break plate and overflow pipe - 5-3/4 inches

Run	ΔP (psig)	Underflow			Overflow			Time (sec.)	Flow Rate (lbs./sec.)	
		Tare	Wt.	Lbs.	Tare	Wt.	Lbs.		O.F.	U.F.
IV-M-1	14.9	63.0	113.5	50.5	56.0	194.3	138.3	10	13.83	5.05
IV-M-2	11.1	62.5	115.2	53.2	56.0	175.0	119.0	10	11.90	5.32
IV-M-3	7.0	62.5	105.0	42.5	56.0	152.0	96.0	10	9.60	4.25
IV-M-4	3.0	62.5	96.0	33.5	56.5	118.0	61.5	10	6.15	3.35
IV-M-5	1.0	63.5	82.5	19.5	56.0	121.0	65.0	15	4.33	1.30
IV-M-6	See data for III-M-3									
IV-M-7	2.5	62.0	114.0	52.0	56.0	92.0	36.0	10	3.60	5.20

(Continued)

Table 4. Operative Data of Separation Investigation (Continued)

Run V-M

Equipment setup same as run IV-M with the exception that the ring diameter was equal to 4.00 inches.

Run	ΔP (psig)	Underflow Tare	Wt.	Lbs.	Overflow Tare	Wt.	Lbs.	Time (sec.)	Flow Rate (lbs./sec.) U.F.	O.F.
V-M-1	13.75	62.2	116.2	54.0	56.0	208.0	152.0	10	5.4	15.2
V-M-2	9.50	62.5	103.5	41.0	56.0	166.5	110.5	10	4.1	11.05
V M-3	7.30	62.5	103.5	41.0	56.0	161.0	105.0	10	4.1	10.5
V-M-4	3.00	62.7	85.0	22.3	56.0	129.0	73.0	10	2.23	7.3
V-M-5	1.00	63.5	84.5	21.0	56.5	157.0	100.5	20	1.05	5.02

Run VI-M

Equipment setup same as run IV-M with the exception that the break plate was 1-1/2 inches from top of overflow pipe.

Run	ΔP (psig)	Overflow Tare	Wt.	Lbs.	Underflow Tare	Wt.	Lbs.	Time (sec.)	Flow Rate (lbs./sec.) O.F.	U.F.
VI-M-1	14.00	56.0	192.0	136.0	62.0	96.0	34.0	10	13.60	3.40
VI M-2	10.75	56.5	175.0	118.5	63.0	93.0	30.0	10	11.85	3.00
VI M-3	6.90	56.5	157.0	100.5	63.0	88.5	25.5	10	10.05	2.55
VI-M-4	2.50	56.0	121.5	65.5	63.0	76.0	13.0	10	6.55	1.30
VI-M-5	1.25	56.5	139.0	82.5	63.0	75.0	12.0	20	4.13	0.60

Run VII-M

Same conditions as run IV-M except overflow pipe was 14.25 inches longer and test section height was 32.25 inches.

Run	ΔP (psig)	Overflow Tare	Wt.	Lbs.	Underflow Tare	Wt.	Lbs.	Time (sec.)	Flow Rate (lbs./sec.) O.F.	U.F.
VII-M-1	14.25	55.0	196.0	141.0	61.5	102.0	40.5	10	14.10	4.05
VII-M-2	9.40	56.5	166.0	109.5	62.5	96.5	34.0	10	10.95	3.40
VII-M-3	6.50	56.0	146.5	90.5	63.2	93.75	30.55	10	9.05	3.055
VII-M-4	2.90	56.2	116.0	59.8	62.5	80.0	17.5	10	5.98	1.75
VII-M-5	1.30	56.5	127.0	70.5	62.5	77.5	15.0	20	3.525	0.750

Run VIII-M

Same as run VII-M except the overflow height was 19 inches from tail cone of impeller.

Run	ΔP (psig)	Overflow Tare	Wt.	Lbs.	Underflow Tare	Wt.	Lbs.	Time (sec.)	Flow Rate (lbs./sec.) O.F.	U.F.
VIII-M-1	11.50	56.0	200.0	144.0	62.5	105.5	43.0	10	14.40	4.30
VIII-M-2	9.30	57.5	179.0	121.5	62.9	94.5	31.6	10	12.15	3.16
VIII-M-3	6.25	56.0	166.0	110.0	62.7	99.6	36.9	10	11.00	3.69
VIII-M-4	3.00	56.0	134.0	78.0	62.5	82.5	20.0	10	7.80	2.00
VIII-M-5	1.90	56.5	149.5	93.0	62.7	80.0	17.3	20	4.65	0.865

Run IX-M

Same as run IV-M except tangential discharge.

Run	ΔP (psig)	Overflow Tare	Wt.	Lbs.	Underflow Tare	Wt.	Lbs.	Time (sec.)	Flow Rate (lbs./sec.) O.F.	U.F.
IX-M-1	10.50	55.5	179.0	123.5	62.5	125.2	62.7	10	12.35	6.27
IX-M-2	8.40	56.5	175.0	118.5	64.5	107.0	42.5	10	11.85	4.25
IX-M-3	5.00	56.5	148.0	91.5	62.8	97.2	34.4	10	9.15	3.44
IX-M-4	2.74	56.5	122.0	65.5	62.7	85.5	22.8	10	6.55	2.28
IX-M-5	1.31	56.5	148.0	91.5	63.2	94.0	30.8	20	4.575	1.54

(Continued)

Table 4. Operative Data of Separation Investigation (Continued)

Run X-M

Same as run IV-M except low (approximately 40 per cent) solids in underflow.

Run	ΔP (psig)	Overflow			Underflow			Time (sec.)	Flow Rate (lbs./sec.)	
		Tare	Wt.	Lbs.	Tare	Wt.	Lbs.		O.F.	U.F.
X-M-1	10.75	55.5	175.0	119.5	62.0	124.5	62.5	10	11.95	6.25
X-M-2	8.00	56.5	158.5	102.0	62.5	114.0	51.5	10	10.20	5.15
X-M 3	5.10	56.5	142.0	85.5	62.5	100.75	38.25	10	8.55	3.825
X-M-4	2.75	56.5	118.0	61.5	62.7	91.2	28.5	10	6.15	2.85
X-M-5	1.40	56.5	145.5	89.0	62.5	101.8	39.3	20	4.45	1.965

Run XI-M

Same as run IV-M except feed concentration is approximately 25 per cent solids.

Run	ΔP (psig)	Overflow			Underflow			Time (sec.)	Flow Rate (lbs./sec.)	
		Tare	Wt.	Lbs.	Tare	Wt.	Lbs.		O.F.	U.F.
XI-M-1	9.75	55.5	159.0	103.5	63.2	159.5	91.3	10	10.35	9.13
XI-M-2	7.25	56.0	145.5	89.5	63.0	144.5	81.5	10	8.95	8.15
XI-M-3	4.75	56.5	129.5	73.0	63.2	130.2	67.0	10	7.30	6.70
XI-M-4	2.50	56.0	109.0	53.0	62.7	117.5	54.8	10	5.30	5.48
XI-M-5	1.00	56.0	129.0	73.0	63.0	140.2	77.2	20	3.65	3.86

Run XII-M

Same as run XI-M-1 except underflow solids were approximately 70 per cent.

XII-M-1	11.00	56.5	205.0	148.5	63.0	111.0	48.0	10	14.85	4.80

Runs V-M-5, II-M-5, and I-M-4 Repeat Data

Run	ΔP (psig)	Overflow			Underflow			Time (sec.)	Flow Rate (lbs./sec.)	
		Tare	Wt.	Lbs.	Tare	Wt.	Lbs.		O.F.	U.F.
V-M-5 (a)	2.00	56.5	142.0	85.5	62.5	90.5	28.0	15	5.7	1.87
II-M-5(a)	2.00	56.2	117.0	60.8	64.0	79.1	15.10	30	2.03	0.503
I-M-4 (a)	2.60	56.5	110.0	53.5	62.4	80.0	17.60	10	5.35	1.76

Run XIII-M

Same as run IV except barytes (density of 4.42 grams per cubic centimeter) was substituted for the sand.

Run	ΔP (psig)	Overflow			Underflow			Time (sec.)	Flow Rate (lbs./sec.)	
		Tare	Wt.	Lbs.	Tare	Wt.	Lbs.		U.F.	O.F.
XIII-M-1	11.9	56.0	195.5	139.5	61.0	104.4	43.4	10	4.34	13.95
XIII-M-2	8.7	56.0	176.0	120.0	61.5	97.0	35.5	10	3.55	12.00
XIII-M-3	6.1	56.0	155.0	99.0	61.5	90.8	29.3	10	2.93	9.90
XIII-M-4	3.1	56.2	128.0	71.8	61.3	78.2	16.9	10	1.69	7.18
XIII-M-5	1.9	58.0	223.0	165.0	68.0	94.5	26.5	30	0.883	5.50

Table 5. Analytical Data for Separation Investigations

Run I-M - Analysis

	I-M-1			I-M-2			I-M-3			I-M-4			I-M-5		
	O.F.-1	O.F.-2	U.F.	O.F.-1	O.F.-2	U.F.	O.F.-1	O.F.-2	U.F.	O.F.-1	O.F.-2	U.F.	O.F.-1	O.F.-2	U.F.
Wt. jar and sample	2426.2	2337.4	1560.0	2203.2	2204.5	1394.6	2443.1	2397.5	1445.1	2413.3	2385.5	1574.5	2439.7	2372.9	1216.5
Wt. jar	707.6	706.3	683.8	659.9	687.1	683.8	689.0	684.2	688.4	687.4	683.3	687.2	685.5	684.1	687.6
Wt. sample	3349.7		876.2	3030.7		710.8	3467.4		756.7	3426.1		687.3	3543.0		528.9
Wt. sand	13.6		326.9	42.6		355.9	53.2		371.8	93.3		294.5	134.9		253.4
Screen Analysis															
+40	-----		145.5	-----		140.8	-----		137.25	-----		110.75	----		67.80
+50	0.2		48.35	2.10		67.25	2.5		82.15	6.2		52.35	5.0		58.10
+70	0.4		35.65	2.4		57.35	3.6		49.55	23.6		37.85	8.9		39.60
+100	1.5		41.25	5.3		32.15	7.0		34.15	9.8		34.85	23.0		37.25
+140	2.5		29.95	8.8		33.85	12.9		36.95	18.6		31.95	43.0		29.35
+200	3.6		18.75	10.4		17.55	11.6		21.25	17.7		16.45	30.5		14.75
+250	1.278		4.751	4.62		4.69	4.52		5.01	5.20		4.41	24.5		4.85
+325	1.022		1.672	2.68		1.54	3.58		1.76	3.66		1.077	----		-----
-325	3.099		0.572	6.30		0.568	7.50		0.682	8.55		0.86	----		-----

Run II-M - Analysis

	II-M-1		II-M-2			II-M-3			II-M-4			II-M-5		
	O.F.	U.F.	O.F.-1	O.F.-2	U.F.	O.F.-1	O.F.-2	U.F.	O.F.-1	O.F.-2	U.F.	O.F.-1	U.F.	
Wt. jar and sample	2212.6	854.4	2182.8	2139.0	808.8	2209.8	2322.3	876.4	2457.0	2219.1	910.8	2302.8	928.3	
Wt. jar	684.1	682.6	684.4	683.8	68.18	681.9	685.5	686.5	685.6	684.1	688.7	680.9	687.5	
Wt. sample	1528.5	171.8	2953.6		127.0	3164.7		189.9	3306.4		222.1	1621.9	240.8	
Wt. sand	7.9	94.43	12.99		55.01	20.71		101.553	44.827		137.654	48.54	134.895	
Screen Analysis														
40	----	32.87	-----		17.73	------		------	------		------	-----	------	
50	----	18.88	-----		9.65	0.283		56.742	0.035		91.63	2.67	95.92	
70	0.27	10.76	-----		7.61	0.082		9.83	0.233		11.72	3.50	13.26	
100	0.12	11.62	-----		7.16	0.532		11.83	1.268		13.01	7.16	12.18	
140	0.11	9.95	-----		6.88	1.124		12.43	9.499		12.46	13.43	8.88	
200	0.48	6.97	0.44		4.80	3.155		7.70	12.45		6.58	10.96	3.59	
250	0.22	1.72	0.49		1.18	2.554		1.77	5.177		1.32	3.38	0.671	
325	0.72	1.03	1.32		0.74	2.702		0.775	4.60		0.565	2.16	0.213	
-325	5.98	0.63	10.74		0.26	10.278		0.486	11.565		0.369	5.28	0.181	

(Continued)

Table 5. Analytical Data for Separation Investigation (Continued)

Run III-M - Analysis

	III-M-1				III-M-2				III-M-3			
	O.F.-1		O.F.-2	U.F.	O.F.-1		O.F.-2	U.F.	O.F.-1		O.F.-2	U.F.
Wt. jar and sample	2351.0		2283.7	1022.2	2372.5		2296.4	985.8	2349.4		2250.0	1195.4
Wt. jar	683.6		688.8	683.5	683.4		683.6	684.9	688.5		683.2	686.2
Wt. sample		3262.3		338.7		3301.9		300.9		3227.7		509.2
Wt. sand		25.32		185.92		37.65		166.60		62.28		271.95
Screen Analysis												
40		-----		-----		-----		-----		-----		97.72
50		-----		91.38		-----		81.03		1.99		53.36
70		0.21		25.0		0.42		22.15		2.00		29.18
100		0.17		24.40		0.62		22.42		4.58		31.45
140		0.81		22.33		2.00		20.24		8.36		30.31
200		2.23		14.90		4.70		14.12		11.72		20.02
250		1.92		3.75		3.41		2.98		5.28		4.40
325		2.98		2.41		4.78		2.00		5.97		2.75
-325		17.00		1.75		21.72		1.66		22.78		2.76

Run IV-M - Analysis

	IV-M-1				IV-M-2			IV-M-3		IV-M-4		IV-M-5		IV-M-7		
	O.F.-1		O.F-2	U.F.	O.F.-1		O.F.-2	U.F.	O.F.	U.F.	O.F.	U.F.	O.F.	U.F.	O.F.-1(a)	O.F.-2(b)	U.F.
Wt. jar and sample	2176.7		2175.0	930.0	2263.5		2182.8	1100.7	2411.7	1009.1	2484.2	975	2500.9	1070.0	2384.5	2381.1	948.1
Wt. jar	684.4		683.3	682.7	683.9		685.8	681.9	687.9	684.0	686.7	684.3	685.0	687.4	683.5	684.5	683.3
Wt. sample		2983.9		247.3		3078.6		418.8	1723.8	325.1	1797.5	290.7	1815.9	382.6	170.1	1696.3	264.8
Wt. sand		46.58		142.24		49.82		206.9	38.54	165.47	40.33	128.45	87.46	178.67	------	------	138.23
Screen Analysis																	
40		-----		44.99		-----		64.20	-----	51.90	-----	40.82	-----	44.60	-----	-----	48.96
50		1.15		25.31		1.13		39.20	1.38	34.10	1.21	21.64	5.12	40.92	2.46	2.53	25.26
70		1.55		20.79		1.51		29.00	1.80	18.05	1.39	17.80	5.19	28.35	2.77	3.27	21.17
100		3.12		17.19		3.23		25.35	2.83	21.79	3.26	16.72	11.52	27.16	5.72	6.75	17.04
140		5.68		16.05		6.29		22.42	5.69	19.91	6.24	15.70	19.42	21.31	10.51	11.83	15.99
200		8.68		12.27		9.13		17.44	8.20	13.33	8.59	10.62	20.84	10.95	12.80	14.41	8.57
250		3.69		2.72		4.11		4.21	3.32	2.87	3.13	2.18	5.21	2.22	4.54	4.86	1.58
325		4.56		1.71		4.65		2.67	3.55	1.73	3.70	1.40	5.46	1.39	4.48	4.93	0.51
-325		18.15		1.21		19.77		2.41	11.77	1.79	12.81	1.57	14.70	1.81	13.87	13.92	1.15

(Continued)

Table 5. Analytical Data for Separation Investigation (Continued)

Run V-M - Analysis

	V-M-1			V-M-2			V-M-3			V-M-4			V-M-5	
	O.F.-1	O.F.-2	U.F.	O.F.-1	O.F.-2	U.F.	O.F.-1	O.F.-2	U.F.	O.F.-1	O.F.-2	U.F.	O.F.	U.F.
Wt. jar and sample	2289.8	2344.2	855.9	2260.2	2411.0	994.4	2391.4	2409.1	988.8	2425.0	2408.2	950.8	2550.0	920.5
Wt. jar	688.5	685.1	683.4	683.8	686.2	684.7	685.7	686.2	688.3	681.8	688.7	683.1	686.0	687.2
Wt. sample	3260.4	172.5		3301.2	309.7		3428.6	300.1		3462.7	267.7		1864.0	233.3
Wt. sand	56.71	90.33		56.77	163.06		81.07	159.13		106.07	142.66		84.68	131.06
Screen Analysis														
40	-----	24.94		-----	44.23		-----	45.96		-----	44.28		-----	47.46
50	0.75	18.23		0.60	29.06		1.27	27.49		3.41	25.28		3.02	25.80
70	1.02	13.01		0.86	23.35		1.67	23.57		4.76	20.87		4.30	19.06
100	2.52	14.66		1.26	23.42		4.44	21.14		11.75	18.94		10.47	16.67
140	6.12	12.47		5.73	21.57		10.47	20.48		27.53	16.11		18.24	11.47
200	9.77	3.22		10.15	15.20		17.18	14.05		29.19	9.59		18.91	6.52
250	4.64	1.85		4.63	2.61		6.96	2.96		7.19	4.98		6.30	1.44
325	5.72	1.14		5.90	1.93		7.55	1.78		9.64	1.18		5.64	1.68
-325	26.17	0.81		27.64	1.64		31.53	1.70		12.60	1.43		17.80	0.96

Run VI-M - Analysis 4/30/55

	VI-M-1			VI-M-2			VI-M-3			VI-M-4			VI-M-5	
	O.F.-1	O.F.-2	U.F.	O.F.-1	O.F.-2	U.F.	O.F.-1	O.F.-2	U.F.	O.F.-1	O.F.-2	U.F.	O.F.	U.F.
Wt. jar and sample	2265.1	2221.5	1198.0	2324.2	2318.0	998.3	2371.5	2432.2	993.4	2456.1	2365.6	939.3	2572.0	965.0
Wt. jar	686.2	686.1	687.1	683.7	684.7	683.2	685.2	682.7	688.0	681.7	698.4	683.1	680.9	683.4
Wt. sample	3114.3		510.9	3273.8		315.1	3455.8		305.4	3431.6		256.2	1891.1	281.6
Wt. sand	95.10		265.04	92.47		153.55	128.82		162.68	163.79		134.38	106.03	142.63
Screen Analysis														
30										-----		-----	-----	51.31
40	-----		81.56	-----		44.51	-----		60.33	-----		49.80	2.22	1.11
50	1.49		50.08	1.33		27.36	3.27		25.44	8.91		25.29	5.34	28.10
70	2.31		35.13	2.57		20.60	5.56		22.36	12.55		18.58	9.32	19.76
100	6.76		31.83	7.57		25.68	14.16		22.26	24.40		16.43	16.10	16.93
140	15.69		31.64	15.65		16.93	27.75		17.15	34.58		12.11	21.28	12.81
200	22.13		23.88	20.47		12.03	26.66		10.01	30.15		8.00	20.57	8.20
250	8.03		4.34	6.41		2.34	9.24		1.92	10.01		1.58	5.74	1.58
325	9.01		3.02	7.66		1.91	9.19		1.36	9.05		1.02	6.06	1.13
-325	29.68		3.56	30.53		2.19	32.99		1.85	34.04		1.57	19.40	1.70

(Continued)

Table 5. Analytical Data for Separation Investigations (Continued)

Run VII-M - Analysis 8/1/55

	VII-M-1			VII-M-2			VII-M-3			VII-M-4			VII-M-5		
	O.F.-1	O.F.-2	U.F.	O.F.-1	O.F.-2	U.F.	O.F.-1	O.F.-2	U.F.	O.F.-1	O.F.-2	U.F.	O.F.-1	O.F.-2	U.F.
Wt. jar and sample	2350.7	2357.8	949.5	2355.1	2385.8	976.5	2228.0	2475.2	991.6	2497.7	2348.2	953.2	2378.3	2462.0	940.7
Wt. jar	685.1	685.1	686.8	685.1	685.1	689.1	685.1	685.1	684.6	685.1	685.1	686.7	685.1	685.1	689.0
Wt. sample	3338.3		262.7	3370.7		287.4	3333.0		307.0	3475.7		266.5	3470.1		255.7
Wt. sand	62.56		140.99	65.68		155.24	76.59		168.17	125.68		148.60	147.21		131.30
Screen Analysis															
40	-----		38.52	-----		44.05	-----		51.39	-----		48.36	-----		44.63
50	0.80		22.40	0.57		26.49	1.04		30.63	3.35		27.64	5.99		24.76
70	1.03		18.17	1.10		18.95	1.62		22.12	4.94		19.91	7.09		17.82
100	2.67		20.18	2.92		22.10	3.71		20.44	12.49		19.64	17.09		17.81
140	5.51		18.76	6.61		20.01	7.91		20.44	21.41		16.77	26.92		13.56
200	8.43		14.74	9.95		15.09	11.90		14.99	25.24		10.66	30.79		8.17
230	3.97		3.29	4.67		3.65	6.15		3.44	8.99		2.54	8.65		1.75
325	5.63		2.60	6.25		2.54	7.51		2.44	10.23		1.34	10.88		1.16
-325	34.52		2.33	33.61		2.36	36.75		2.28	39.03		1.74	39.80		1.64

Run VIII-M - Analysis

	VIII-M-1			VIII-M-2			VIII-M-3			VIII-M-4			VIII-M-5		
	O.F.-1	O.F.-2	U.F.	O.F.-1	O.F.-2	U.F.	O.F.-1	O.F.-2	U.F.	O.F.-1	O.F.-2	U.F.	O.F.-1	O.F.-2	U.F.
Wt. jar and sample	2062.2	2169.6	900.0	2198.5	2203.0	994.5	2314.8	2319.7	926.0	2440.4	2282.3	990.5	2518.6	2538.6	1023.7
Wt. jar	684.6	687.5	683.5	684.9	685.1	671.1	707.9	695.1	665.4	703.7	664.7	694.9	693.4	698.0	667.7
Wt. sample	2859.7		216.5	3033.5		323.4	3231.5		260.6	3354.3		295.6	3665.8		356.0
Wt. sand	73.41		109.67	84.35		177.13	105.51		133.56	123.40		153.57	208.24		196.63
Screen Analysis															
40	-----		37.45	-----		63.13	-----		56.85	-----		57.06	-----		84.91
50	1.71		14.33	1.77		31.26	2.50		25.35	3.81		26.59	9.46		52.57
70	2.86		13.94	2.43		27.89	3.57		16.31	5.19		19.60	13.44		25.63
100	8.36		16.31	5.95		27.27	8.48		12.59	12.93		21.10	29.39		15.18
140	10.67		13.87	11.66		11.98	15.33		9.79	26.54		16.84	45.37		8.63
200	11.20		8.93	16.33		9.54	21.24		7.81	18.93		7.28	40.51		5.31
230	4.53		1.92	6.33		2.07	6.04		1.82	6.67		1.89	12.49		1.41
325	4.33		1.40	5.51		1.91	8.11		1.22	6.86		1.24	13.23		1.00
-325	29.75		1.52	34.37		2.08	40.24		1.82	42.47		1.97	44.35		1.99

(Continued)

Table 5. Analytical Data for Separation Investigations (Continued)

Run IX-M - Analysis

	IX-M 1			IX-M-2			IX-M-3			IX-M-4			IX-M-5		
	O.F.-1	O.F.-2	U.F.	O.F.-1	O.F.-2	U.F.	O.F.-1	O.F.-2	U.F.	O.F.-1	O.F.-2	U.F.	O.F.-1	O.F.-2	U.F.
Wt. jar and sample	2316.5	2253.7	866.0	2114.5	2191.7	981.8	2312.3	2186.8	900.8	2276.6	2209.0	875.9	2529.0	2484.0	1035.7
Wt. jar	668.7	699.3	707.6	667.0	698.8	671.9	668.8	704.6	685.5	667.8	675.5	681.5	689.8	670.3	683.3
Wt. sample	3202.2		158.4	2940.4		309.9	3125.7		215.3	3142.3		194.4	3652.9		352.4
Wt. sand	73.77		77.39	77.44		172.26	96.08		100.45	108.59		107.03	156.38		177.17
Screen Analysis															
40	-----		22.42	-----		57.95	-----		33.89	-----		35.01	-----		62.79
50	1.52		13.16	1.74		34.38	2.45		13.24	3.28		18.81	7.98		30.57
70	1.54		9.65	1.90		21.38	3.30		11.88	3.84		14.59	8.85		22.10
100	4.03		10.43	4.54		18.17	6.32		13.23	8.24		13.60	17.33		22.28
140	8.16		9.52	8.69		17.83	11.70		13.01	15.63		12.59	29.10		18.90
200	10.54		7.66	12.77		13.90	17.88		10.01	22.10		8.00	36.19		12.80
230	5.06		1.94	5.03		3.51	7.26		2.09	7.74		1.65	10.62		2.86
325	5.80		0.98	7.03		2.43	8.23		1.48	8.30		1.20	12.73		2.09
-325	37.12		1.63	35.74		2.71	38.94		1.62	39.46		1.58	46.91		2.78

Run X-M - Analysis

	X-M-1			X-M-2			X-M-3			X-M-4			X-M-5		
	O.F.-1	O.F.-2	U.F.	O.F.-1	O.F.-2	U.F.	O.F.-1	O.F.-2	U.F.	O.F.-1	O.F.-2	U.F.	O.F.-1	O.F.-2	U.F.
Wt. jar and sample	2252.1	2196.3	990.6	2218.2	2335.1	982.4	2216.0	2301.8	968.8	2385.0	2470.3	924.4	2233.8	2446.0	990.0
Wt. jar	703.5	675.0	725.1	676.7	704.1	711.0	698.5	685.0	672.0	662.3	681.0	670.4	666.9	706.4	663.3
Wt. sample	3069.9		265.5	3172.5		271.4	3134.3		296.8	3512.0		254.0	3308.5		326.7
Wt. sand	69.61		114.38	71.08		120.38	77.38		127.23	112.23		-----	129.55		146.70
Screen Analysis															
40	-----		32.93	-----		36.26	-----		34.90	-----		37.31	-----		44.26
50	1.12		18.00	1.07		19.32	1.47		20.37	3.09		22.42	5.47		25.68
70	1.59		14.44	1.52		15.39	1.92		17.97	3.61		19.49	3.33		20.44
100	3.36		14.99	3.36		15.69	4.02		16.57	8.53		15.17	10.91		20.43
140	6.15		14.49	6.63		14.37	8.03		17.10	14.72		13.30	19.68		16.85
200	8.87		11.61	10.06		11.65	11.76		12.04	20.38		9.20	25.66		11.67
230	8.79		2.99	4.51		2.95	5.14		3.16	7.79		2.33	9.11		2.56
325	5.14		2.24	5.76		2.07	6.77		2.19	9.51		1.49	10.07		1.77
-325	34.59		2.69	38.17		2.68	38.27		2.93	44.60		2.36	43.32		3.04

(Continued)

Table 5. Analytical Data for Separation Investigations (Continued)

Run XI-M - Analysis

	XI-M-1 O.F.-1	O.F.-2	U.F.	XI-M-2 O.F.-1	O.F.-2	U.F.	XI-M-3 O.F.-1	O.F.-2	U.F.	XI-M-4 O.F.-1	O.F.-2	U.F.	XI-M-5 O.F.-1	U.F.
Wt. jar and sample	2278.4	2251.5	1070.3	2357.0	2379.8	941.2	2313.8	2225.4	1135.5	2372.6	2465.0	870.0	2540.0	854.6
Wt. jar	684.7	683.2	687.5	683.5	684.7	684.0	681.9	687.7	685.5	686.0	683.5	681.5	681.0	683.3
Wt. sample	3162.0		392.8	3568.6		257.2	3169.6		450.0	3468.1		188.5	1859.0	171.3
Wt. sand	79.65		202.54	102.83		128.09	117.02		253.19	178.94		101.41	120.47	92.23
Screen Analysis														
40	-----		65.58	-----		37.20	-- --		92.97	-----		33.68	-----	32.60
50	1.17		30.60	1.71		20.36	2.54		43.11	6.75		17.63	8.25	16.54
70	1.50		28.45	2.47		16.56	3.24		30.56	7.57		12.61	7.29	12.52
100	3.87		26.12	5.85		17.67	8.09		31.47	17.74		13.43	14.91	11.38
140	7.42		22.06	11.58		16.12	15.87		25.16	28.81		11.17	21.21	9.15
200	11.18		18.15	17.02		12.08	21.69		18.74	36.85		8.30	25.13	6.45
230	5.66		4.64	7.39		3.25	7.91		4.07	12.34		1.61	8.24	1.30
325	6.07		3.28	8.74		2.09	9.81		3.02	13.87		1.17	8.48	0.73
-325	42.78		3.66	48.07		2.76	47.87		4.09	55.01		1.81	26.96	1.56

Run XII-M - Analysis

	XII-M-1 O.F. 1		O.F.-2	U.F.	Screen Analysis	Ave.	U.F.	Screen Analysis	Ave.	U.F.
Wt. jar and sample	2228.3		2093.0	977.4	40	------	63.24	200	39.40	19.94
Wt. jar	684.4		686.5	683.1	50	8.83	34.52	230	14.13	3.64
Wt. sample		2951.4		294.3	70	8.24	28.98	325	13.37	2.28
		185.82		212.80	100	17.59	31.78	-325	50.79	2.12
					140	33.47	26.30			

Run XIII-M - Analysis

	XIII-M-1 O.F.-1	O.F.-2	U.F.	XIII-M-2 O.F.	U.F.	XIII-M-3 O.F.	U.F.	XIII-M-4 O.F.-1	Q.F.-2	U.F.	XIII-M-5 O.F.-1	O.F.-2	U.F.
Wt. jar and sample	2131.8	2157.8	886.3	2061.8	952.0	2272.3	684.0	2312.6	2370.0	714.0	2401.4	2321.7	695.6
Wt. jar	686.7	686.7	687.0	659.6	689.0	664.0	382.1	702.9	671.4	398.2	703.6	670.5	397.2
Wt. sample	2916.2		199.3	1402.2	263.0	1608.3	301.9	3308.3		315.8	3349.0		298.4
Wt. $BaSO_4$	113.80		113.05	59.76	150.87	77.78	155.34	182.76		159.04	210.03		152.86
Screen Analysis													
40	-----		16.94	-----	25.47	-----	18.32	-----		12.79	-----		12.96
50	0.21		14.47	0.41	20.53	0.21	21.56	0.26		19.42	0.30		17.10
70	0.60		13.43	0.33	18.17	0.35	18.98	0.48		17.23	0.61		17.74
100	1.11		18.24	0.79	23.51	0.74	25.89	1.49		26.08	1.58		25.08
140	2.30		15.55	0.99	20.44	1.43	21.02	3.46		26.01	4.67		24.99
200	4.40		13.26	2.04	16.64	2.47	19.34	7.61		23.22	10.57		24.15
230	3.70		4.83	1.60	6.93	2.55	7.24	5.86		9.08	7.87		8.04
325	2.24		6.72	3.39	7.74	4.07	8.81	11.96		10.19	18.39		10.23
-325	99.23		9.61	50.21	11.44	65.96	14.18	151.64		15.02	166.04		12.57

Table 6. Operative Data of Pressure Drop Studies

O.F. Height	4-5/8 inches
Section Height	18 inches
Ring Height	10-3/8 inches
Ring Diameter	5.00 inches
Distance between break plate and overflow pipe	5-3/4 inches
Liquid	Water
Static Pressure	2.2 psig

O.F. Diameter Nom. Pipe Size (inches)	U.F. Diameter Nom. Pipe Size (inches)	Gage Pressure (psig)	Flow Rate (lbs./sec.) U.F.	O.F.
2-1/2	1	5.3	6.90	6.90
2-1/2	3/4	10.6	4.80	10.00
2-1/2	3/8	11.7	1.52	13.00
2	1	7.0	7.85	5.50
2	3/4	10.6	5.35	8.35
2	3/8	14.8	1.80	11.55
1-1/2	1	12.1	11.00	4.55
1-1/2	3/4	15.0	5.51	7.10
1-1/2	3/8	20.2	2.30	10.50
1-1/4	1	14.2	10.37	4.10
1-1/4	3/4	18.3	6.85	6.50
1-1/4	3/8	23.9	2.62	9.55

Table 7. Calculated Data for Pressure Drop Studies

Corrected Pressure (ft. H_2O)	Flow Rate ($ft.^3/sec.$) Feed	U.F.	Velocity Head (ft. H_2O) Feed	U.F.	Head Loss h_L (ft. H_2O)	GPM/ $h_L^{0.5}$	O.F. Diameter Approximate (inches)	U.F. Diameter Approximate (inches)
7.16	0.2212	0.1106	0.126	5.274	4.93	44.7	2.47	1.05
19.40	0.2372	0.0769	0.145	6.699	15.77	26.8	2.47	0.824
21.95	0.2327	0.0244	0.139	5.257	19.75	23.5	2.47	0.493
11.09	0.2139	0.1258	0.118	6.828	7.30	35.4	2.07	1.05
19.40	0.2195	0.0857	0.124	8.329	14.12	26.3	2.07	0.824
29.11	0.2139	0.0288	0.118	7.325	24.82	19.3	2.07	0.493
22.87	0.2492	0.1763	0.160	13.403	12.55	31.6	1.61	1.05
29.57	0.2021	0.0883	0.105	8.840	23.75	18.7	1.61	0.824
41.58	0.2052	0.0369	0.108	12.027	32.58	16.2	1.61	0.493
27.72	0.2319	0.1662	0.138	11.914	18.86	24.0	1.38	1.05
37.19	0.2140	0.1098	0.118	13.679	26.56	18.6	1.38	0.824
50.13	0.1950	0.0420	0.098	15.574	37.57	14.3	1.38	0.493

CALCULATION FOR IMPELLER DESIGN

Conditions:

1. feed rate = 150 GPM,
2. tube diameter = 5.5 in.,
3. hub diameter = 4.0 in.,
4. distance between trailing edge of blade and break plate = 10 in., and
5. revolutions of liquid = $\frac{10 \text{ in.}}{1.5 \text{ in. per revolution}}$.

Area at leading edge

$$A \frac{\pi}{4} [(5.5)^2 - (4.0)^2] = 0.0786 \text{ sq. ft.}$$

$$\text{Velocity} = u_1 = \frac{150}{7.48} \cdot \frac{1}{0.0786 \times 60} = 4.25 \text{ ft./sec.}$$

Time for fluid to move from trailing edge to break plate = t

$$t = \frac{10 \text{ in.}}{12 \frac{\text{in.}}{\text{ft.}} \times 4.2 \frac{\text{ft.}}{\text{sec.}}} = 0.196 \text{ sec.}$$

Now, Vr = constant, when V = minimum, r = 2.25 in. and V = maximum, r = 1.00, since maximum V is found at radius to be approximately equal to radius of overflow pipe. The average tangential velocity is located at radius

$$\frac{2.25 + 1.0}{2} = 1.67 \text{ inches.}$$

Fluid at this point makes 6.67 revolutions in 0.196 seconds. Therefore, at this point

$$V = \frac{2\pi(1.67)(6.67)}{12(0.196)} = 29.7 \text{ ft./sec.}$$

Then

$$\Gamma = 2\pi rV = 2\pi \frac{(1.67)(29.7)}{12} = 25.8 \text{ ft.}^2/\text{sec.},$$

and

$$\tan \alpha = \frac{u}{V} = \frac{4.25}{29.7} = 0.143$$

or

$$\alpha = 8 \text{ degrees } 9 \text{ minutes}$$

and

$$C = \frac{\Gamma \cos\left(\frac{90° - \alpha}{2}\right) \sin\left(90° - \frac{90° - \alpha}{4}\right)}{\pi Nu \cos\left(90° + \frac{90° - \alpha}{4}\right)}$$

$$\sin\left(90° - \frac{90° - \alpha}{4}\right) = 0.9369$$

$$\cos\left(90° + \frac{90° - \alpha}{4}\right) = 0.3497$$

$$\cos\left(\frac{90° - \alpha}{2}\right) = 0.755.$$

Then

$$C = \frac{25.8 \text{ ft.}^2/\text{sec.} \times 0.7555 \times 0.9369}{3.1416 \times N \times 4.2 \text{ ft./sec.} \times 0.3497}$$

$$C = \frac{3.95}{N}.$$

If 12 blades are chosen

$$C = 0.33 \text{ ft.}$$

Now,

$$\cos \alpha = \frac{C}{R}$$

$$= 8 \text{ degrees } 9 \text{ minutes}$$

$$\cos \alpha = 0.989$$

$$R = \frac{0.33}{0.989} = 0.34 \text{ ft.}$$

Now,

$$F = \frac{\pi}{N} \rho u V \, r^2 \Big|_{r_1}^{r_2}$$

where r is in feet

$$F = \frac{3.1416}{12} \; \frac{70.42 \text{ lb./ft.}^3}{32.2 \text{ ft./sec.}^2} \left(4.25 \frac{\text{ft.}}{\text{sec.}}\right)\left(29.7 \frac{\text{ft.}}{\text{sec.}}\right)[(0.458)^2 - (0.33)^2]$$

$$= 7.3 \text{ lbs.}$$

Thus, 0.067-in. steel rolled pins with strength of about 500 lbs. in shear would carry the load.

If the blade thickness is chosen at 0.125 in. (steel) and the supports are placed 1.5 in. from the trailing edge

$$Y = \frac{7.3 \text{ lb.} \times \frac{1.5}{2} \times (1.5)^3}{8 \times 30 \times 10^6 \text{v} \; \frac{0.75 \times (0.125)^3}{12}} = 0.00021$$

and the deflection is negligible.

Thus, for the specified conditions

blade length = C = 0.33 ft.,

radius of blade arc = R = 0.34 ft.,

blade angle = 8 degrees 9 minutes, and

blade thickness = d = 0.125 in.

SAMPLE CALCULATIONS

Calculation of 50 Per Cent Separation Point

Let X = flow rate of overflow (lbs./sec.),

Y = flow rate of underflow (lbs./sec.),

Mx = fraction of a specific screen size in overflow sample, and

My = fraction of a specific screen in underflow sample.

Then,

(X)(Mx) = weight of a specific size reporting to overflow (lbs./sec.),

(Y)(My) = weight of a specific size reporting to underflow (lbs./sec.),

(X)(Mx) + (Y)(My) = weight of a specific size entering in feed (lbs./sec.), and

$\frac{(Y)(My)}{(X)(Mx) + (Y)(My)} \times 100$ = percentage of a specific screen size reporting to underflow.

The calculations for run I-M-3 appear below.

Flow rate overflow (X) = 7.89 lbs./sec. and

underflow (Y) = 3.97 lbs./sec.

Weight of sample overflow = 3467.4 gm. and

underflow = 756.7 gm.

$$Mx = \frac{\text{Weight in overflow on a specific screen}}{\text{Weight of overflow sample}} .$$

$$My = \frac{\text{Weight in underflow on a specific screen}}{\text{Weight of underflow sample}} .$$

For 50-mesh screen

$$(X)(Mx) = \frac{(7.89)(2.5)}{3467.4}$$

$$= 0.00569,$$

$$(Y)(My) = \frac{(3.97)(82.15)}{756.7} = 0.431,$$

$$(X)(Mx) + (Y)(My) = 0.43669, \text{ and}$$

$$\frac{(Y)(My) \times 100}{(X)(Mx) + (Y)(My)} = 98.6 \text{ per cent.}$$

This calculation was repeated for each screen size shown in the following tabulation:

Mesh Size	Size Opening (microns)	Percentage reporting to U.F.	Average Particle Size (microns)
40	420	100	505
50	297	98.6	359
70	210	96.8	254
100	149	91.8	180
140	105	86.8	127
200	74	80.9	90
230	62	71.9	68
325	44	53.2	53
-325	---	17.4	22

The average particle size is the arithmetic average of the openings in the screen on which the material was retained and the next larger screen. For example:

50 mesh is equivalent to 297 microns,

40 mesh is equivalent to 420 microns, and

$\frac{297 + 420}{2}$ = average particle size for 50-mesh screen = 359.

The average particle size was plotted versus the percentage of that particular particle size reporting to the underflow as shown in Figure 16. The intersection of a smooth curve through these points with the 50 per cent line was taken as the 50 per cent separation point.

Calculation of Solids Concentration

S_o = percentage solids in overflow

$$= \frac{\text{total weight of material in overflow sample}}{\text{weight of overflow sample}} .$$

For run I-M-3

$$\text{Percentage of solids} = \frac{53.2}{3467.4} \times 100 = 1.53, \text{ and}$$

S_v = percentage of solids in underflow

$$= \frac{\text{total weight of material in underflow}}{\text{weight of underflow sample}} .$$

For run I-M-3

$$\text{percentage of solids in underflow} = \frac{371.8}{756.7} \times 100 = 49.13.$$

Percentage solids in feed:

weight of solids reporting to overflow =

fraction of solids in overflow times overflow rate (lbs./sec.).

Weight of solids reporting to underflow =

fraction of solids in underflow times underflow rate.

Percentage of solids in feed =

$$\frac{\text{weight of solids reporting to O.F. + weight of solids reporting to U.F.}}{\text{total flow rate}} .$$

For run I-M-3

S_c = percentage of solids in feed

$$= \frac{\left[\left(\frac{53.2}{3467.4}\right)(7.89) + \left(\frac{371.8}{756.7}\right)(3.97)\right] \times 100}{7.89 + 3.97} = 17.46.$$

Percentage Coarse and Fine Separation

$$\text{Percentage of coarse-particle separation} = \frac{W_v}{W_c} 100.$$

where W_v = weight of solids > 50 per cent particle size in underflow, and

W_c = weight of solids > 50 per cent particle size in feed.

A tabulation of values used in computing coarse and fine separation is shown below:

Run I-M-3

Particle Size (microns)	XMx	YMy	Accumulative XMx	Accumulative YMy	Accumulative XMx + YMy
505	0	72.0	0	72.0	72.0
359	0.569	43.1	0.569	115.1	115.7
254	0.820	26.1	1.39	141.2	142.6
180	1.595	17.9	2.98	159.1	162.1
127	2.935	19.38	5.92	178.5	184.4
90	2.64	11.1	8.56	189.6	198.2
68	1.03	2.63	9.59	192.2	201.8
53	0.813	0.925	10.4	193.1	203.5
22	1.70	0.358	12.1	193.5	205.6

50 per cent separation point = 50 microns.

Accumulative (Y)(My) = 193.1 for 53 microns

= 193.5 for 22 microns.

By linear interpolation,

$$W_v = 193.2.$$

Accumulative (X)(Mx) + (Y)(My) = 203.5 for 53 microns

= 205.6 for 22 microns.

Likewise,

$$W_c = 203.7.$$

$$\text{Percentage of coarse separation} = \frac{193.2}{203.7} \times 100 = 94.85.$$

$$\text{Percentage of fine separation} = \frac{W_o}{W_F} \ 100$$

where W_o = weight of solids < 50 per cent point in overflow and

W_F = weight of solids < 50 per cent point in feed.

Accumulative XMx = 10.4 for 53 microns

= 12.1 for 22 microns.

By linear interpolation, for the 50 per cent point

XMx = 10.56.

W_o = total accumulative XMx - XMx for 50 per cent point

= 12.10 - 10.56 = 1.54.

W_F = total accumulative XMx + YMy - XMx + YMy for 50 per cent point

= 205.6 - 203.7 = 1.90.

$$\text{Percentage fine separation} = \frac{1.54}{1.90} \times 100 = 81.05.$$

Least-Squares Calculation for Flow Rate Versus 50 Per Cent Particle Size

Since the data presented in Figure 17 can be approximately represented by an equation of the form

$$\log \mu = m \log G + \log A$$

where μ = particle size in microns, and

G = flow rate in lbs./sec.

Letting $y = \log \mu$, $X = \log G$, and $b = \log A$, we have

$$Y = mX + b.$$

By the least squares method,

$$\Sigma Y = m\Sigma X + bn$$

and

$$\Sigma XY = m\Sigma X^2 + b\Sigma X$$

from which

$$m = \frac{\Sigma y \Sigma x - N\Sigma xy}{(\Sigma x)^2 - N\Sigma X^2}.$$

For run I-M, the least-squares calculation for the slope are tabulated as follows.

Run	G (lbs./sec.)	μ (microns)	log G (X)	log μ (Y)	XY	X^2
I-M-1	20.20	35	1.3054	1.5441	2.0157	1.7041
I-M-2	15.26	45	1.1836	1.6532	1.9567	1.4009
I-M-3	11.86	50	1.0741	1.6990	1.8249	1.1537
I-M-4a	7.11	70	0.8519	1.8451	1.5718	0.7257
I-M-5	3.88	110	0.5888	2.0414	1.2020	0.3467
			5.0038 $= \Sigma X$	8.7828 $= \Sigma Y$	8.5711 $= \Sigma XY$	5.3311 $= \Sigma X^2$

$$m = \frac{(5.0038)(8.7828) - (5)(8.5711)}{(5.0038)^2 - (5)(5.3311)} = -\frac{1.09187}{1.61749} = -0.675.$$

Using this method, the slopes for runs II and IV were found to be -0.690 and -0.704, respectively.

Least-Squares Calculation for Overflow Diameter Versus 50 Per Cent Particle Size

The data shown in Figure 18 indicate that the relationship between the overflow diameter, e, (actual inside diameter in inches) and the 50 per cent particle size (microns) may be represented by an equation of the form

$$\log \mu = m' \log e + \log A'.$$

Calculation using the least-squares method are shown as follows.

Run	e (inches)	μ (microns)	log e (X)	log μ (Y)	XY	X^2
I-M	2.067	51	0.3153	1.7076	0.5384	0.0994
II-M	1.049	30.5	0.0208	1.4843	0.0309	0.0004
III-M-1	1.380	35	0.1399	1.5441	0.2160	0.0196
III-M-2	1.610	40	0.2068	1.6021	0.3313	0.0428
III-M-3	2.469	57	0.3925	1.7559	0.6892	0.1541
			1.0753 = ΣX	8.0940 = ΣY	1.8058 = ΣXY	0.3163 = ΣX^2

$$m = \frac{(1.0753)(8.0946) - (5)(1.8058)}{(1.0753)^2 - (5)(0.3163)} = 0.766 \text{ or } 0.77.$$

Least-Squares Calculation of Correlation Coefficient Versus 50 Per Cent Point

The data shown in Figure 19 indicate that the relationship between the correlation coefficient ($e^{0.77}/G^{0.68}$) and the 50 per cent point may be represented by an equation of the form

$$\log \mu = m'' \log \frac{e^{0.77}}{G^{0.68}} + \log A''.$$

Calculations using the least-squares method are as follows. For convenience in handling logarithms, the reciprocal of the correlation coefficient is used in the calculations.

Run	$\frac{e^{0.77}}{G^{0.68}}$	$\frac{G^{0.68}}{e^{0.77}}$	μ	$\log \frac{G^{0.68}}{e^{0.77}}$ X	$\log \mu$ Y	XY	X^2
I-M-1	0.226	4.425	35	0.6459	1.5441	0.9973	0.4172
I-M-2	0.274	3.649	45	0.5622	1.6532	0.9294	0.3161
I-M-3	0.325	3.076	50	0.4880	1.6990	0.8291	0.2381
I-M-4a	0.459	2.179	70	0.3383	1.8451	0.6242	0.1144
I-M-5	0.693	1.443	110	0.1593	2.0414	0.3252	0.0254
II-M-1	0.207	4.830	33	0.6840	1.5185	1.0387	0.4679
II-M-2	0.240	4.166	37.5	0.6197	1.5740	0.9754	0.3840
II-M-3	0.314	3.184	49	0.5030	1.6902	0.8502	0.2530
II-M-4	0.434	2.304	70	0.3625	1.8451	0.6688	0.1314
III-M-1	0.239	4.184	35	0.6216	1.5441	0.9598	0.3864
III-M-2	0.269	3.717	45	0.5702	1.6021	0.9135	0.3251
IV-M-1	0.273	3.663	42	0.5638	1.6233	0.9152	0.3179
IV-M-2	0.291	3.436	45	0.5361	1.6532	0.8863	0.2874
IV-M-3	0.336	2.976	50	0.4736	1.6990	0.8046	0.2243
IV-M-5	0.620	1.612	101	0.2074	2.0043	0.4157	0.0430
IV-M-6	0.374	2.673	55	0.4270	1.7404	0.7432	0.1823
IV-M-7b	0.458	2.183	66	0.3391	1.8195	0.6170	0.1150
				8.1017 $= \Sigma X$	29.0965 $= \Sigma Y$	13.4936 $= \Sigma XY$	4.2289 $= \Sigma X^2$

$$m = \frac{(8.1017)(29.0965) - (17)(13.4936)}{(8.1017)^2 - (17)(4.2289)} = \frac{6.3399}{6.2538} = 1.00$$

Calculation for Predicted Line of Figure 28, Run XIII-M

Using equation 40 and the following data:

density of sand-water slurry = 1.10 gm./cc.,

density of barytes-water slurry = 1.13 gm./cc.,

density of sand = 2.64 gm./cc.,

density of barytes = 4.42 gm./cc.,

$$\mu = 157 \frac{e^{0.77}}{G^{0.68}} \times \left[\frac{2.64 - 1.10}{4.42 - 1.13}\right]^{0.5}$$

and

$$\mu = 107.4 \frac{e^{0.77}}{G^{0.68}} .$$

Predicted intercept for run XIII-M in Figure 28 is equal to 107.4

Pressure Drop Calculations

An energy balance over the section of the equipment between the pressure tap directly above the impeller and the discharge point of the underflow stream can be written:

$$P_1 v_1 + \frac{u_1^2}{2g} + Z_1 = P_2 v_2 + \frac{u_2^2}{2g} + Z_2 + h_1$$

where P_1 = pressure at tap above impeller,

P_2 = pressure at discharge from underflow pipe or atmospheric pressure,

$v_1 = v_2$ = specific volume (lbs./ft.^{3}),

Z_1 and Z_2 = heights of pressure tap and of underflow discharge, respectively, from an arbitrary datum plant,

u_1 = flow velocity in equipment at pressure tap (ft./sec.), and

h_L = head loss through equipment including velocity head from overflow discharge which is assumed nonrecoverable.

Taking the datum plane through Z_2, this equation reduces to:

$$P_1 v_1 + \frac{u_1^2}{2g} + Z_1 = \frac{u_2^2}{2g} + h_L$$

or

$$h_L = P_1 v_1 + \frac{\Delta u_{1\text{-}2}^2}{2g} + Z_1.$$

For run III-P-1 with underflow of 1-in. nominal pipe diameter,

flow to U.F. = 6.90 lbs./sec.,

flow to O. F. = 6.90 lbs./sec.,

P_1 = 3.1 psig,

$$A_1 = \frac{\pi [(5.5)^2 - (4)^2]}{(4)(144)}$$

$$= 0.0777,$$

A_2 = 0.006 ft.^{2},

Z_1 = 2.92 ft.,

total feed rate = 13.80 lbs./sec.,

$$\frac{u_1^2}{2g} = \left[\frac{13.80}{(62.4)(0.0777)}\right]^2 \frac{1}{64.4} = 0.126 \text{ ft.},$$

$$\frac{u_2^2}{2g} = \left[\frac{6.90}{(62.4)(0.006)}\right]^2 \frac{1}{64.4} = 5.274 \text{ ft., and}$$

$$P_1 v_1 = \frac{(3.1)(144)}{(62.4)} = 7.15 \text{ ft.}$$

Therefore,

$$h_L = 7.15 + 0.13 - 5.27 + 2.92 = 4.93 \text{ ft. } H_2O.$$

The capacity ratio is defined as

$$\frac{Q}{(h_L)^{0.5}},$$

where Q = feed rate (GPM)

$$Q = \frac{(13.80)(60)}{8.33} = 99.4,$$

$$\text{capacity ratio} = \frac{99.4}{(4.93)^{0.5}} = 44.7.$$

Taggart Efficiency

The Taggart efficiency is defined by

$$E = \frac{C - \frac{(100 - c)G}{100 - f}}{\frac{fF}{100}} \times 100$$

where C = weight of solids to overflow,

100 - c = percentage of oversize in overflow,

100- f = percentage of oversize in feed, and

F = weight of solids in feed.

Referring to sample calculation III, we find that C = 12.1, and F = 205.6.

$$100 - f = \frac{W_c}{F} \times 100 = \frac{203.7}{205.6} \times 100 = 99.07$$

$$100 - c = \left(\frac{C - W_o}{C}\right) 100 = \left(\frac{12.10 - 1.54}{12.10}\right) 100 = 87.27$$

$$f = 100 - (100 - f) = 0.93$$

$$E = \frac{12.1 - \frac{(87.27)(12.1)}{99.07}}{0.93\left(\frac{205.6}{100}\right)} \times 100 = 75.39\ \%$$

Calculation of Water Split

H_s = water split = percentage of water to underflow

$$= \frac{Y - S_v Y}{G - S_c G}$$

where S_v = percentage solids in underflow,

S_c = percentage solids in feed, and

G = feed rate (lbs./sec.).

For run I-M-3

$Y = 3.97$,

$S_v = 49.13$,

$G = 11.86$, and

$S_c = 17.46$.

$$H_s = \left[\frac{3.97 - (0.4913)(3.97)}{11.86 - (0.1746)(11.86)}\right] 100 = 20.63\ \%$$

PRELIMINARY INVESTIGATION OF 10-INCH FIXED-IMPELLER DEVICE

Equipment and Procedure

The DallaValle-Moder model (Figure 2) was assembled in the lower laboratory of the Chemical Engineering Department and was placed in a closed circuit with reservoir and pumps (Figure 33). A series of exploratory tests were conducted with sand and water slurries of several solids concentrations. The flow rates, underflow pipe diameters, and position of the overflow with respect to the fixed blade were considered. Also tests were conducted without the insert ring to determine its effect on operation. In order to evaluate from a design viewpoint, the bottom discharge for the overflow (this is contrary to conventional cyclones with discharge at the top), the feed header was modified with a tangential inlet. With the fixed blade removed, runs were made with the modified hydroclone at two pressure drops and compared with other runs using a 9-inch conventional cyclone.

Flow rates, pressure drops, and samples of the underflow and overflow streams were taken for each set of conditions. Screen analyses and solids concentration determinations of the samples were performed. The data obtained were used to calculate (1) percentage of solids in the underflow and overflow streams, (2) percentage of solids in the feed stream, and (3) percentage of a specific mesh-size particle reporting to the underflow and overflow. Plots were made of the percentage of a specific mesh-size particle reporting to the underflow and overflow versus particle size. Thus, the classification point or 50 per cent point was determined based on the Dahlstrom method (3). This is defined as a point at which a particle of a specific size reports 50 per

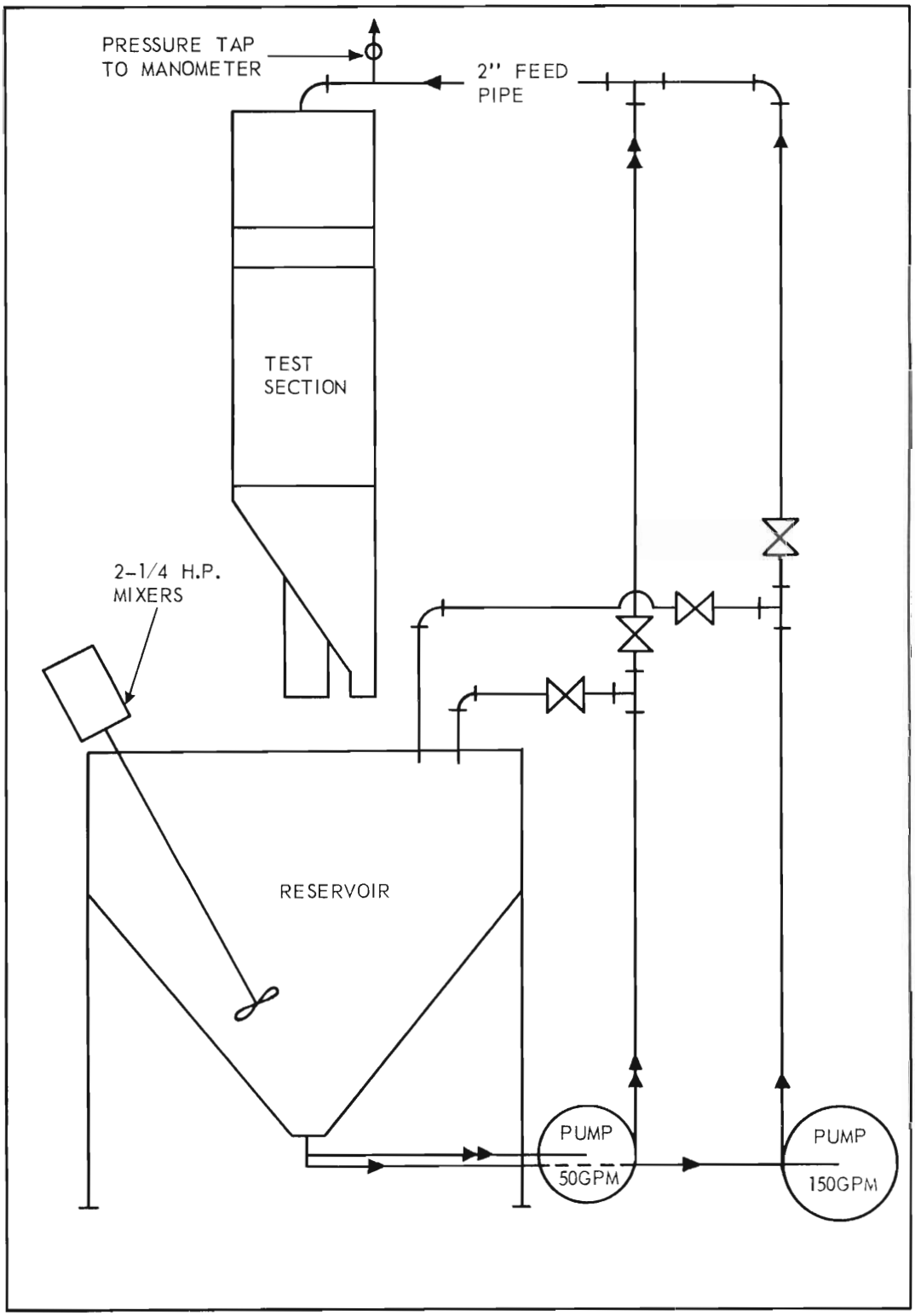

Figure 33. Sketch of Equipment Layout for 10-Inch Model.

cent (by weight) to the underflow and 50 per cent to the overflow. This method presents a clear picture of the classification point, and the slope of the curves indicates the sharpness of the separation. Sample calculations, operative and analytical data are included in this Appendix.

Results and Discussion

Table 8 presents the results of several of the control tests. As previously stated these experiments were carried out on the exploratory basis to obtain indicative design information for future model study. Whereas these tests did not cover an extensive range of investigations, data obtained indicate several qualitative relationships which were most useful in future design and operation.

Effect of solids concentration.--Comparison of run VI-2 with run IX-2 (Table 8) indicates that increased solids concentration in the feed results in an increase in the particle size at the 50 per cent point. This would be expected as particles moving toward the periphery of the cylindrical section of the hydroclone would encounter more collisions with other particles per unit distance. This effect of concentration is also shown, to a lesser degree, by comparing runs VI-3 with IX-2. The difference in magnitudes of this differential in 50 per cent point particle size at high- and low-flow rates would not be expected. This will be discussed under "Effect of Flow Rate."

Effect of underflow outlet diameter.-- Effect of the diameter of the underflow on the 50 per cent point is indicated by comparing the runs VI-1 with VI-2 and VII-1 with VII-2. A 1-inch underflow diameter gave a separation at a particle size of about 100 microns smaller than the 1/2-inch diameter. This would be expected since a greater part of the

Table 8. Data of 10-Inch Fixed-Impeller Studies

Run and Test Number	50 Per Cent Point (microns)	O.F. Diameter (Nominal Pipe Size) (inches)	U.F. Diameter (Nominal Pipe Size) (inches)	O.F. Rate (lb./ sec.)	U.F. Rate (lb./ sec.)	Solids in O.F. (%)	Solids in U.F. (%)	Solids in Feed (%)
Run VI								
Test 1	660	3	1	22.7	3.8	14.7	38.4	18.1
2	790	3	1/2	24.9	1.8	14.7	60.4	17.8
3	540	3	1/2	9.23	1.03	15.7	68.0	20.9
Run VII								
Test 1	840+	3	1/2	26.0	1.88	14.9	53.5	17.5
2	760	3	1	21.6	3.8	13.4	32.5	16.3
Run VIII								
Test 1	840+	3	1/2	23.7	1.77	17.4	60.7	20.4
2	840+	3	3/4	26.9	2.02	17.9	49.8	20.1
3	780	3	1	20.72	3.71	16.6	40.6	20.2
Run IX								
Test 1	490	3	1/2	25.9	2.08	7.95	46.55	10.74
2	450	3	1/2	8.7	0.81	8.45	53.3	12.27
3	460	3	1/2	12.73	1.04	8.02	52.6	11.38
Run X								
Test 1	620	3	1/2	24.85	1.68	6.98	41.65	9.18
2	730	3	1/2	14.23	1.09	8.18	47.23	10.95
3	840+	3	1	25.3	3.84	8.45	22.35	10.29
4	290	3	1	12.6	2.52	7.27	27.55	10.65

feed would report to the underflow with the 1-inch diameter. The underflow would be expected to contain a larger percentage of the larger size particles with a lower total percentage of solids. This is shown to be the case in runs VI-1 and VI-2 with 38.4 per cent and 60.4 per cent solids in the underflow, respectively.

Effect of baffle ring.-- In order to obtain a preliminary evaluation of the baffle ring (Figure 2), run VIII was made with the ring removed. It is evident upon comparison of runs VI-1 and 2 with VIII-1 and 3 that the ring has some effect on the flow pattern and separation characteristics of the equipment. However, the difference between the 50 per cent point for these runs cannot be attributed solely to the ring, since the solids concentrations of the feed were not identical. It appears that the ring assists to a limited extent in separation at a smaller particle size.

Effect of flow rate.--Effect of flow rate, which in effect is an index of efficiency or adequacy of the fixed blade, is shown by comparing runs VI-1 and 2. If the blade section were designed properly, an increase in flow rate should cause the separation to occur at a smaller particle size. It is evident upon comparing the above-mentioned runs with one another and run IX-1 with IX-2 and 3 that the reverse is true for the blade section used. This is attributed to short-circuiting of the slurry through the blade directly into the overflow pipe. It indicates inefficient blade design.

Effect of overflow pipe location.--Preliminary studies on the effect of the overflow-pipe location relative to the blade section were made by extending the overflow pipe upward to within 11 inches of the blade. These data are shown in run X. Run IX was made with the overflow pipe 16 inches below the blade. Upon comparing results of these two runs, it appears that during run X a larger portion of the slurry short-circuited directly into the overflow pipe than in run IX. If short-circuiting were not present, one would expect to obtain separation at smaller particle sizes.

Evaluation of bottom discharge overflow pipe (comparison with 9-inch cyclone).--Run XII was made with a tangential feed inlet into the header and with the blade section removed. Run XII was made with the conventional 9-inch cyclone. Table 9 presents the data obtained. Figure 34 is a plot of the percentage (by weight) of a specific particle size reporting to the underflow versus particles size in microns. The scatter of the data is attributed to unstable operation. The pressure drop for the cyclone was increased by 2 inches of mercury to compensate for an additional 2 feet of head in the modified hydroclone setup. Even with this increased pressure the cyclone did not exhibit stable operation in run XIII, whereas in run XII the modified hydroclone operated with practically no fluctuation.

It is apparent from Figure 34 and Table 9 that sharper separation (as indicated by the slope of the curves) was obtained with the cyclone at a smaller particle size (50 per cent point) than with the modified hydroclone. This difference indicates that the greater pressure drop in the cyclone represents greater energy application to the separation of the solid from the liquid. Dahlstrom's (3) work shows that an increase in cone angle of a conventional cyclone results in the 50 per cent separation point at a larger particle size. With the flat bottom of the hydroclone, the cone angle has been extended to the limit or zero. A 50 per cent point would be expected to be at a larger particle size. Run XII indicates that this has occurred. A most significant factor from this comparison of the conventional cyclone with the modified hydroclone is the relative stability of the operation of the two test sections. It appears that the bottom discharge for the overflow with

Table 9. Data of Comparison Test of 10-Inch Model with 9-Inch Cyclone

Run and Test Number	50 Per Cent (microns)	O.F. Diameter (Nominal Pipe Size) (inches)	U.F. Diameter (Nominal Pipe Size) (inches)	O.F. Rate (lb./sec.)	U.F. Rate (lb./sec.)	Solids in O.F. (%)	Solids in U.F. (%)	Solids in Feed (%)	Inlet Pressure (inches of mercury)
Run XII									
Test 1	66	3	1/4	26.1	2.35	0.31	64.5	5.6	5.8
2	72	3	1/4	12.3	1.45	0.65	67.6	7.6	2.0
Run XIII									
Test 1	37	3	3/4	8.32	3.15	0.094	56.8	15.6	4.1
2	24	3	1-1/4	13.9	6.25	0.096	51.3	15.9	6.8

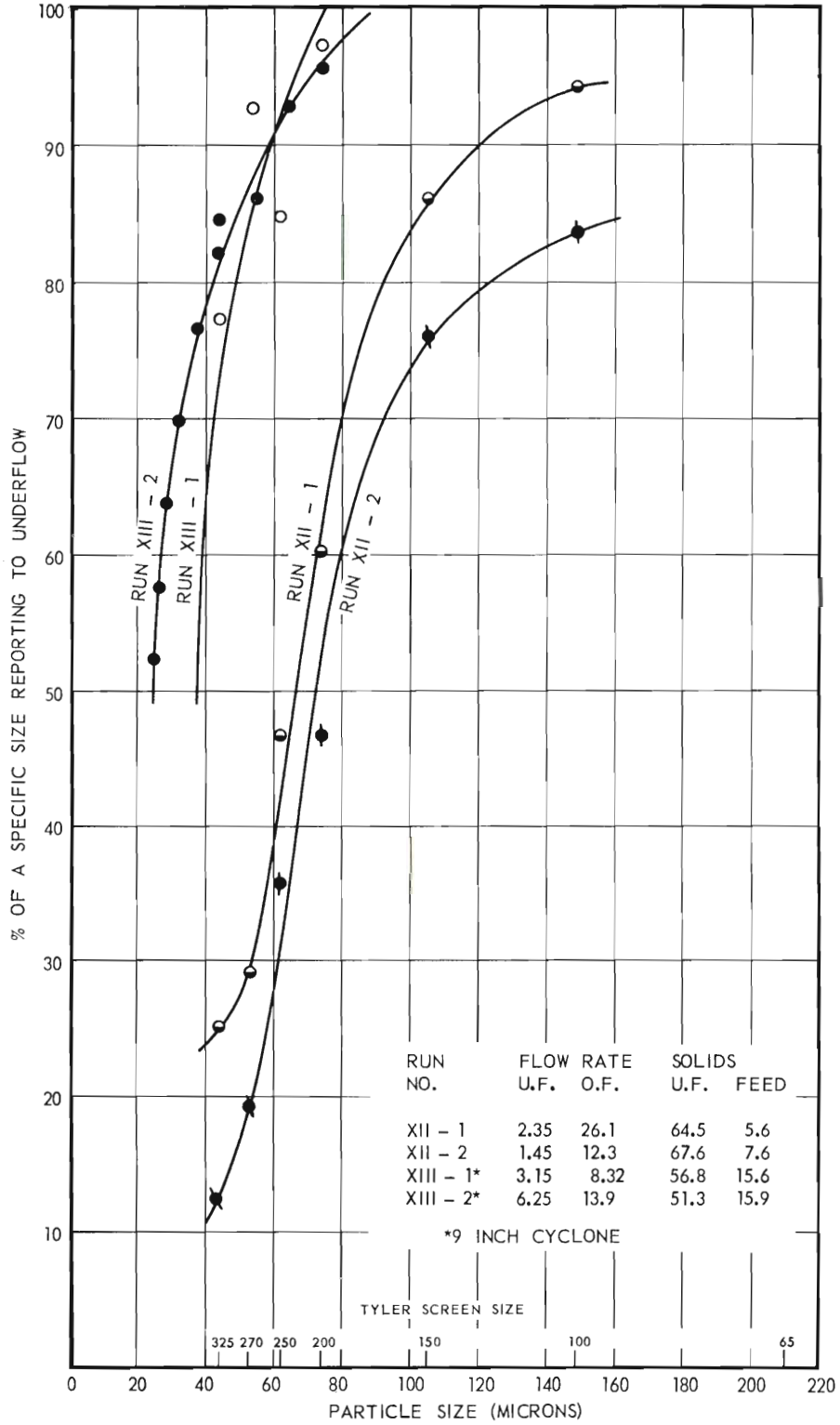

Figure 34. Comparison Test for 10-Inch Model with 9-Inch Model.

a flat-bottom arrangement will permit separation at lower pressure drops than with the cyclone. This might well be the starting point for development of a separator that will do the same job as the conventional cyclone at considerably lower pressure drops.

Conclusions and Recommendations

Results of the exploratory tests under phase II of the subject program indicate:

1. That separation could be obtained with a fixed-blade hydroclone as designed within the particle-size range of 290 to 840 microns, however, the separation was not sharp. Consequently, additional design and investigation would be required to attain satisfactory separation.

2. That the most significant factor in the DallaValle-Moder 10-inch model was the inefficient impeller section which results in short-circuiting which overshadowed the effect of flow rate and overflow pipe location.

3. That the baffle ring had limited effect on operation with the impeller section used.

4. That increased solids concentration in the feed resulted in the increase in particle size at the 50 per cent point.

5. That an increase in the underflow diameter resulted in a 50 per cent separation point at a smaller particle size.

6. That with a tangential inlet header the bottom discharge for the overflow and flat-bottom arrangement resulted in effective stable operation at a lower pressure drop than the conventional cyclone.

7. That the 50 per cent separation point occurred at a larger

particle size for a specific pressure drop with the modified hydroclone than with the conventional cyclone.

SAMPLE CALCULATION FOR 10-INCH MODEL

Run IX-1

O.F. rate = 25.9 lbs./sec.

U.F. rate = 2.08 lbs./sec.

	O.F.	U.F.
Weight of sample (gm.)	1071.85	578.05
Weight of solids in sample (gm.)	85.25	268.85

Screen Analysis

Mesh	Overflow Weight	Underflow Weight
20	0.10	2.2
28	12.25	93.95
35	0.77	3.85
48	16.88	75.7
65	23.0	50.56
100	17.6	28.89
150	8.85	9.26
200	3.5	3.04
-200	2.1	1.00

For 20 mesh

overflow

$$\frac{\text{20-mesh screen}}{\text{sample wt.}} \times \text{flow rate} = \frac{0.10}{1071.85} \times 25.9 \text{ lbs./sec.} = 0.00233$$

underflow

$$\frac{2.2}{578.1} \times 2.08 \text{ lbs./sec.} = 0.00792$$

$$\frac{0.00233}{0.00233 + 0.00792} = \text{fraction reporting to O.F.} = 0.2295$$

$$1.00 - 0.2295 = 0.7725 \text{ reporting to U.F.}$$

This calculation is repeated for each mesh size.

Mesh	Fraction to Overflow	Fraction to Underflow
28	0.228	0.773
28	0.465	0.535
35	0.566	0.434
48	0.598	0.402
65	0.752	0.248
100	0.796	0.204
150	0.866	0.134
200	0.885	0.115
-200	0.934	0.066

Separation (50 per cent point) for this run falls between 28 and 35 mesh. A plot of fraction to overflow or underflow versus particle size gives an intersection of the curve with the 50 per cent line at 490 microns (Figure 35).

Percentage of Solids in Overflow, Underflow, and Feed

Since representative samples of the feed are most difficult to obtain in liquid-solid separation equipment, the feed percentage of solids is calculated from the overflow and underflow streams.

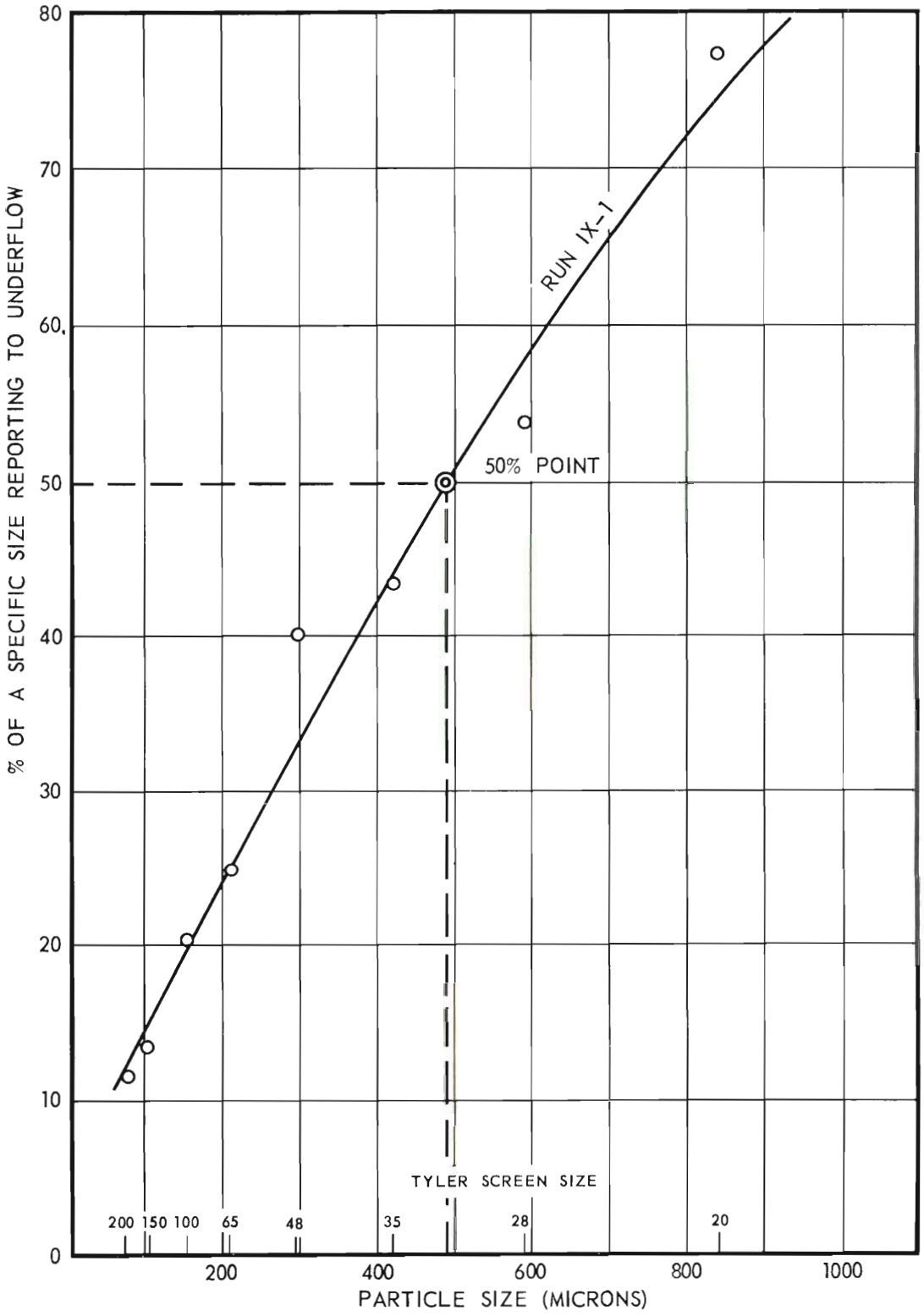

Figure 35. Plot for 50 Per Cent Point, Run IX-1 (10-Inch Model).

Run IX-1

For overflow:

$$\text{percentage of solids in O.F.} = \frac{\text{wt. solids in sample}}{\text{total wt. of sample}} \times 100$$

$$= \frac{85.25}{1071.85} = 7.95.$$

For underflow:

$$\text{percentage of solids in U.F.} = \frac{268.85}{578.05} \times 100 = 46.55.$$

For feed:

percentage of solids in feed =

$$\frac{(\%\ \text{solids O.F.} \times \text{O.F. rate}) + (\%\ \text{solids U.F.} \times \text{U.F. rate})}{\text{total feed rate}} \times 100 =$$

$$\frac{(7.95 \times 25.9) + (46.55 \times 2.08)}{27.98} \times 100 = 10.74.$$

REFERENCES CITED

1. Dahlstrom, D. A., "High Speed Classification and Desliming With the Liquid-Solid Cyclone." Mining Engineering (February 1951) and Transactions, A.I.M.E. (1951).

2. Dahlstrom, D. A., Prediction of Energy Requirements and Solid Elimination Efficiency for the Liquid-Solid Cyclone. Ph.D. Thesis, Northwestern University, 1949.

3. Dahlstrom, D. A. "Cyclone Operating Factors and Capacities on Coal and Refuse Slurries." Transactions A.I.M.E. 184, (1949), 331-34.

4. Driessen, M. G. "The Use of Centrifugal Force for Cleaning Fine Coal in Heavy Liquids and Suspensions with Special Reference to the Cyclone Washer." Journal of the Institute of Fuel (December 1945).

5. Driessen, M. G., "The Use of Hydraulic Cyclones in Thickeners and Washers in Modern Coal Preparation." Coal Technology, TP 2135 (August 1947) and Transactions A.I.M.E. (1948), 177, 240.

6. Fitch, E. B., and Johnson, E. G., "Operating Behavior of Liquid-Solid Cyclones." Mining Engineering (March 1953).

7. Rastatter, E. L. and Group, A. H., "Hammermill Dirt Separation." Tappi 35, No. 5 (May 1952).

8. Sutherland, R. L., "Recovering and Desliming Fine Coal with Cyclones." Cincinnati Meeting, American Mining Congress, April 1950.

9. Tille, R., "Contribution a L'Etude du Lavage des Charbons au Cyclone Driessen." Extrait des Annales Mines de Delgique (1951).

10. Weems, F. T., "Some Metallurgical Applications of the Dorrclone." Transactions A.I.M.E. 190 (1951), 681-90.

11. Criner, H. E., The Vortex Thickener. International Conference on Coal Preparation, Paris, France, June 1950.

12. Dahlstrom, D. A., "High Efficiency Desliming by Use of Hydraulic Water Additions to the Liquid-Solid Cyclone." Mining Engineering (August 1952).

13. Driessen, M. G., and Criner, H. E., "Cyclone Thickener Applications in Coal Industry." Mining Engineer 187 (January 1950), 102-108.

14. Hyer, J. W., "Heavy-Density Separation--A Review of Its Literature." Quarterly, Colo. School of Mines 43, No. 13 (1948) 36-42.

15. Moder, J. J., Close Gravity Solids Separation with Heavy Liquids and the Liquid-Solid Cyclone. Ph.D. Thesis, Northwestern University, 1950.

16. Moder, J. J., and Dahlstrom, D. A., "Fine-Size, Close-Specific Gravity Separation with the Liquid-Solid Cyclone." Chemical Engineering Progress 48 (February 1952).

17. Kelsall, D. F., A Study of the Motion of Solid Particles in a Hydraulic Cyclone. Symposium on Mineral Dressing, The Institution of Mining and Metallurgy, London, England, September 23-25, 1952.

18. Dahlstrom, D. A., Fundamental and Applications of the Liquid Cyclone, presented at American Institute of Chemical Engineers, Biloxi, Mississippi, March 7-10, 1953.

19. Streeter, Victor L., Fluid Dynamics. McGraw-Hill, New York, 1948.

20. Eshbach, Ovid W., Handbook of Engineering Fundamentals, John Wiley & Sons, New York, 1944.

21. Taggart, A. F., Handbook of Mineral Dressing, John Wiley & Sons, New York, 1945.

22. Emmett, Robert C., and Dahlstrom, D. A., "The Application of Centrifugal Forces to Gravitational Classifiers." Mining Engineering (October 1953).

VITA

Henry Howard Sineath, son of Ruth Butler Sineath and Francis Henry Sineath, was born on December 4, 1921, in Savannah, Georgia. At an early age, he moved with his family to Jacksonville, Florida, where he attended elementary and high school.

Upon graduation from Andrew Jackson High of Jacksonville in 1940, he enrolled at the School of Chemical Engineering of the University of Tennessee, Knoxville, Tennessee. During his undergraduate years, he was an above average student and was a very active participant in many student activities and organizations. In recognition of his leadership in student activities, he was elected to Who's Who Among Students in American Colleges and Universities in 1944. While an undergraduate (1942 to 1943), he was a co-op student employed by E. I. du Pont de Nemours Co., Richmond, Virginia, as a process student in the cellophane industry. He also worked for the TVA at the University of Tennessee as a part-time student employee (1943 to 1944) and for the Glidden Company, Jacksonville, Florida, as a control operator. He received the Bachelor of Science Degree in Chemical Engineering in 1944.

Upon graduation from the University of Tennessee, he entered the United States Army. The major part of his service was with the Corps of Engineers as a military engineer. While on this tour of duty, he was assigned as post engineer of Fort Gulick, Panama Canal Zone. In August 1947, he was relieved from active duty and assigned an inactive status in the Reserve Corps as a First Lieutenant.

After a brief period in the construction field, he entered the University of Tennessee in 1948 as a Graduate Student in Chemical Engineering. While doing graduate work there (1948 to 1949), he received a Departmental Research Fellowship, was an instructor in the Chemical Engineering Department, and assisted the Department Maintenance Section in design and construction of equipment and instrumentation. He received the Master of Science Degree in 1949, majoring in Chemical Engineering and minoring in Fluid Mechanics and Mathematics. The title of his Master of Science thesis is "Heat Transfer to Mercury--the Asymmetric Case."

Upon graduation he was employed by International Minerals and Chemical Corporation as a Research Engineer in the chemical engineering pilot plant group. Subsequently, he was assigned as Group Leader of this section and held that position until February 1951.

In February 1951, he joined the Georgia Institute of Technology as a Research Assistant in the Engineering Experiment Station and entered the Graduate School on a part-time basis. While at the Georgia Tech Engineering Experiment Station, he served as a Project Director on a large Industrial Market Research Project (1951 to 1952), as Assistant to the Director (1953 to 1955), and as supervisor of the Industrial Projects Laboratory (1955). While Assistant to the Director, he supervised the Service Groups of the Station and served as Secretary of the Patent Committee.

He is married to the former Miss Blanche Betty Hajek of Winamac, Indiana, and is the father of four children.

He is a registered Professional Engineer in the state of Georgia and is a member of the following organizations:

The American Institute of Chemical Engineers

The American Chemical Society

The National Society of Professional Engineers

The Society of Sigma Xi

Alpha Chi Sigma

Reserve Officer Corps.

Toastmasters International

Upon completion of the requirements for the degree of Doctor of Philosophy in Chemical Engineering, he plans to continue his work in research in the field of solid-liquid separation and diffusion processes.